PR

QP
84
.A1
G88

Vol. 24
no. 3

GROWTH

A JOURNAL FOR STUDIES OF DEVELOPMENT AND INCREASE

UNIVERSITY
OF MICHIGAN

MAR 1 1961

SCIENCE
LIBRARY

VOLUME XXIV, NUMBER 3
PAPERS 590-594

SEPTEMBER, 1960 $6.00 A YEAR

Second-Class postage paid at Worcester, Mass.

GROWTH

A journal for the coordination of studies of increase and development as general properties of nature. Published by contributors and subscribers on a cooperative, non-profit, non-salary basis. The field of investigation is primary and work will be published in which the approach is through mathematics, physics, chemistry, genetics, embryology, philosophy, and anthropology; just as will studies of development in its several expressions, and of mass increase and the part played therein by nutrition, vitamins, and hormones.

It is published four times a year during March, June, September and December at $6.00 per volume (outside U. S. and Canada, $6.50). Single numbers $2.00. There will be one volume each year.

All manuscripts and subscriptions should be sent to: The Editors of Growth, The Institute for Cancer Research, Fox Chase, Philadelphia 11, Pa.

THE EDITORS OF GROWTH

Managing Editor

STANLEY P. REIMANN, M.D.

Institute for Cancer Research, Fox Chase, Philadelphia, Pa.

Editor-in-Chief

IRENE COREY DILLER, PH.D.

Institute for Cancer Research, Fox Chase, Philadelphia, Pa.

John T. Bonner, Princeton University
Donald P. Costello, Univ. of N. Carolina
S. A. Courtis, University of Michigan
Sears Crowell, Indiana University
Harry G. Day, Indiana University
Earl L. Green, Ohio State University
Wm. W. Greulich, Stanford University
Leigh Hoadley, Harvard University
Warren H. Lewis, The Wistar Institute
Olin E. Nelsen, University of Pennsylvania
Willard C. Olson, University of Michigan
E. W. Shrigley, Indiana University Medical Center
E. W. Sinnott, Yale University
Philip R. White, Roscoe B. Jackson Memorial Laboratory
Anna Rachael Whiting, University of Pennsylvania

Growth, 1960, **24**, 203-208.

EFFECT OF HEMOGLOBIN ON TISSUE CELLS CULTIVATED *IN VITRO*[1]

DONALD M. PACE AND JOHN F. BOOKHARDT

Department of Physiology, University of Nebraska, Lincoln

(Received for publication May 9, 1960)

It is common experience among those working with nutrient media containing blood serum occasionally to find hemoglobin in the serum. Naturally, many have expressed concern over the effect this substance may have on cell growth. Baker (1929) found that low concentrations of hemoglobin (e.g., 11.9 mg. per cent) cause noticeable stimulation in growth of normal and malignant rat fibroblasts. Morigami and Enomoto (1936) also noted that hemoglobin in low concentrations stimulates growth of chick heart fibroblasts. More recently, Ehrmann and Gey (1953) observed that rat hemoglobin noticeably stimulates the growth of connective tissue cells. They exposed the cells to 200 mg. per cent hemoglobin over a period of 7 days.

Thus, there seems to be no doubt that hemoglobin in the concentrations used by these investigators stimulates growth and mitosis in fibroblast cells. As yet, no one has tested a wide range of concentrations on either fibroblasts or other cells to ascertain whether or not hemoglobin would have an effect in extremely low concentrations, or would become toxic in high concentrations. The intent of the present study is to ascertain the effects of hemoglobin on cell proliferation and on maximum cell population as well as on structural changes in fibroblasts and liver epithelial cells.

MATERIALS AND METHODS

Tissue culture procedures were employed as described by Pace and Aftonomos (1957). The cells were cultivated in 40 parts horse serum, 40 parts BSS and 20 parts embryo extract (1:1). Two cell types, or clones, obtained through the courtesy of Dr. Wilton R. Earle of the

[1] This investigation was supported by research grant #C-1654 (C2) from the National Cancer Institute, Public Health Service, and in part by funds received from the Cooper Foundation through the University of Nebraska Foundation.

National Cancer Institute, were used in this project—Strain L (NCTC Clone 929) and mouse liver cells (NCTC Clone 1469). Replicate cultures were prepared in D-3.5 Carrel flasks two days before replacing the medium with that containing hemoglobin. The medium was changed every second day in both control and experimental cultures, 1 ml. of fresh medium per flask. Concentrations of hemoglobin ranging from 25 mg. to 2,000 mg. per 100 ml. were used.

The hemoglobin was prepared from horse blood by a modification of the method of Marshall and Welker (Hawk, Oser, and Summerson, 1947). A 2 per cent stock solution was made up with the crystals obtained by this method and the various dilutions made from this solution.

Cell or nuclei counts were made periodically (usually every 2nd day) by selecting, randomly, 3 cultures for each condition. The Strain L cells were trypsinized in order to suspend for counting, but the liver cells were counted by the nuclei enumeration method of Sanford, Earle, *et al.* (1951).

Results

1. *Strain L Cells*

In the first group of tests, only three concentrations of hemoglobin were used—25, 50, and 125 mg. per cent. The cells in the two lower concentrations were carried for 7 days; those in the 125 mg. per cent for 15 days. The results are presented in Table I.

At the end of the 7-day period the cells in all concentrations appear normal and healthy and show no signs of any structural changes.

TABLE I

THE EFFECTS OF DIFFERENT CONCENTRATIONS OF HEMOGLOBIN ON GROWTH IN STRAIN L CELLS

Days after experiment started	Concentration of hemoglobin in mg. per cent			
	0 (control)	25	50	125
	Average for 9 cultures of cells in millions per ml.			
0	0.56	0.56	0.56	0.56
1	0.61	0.80	0.90	—
2	0.77	0.79	0.81	—
3	0.82	0.87	1.17	—
4	0.87	—	—	1.20
7	1.33	2.02	2.00	2.03
10	1.40	—	—	2.60
12	1.35	—	—	2.50
15	1.60	—	—	3.00

It is evident from these results that hemoglobin, at these concentrations, has a stimulating effect on cell proliferation. This is strongly evident after 7 days, at which time the number of cells in all the experimental cultures are approximately equal and show about 58% greater growth than the controls.

In a second series of tests, a wider range of concentrations were used—from 0.1 to 1.0 per cent. The cultures were observed and the cells counted periodically for 17 days. The results are presented in Table II.

TABLE II

THE EFFECTS OF SEVERAL CONCENTRATIONS OF HEMOGLOBIN ON GROWTH IN STRAIN L CELLS

Days after experiment started	Per cent concentration of hemoglobin						
	0 (control)	0.10	0.20	0.40	0.60	0.80	1.0
	Average for 6 cultures of cells in millions per ml.						
0	0.80	0.80	0.80	0.80	0.80	0.80	0.80
3	0.86	0.79	0.89	0.89	0.82	0.98	0.55
7	2.00	2.20	2.40	3.00	3.60	2.76	2.00
10	2.40	3.80	3.20	4.20	4.80	2.50	1.92
12	4.62	4.65	5.00	4.80	4.08	4.90	3.40
14	4.20	3.50	3.00	2.40	3.20	2.00	1.60
17	2.40	2.91	3.60	3.80	2.42	1.17	0.86

Concentrations of hemoglobin from 0.1% to 0.8%, inclusive, appear to stimulate proliferation, or at least they are not inhibitory to Strain L cells. This is true if maximum numbers are considered. Once the cultures have reached their maximum numbers, they usually begin to show necrosis because of crowding; thus it is not possible to draw any valid conclusions beyond the period the cultures have reached maximum cell numbers. As is well known in tissue culture work, a considerable number of the cells may detach after reaching maximum numbers and are discarded at the following medium change. Because of this, the remaining cells begin to proliferate rapidly again and may sometimes reach a higher maximum than the first.

A third series of experiments were carried out over a period of 18 days to ascertain the effects of still higher concentrations of hemoglobin on Strain L cells. The highest concentration used was 2 per cent. The initial cell number was almost twice that of the second series of experiments (Table II). The results are given in Table III. Most of the cells died rapidly once the maximum was reached. A

comparison of the results of Tables II and III indicates that 0.6 per cent hemoglobin is optimum for stimulating proliferation in Strain L cells, but just as in the case of the other cultures, these cells died rapidly once the maximum number (6.25 million per ml.) was reached.

TABLE III

THE EFFECTS OF RELATIVELY HIGH CONCENTRATIONS OF HEMOGLOBIN ON STRAIN L CELLS AS COMPARED TO THE EFFECTS OF LOW CONCENTRATIONS

Days after experiment started	Percent concentration of hemoglobin							
	0 (control)	0.10	0.20	0.40	0.60	0.80	1.0	2.0
	Average for 6 cultures of cells in millions per ml.							
0	1.52	1.52	1.52	1.52	1.52	1.52	1.52	1.52
3	1.62	1.63	2.01	1.64	1.78	1.47	1.40	1.08
5	1.62	3.54	2.00	2.46	1.94	1.89	1.07	1.01
8	1.96	3.27	3.40	2.40	2.85	2.08	1.65	0.69
10	1.97	3.28	3.52	2.40	3.04	1.78	1.26	1.08
12	2.95	4.74	3.40	2.30	5.67	3.60	3.03	0.48
15	2.65	5.55	6.00	5.00	6.25	3.85	3.45	dead
18	4.25	dead	dead	dead	dead	dead	dead	—
21	dead	—	—	—	—	—	—	—

No marked differences in cell morphology are noticeable in the cultures containing up to 0.2% hemoglobin, but the cells in all the higher concentrations become more granular and take on a pink to red color after the second to third day of exposure; nevertheless, the cells seem to grow well.

2. *Mouse Liver Cells:*

The liver cells were exposed to concentrations of hemoglobin similar to those used on Strain L cells—ranging from 0.1 to 2.0 per cent. The results are given in Table IV.

The effect of hemoglobin on liver cells is quite different from that on Strain L. Although proliferation of the liver cells in 0.1% hemoglobin approaches that in the control cultures, there is no stimulation in any of the concentrations used.

DISCUSSION

The amount of hemoglobin found in serum prepared for tissue cell cultivation may vary considerably and naturally has been of real concern to those working in this field. As mentioned previously, several investigators have noted that concentrations up to 200 mg. per

cent actually stimulate growth in fibroblast cells, and the present study confirms this.

The work presented here indicates that hemoglobin stimulates cell proliferation in Strain L fibroblasts and that the optimum concentration is approximately 0.6 per cent. At this concentration, there is

TABLE IV
THE EFFECTS OF VARIOUS CONCENTRATIONS OF HEMOGLOBIN ON MOUSE LIVER CELLS

Days after experiment started	Per cent concentration of hemoglobin							
	0 (control)	0.10	0.20	0.40	0.60	0.80	1.0	2.0
	Average for 9 cultures of cells in millions per ml.							
0	0.50	0.50	0.50	0.50	0.50	0.50	0.50	0.50
3	1.24	1.05	1.42	2.47	1.32	1.00	1.20	1.00
5	1.29	1.18	0.98	2.27	1.10	1.31	1.88	2.95
10	8.45	9.37	5.75	5.60	5.25	4.40	4.50	dead
12	9.50	8.00	6.37	5.25	6.37	3.65	3.20	—
14	5.25	6.27	6.40	6.30	6.80	dead	dead	—
16	dead	dead	dead	dead	dead	—	—	—

NOTE: Because of equipment difficulties, counts could not be made on the 8th day, as originally intended. However, media changes were made.

considerable coloration and granulation in the protoplasm of the cells, suggesting that at least part of the hemoglobin molecule is penetrating the cell membrane. Whether or not the cells are affected osmotically in a medium containing 0.6 per cent hemoglobin is still a question. If the cells are so affected, the stimulating effect of hemoglobin evidently overshadows any other. From the appearance of cells exposed to 2 per cent hemoglobin, it is probable that osmosis does play a role at this concentration. The cells lose volume and some appear to be crenated.

Contrary to the results obtained with connective tissue cells, hemoglobin, except in the lowest concentrations, appears to have very little action on liver epithelial cells, unless it be a slight inhibitory one.

To explain the mechanism of action by which hemoglobin may stimulate or depress cell proliferation demands further investigation. Perhaps hemoglobin may still perform at least part of its original function and supply a greater quantity of oxygen to the cells. However, it is unlikely that any hemoglobin remains, as such, in the medium; it may exist as heme or it is likely that iron itself is having the effect. It is well known that under normal circumstances, liver cells aid in the disintegration of hemoglobin and heme. Perhaps these

cells *in vitro* still continue this function of destroying the hemoglobin or heme before either of the compounds can enhance cell metabolism by providing additional oxygen. Also, since liver cells probably have sufficient iron already within their cytoplasm, any further addition should have very little if any effect. At least, these are thoughts that may soon be investigated.

In any case, hemolysis should be avoided when preparing serum for culture media since hemoglobin does have a stimulatory effect on some cells and an inhibitory effect on others over a wide range of concentrations.

Summary

1. The effects of various concentrations of hemoglobin on proliferation and structure of Strain L and mouse liver cells has been studied.

2. Hemoglobin, in concentrations up to 0.8%, stimulates, while a concentration of 1% hemoglobin and above, inhibits proliferation in Strain L cells.

3. Except for a slight stimulation in 0.1% hemoglobin, growth of mouse liver cells was inhibited progressively in concentrations above this.

4. The cells of Strain L and mouse liver strains, both have a pinkish to reddish appearance and become quite granular in concentrations of hemoglobin above 0.2%.

5. It is suggested that great care be taken to prepare hemoglobin-free serum for tissue culture media because hemoglobin affects tissue cells *in vitro*.

References

1. Baker, L. E. 1929. The chemical nature of the substances required for cell multiplication, action of glutathione, hemoglobin, and ash of liver on growth of fibroblasts. *J. Exper. Med.* **49**, 163-182.
2. Ehrman, R. L., & Gey, G. O. 1953. The use of cell colonies on glass for evaluating nutrition and growth in roller-tube cultures. *J. Natl. Cancer. Inst.*, **13**, 1099-1121.
3. Hawk, P. B., Oser, B. L., & Summerson, W. H. 1947. *Practical Physiological Chemistry*, 441 pp. Blakiston, Philadelphia, Pa.
4. Morigami, S., & Enomoto, T. 1936. Uber den Einfluss des Oxyhemoglobins und des Kohlenmonoxydhemoglobins auf das Wachstum der Fibroblastem *in vitro*. *Niss inizaku*, **25**, 679-686.
5. Pace, Donald M. & Aftonomos, Lefkos. 1957. Effects of cell density on cell growth in a clone of mouse liver cells. *J. Natl. Cancer Inst.*, **19**, 1065-1075.
6. Sanford, K. K., Earle, W. R., Evans, V. J., Waltz, H. K., & Shannon, J. E. 1951. The measurement of proliferation in tissue cultures by enumeration of cell nuclei. *J. Natl. Cancer Inst.*, **11**, 773-795.

Growth, 1960, **24**, 209-214.

STUDIES ON THE EARLY GROWTH OF LONG BONES IN MICE OF TWO STRAINS

NANCY GRAFF*

(Received for publication June 29, 1960)

Complete growth is an irreversible complex process which is closely associated with the availability of substrates and growth hormones (Thimann, 1945). Data on mammals, amphibians and fish reported by Robb (4) support the conclusion that the growth of the whole determines the relative size of its parts. Robb further suggests that restriction of growth in any body tissue is due to some inadequacy of its environment. In unicellular organisms such as bacteria, growth is explained in terms of availability of nutriment and also in terms of concentration of accumulated waste products (Henrici and Ordal, 2).

MATERIALS AND METHODS

Two strains of mice of the inbred colony at the Biological Station in Springville were used in this experiment. They were the Polydactylous (aabbss) (hereafter referred to as Poly), and the A (aabbcc) strains (3). They were taken from average litters of not more than six nor less than four and left with their parents until sacrificed or weaned. At 30 days they were weaned and sexed and remained isolated until killed at 40 or 50 days. At least five males and five females, all of which were virgins, were killed at each of the age periods, newborns-5-10-15-20-30-40-50 days. The animals were killed with ether, skinned immediately, and fixed in 95% ethyl alcohol. For the skeletal study the bones were cleared and stained according to the method of Williams (7) with no modifications. The shaft and the epiphysis of the long bones: radius, humerus, tibia, and femur, of both left and right sides of males and females were measured to within 0.1 mm using an ocular micrometer in a Bausch and Lomb dissecting microscope.

* This experiment has been performed at the Biological Station of Roswell Park Memorial Institute, Springville, N. Y. as part of the trainee program performed in collaboration with Griffith Institute and Central School, Springville, N. Y. Thanks are due to Mr. Leonard Roman, Mr. Harry L. Babbitt and Dr. Leonell C. Strong for advice and help during the time the work was in progress.

The animals were kept in wooden boxes with sawdust and cotton nesting material at 70 to 80 degrees F. temperature. The humidity was kept at about 50%. They were fed mouse blocks supplemented by mixed grain two times a week and bread and milk to which a small amount of cod liver oil had been added once a week. They received water *ad libitum*. The ingredients of mouse blocks are fine ground oat groats, beef scraps (50% protein), ground wheat, dried milk, sodium chloride, wheat germ meal, Brewers yeast, vitamin A and D, fish oil, dehydrated molasses, and calcium pantothenate. This diet is the same as used in the inbred colony for 40 years (5).

It is the purpose of this study to compare the growth of the long bones in mice of two strains from birth to 50 days of age. The data were analyzed by the statistical method of determining the means and standard deviations. Rate of growth was determined by comparing the slopes of the growth curves. Growth indices were obtained by dividing the mean values of 50 day old mice by the mean values of newborns for all long bones studied.

Results

The mean values of the measurements of the radii, humeri, tibiae and femurs, for the two strains, Poly and A, are given in the tables 1 through 4. The data show that there are two similar but slightly different growth patterns in bones of these two strains. The Poly strain shows a definitely longer bone length in the male at 50 days than the female with the exception of the femurs. In the A strain the difference is not as pronounced. The right side of the male is longer than the female and the left side of the female is longer than the male except the femur at 50 days.

In the A strain at 30 days the right tibia of the male is 13.78, the female 14.46; at 40 days the male is 15.16, the female 14.02; at 50 days the male is 16.18 and the female is 15.96 showing that there is no definite longer growth in one sex. First one bone is longer, then the next, conforming to no specific pattern at 50 days. In the Poly mice the male bones at 50 days are longer than the female bones except the femurs. This difference between A and Poly mice appears to confirm the fact that the A mouse is larger than the Poly mouse at maturity.

The right and left tibia of the male at 30 days in the Poly strain are 13.78 $\pm$ 1.4 and 14.04 $\pm$ 1.2 respectively, at 40 days they are

TABLE I

MEAN LENGTH OF THE LONG BONES FOR THE RIGHT SIDE MALE AND FEMALE STRONG A MICE AT BIRTH, 5, 10, 15, 20, 30, 40, 50 DAYS. ALL MEASUREMENTS IN MM.

Age	Radius	Humerus	Tibia	Femur
Right Side A ♀				
New Born	3.88 ± 0.4	4.10 ± 0.4	4.18 ± 0.4	3.80 ± 0.2
5 days	5.34 ± 0.6	5.82 ± 1.2	6.34 ± 1.0	5.42 ± 0.1
10 days	6.08 ± 0.6	6.68 ± 0.6	8.92 ± 1.4	6.74 ± 0.6
15 days	7.44 ± 0.8	7.70 ± 0.6	11.54 ± 1.4	8.02 ± 1.6
20 days	8.50 ± 0.8	9.00 ± 0.8	12.32 ± 1.0	8.90 ± 1.4
30 days	9.42 ± 0.2	9.62 ± 0.4	14.46 ± 0.4	10.32 ± 0.6
40 days	9.88 ± 1.2	10.14 ± 0.4	14.02 ± 2.0	10.60 ± 0.6
50 days	10.28 ± 0.4	10.56 ± 0.6	15.96 ± 1.8	12.14 ± 2.0
Right Side A ♂				
New Born	3.52 ± 0.4	3.80 ± 0.6	4.28 ± 0.8	3.68 ± 0.8
5 days	5.28 ± 0.4	5.96 ± 0.6	7.56 ± 0.6	5.54 ± 0.6
10 days	6.80 ± 0.4	7.10 ± 1.0	9.62 ± 0.8	7.54 ± 0.8
15 days	7.78 ± 1.0	7.44 ± 1.2	11.84 ± 1.0	8.04 ± 1.4
20 days	8.70 ± 1.0	8.92 ± 1.6	12.74 ± 1.0	9.76 ± 0.6
30 days	9.06 ± 1.4	9.00 ± 0.8	13.78 ± 1.4	10.32 ± 1.0
40 days	9.94 ± 1.0	10.46 ± 1.8	15.16 ± 2.0	10.86 ± 1.0
50 days	10.58 ± 0.8	10.78 ± 0.8	16.18 ± 1.2	11.94 ± 0.6

TABLE II

MEAN LENGTH OF THE LONG BONES FOR THE LEFT SIDE MALE AND FEMALE STRONG A MICE AT BIRTH, 5, 10, 15, 20, 30, 40, 50 DAYS. ALL MEASUREMENTS IN MM.

Age	Radius	Humerus	Tibia	Femur
Left Side A ♀				
New Born	3.60 ± 0.4	4.28 ± 0.8	4.40 ± 0.4	4.04 ± 0.6
5 days	5.40 ± 0.6	5.80 ± 0.8	7.56 ± 1.2	5.54 ± 1.2
10 days	6.22 ± 0.8	6.80 ± 0.6	8.74 ± 1.2	6.64 ± 0.8
15 days	7.98 ± 1.4	7.80 ± 0.8	11.68 ± 0.8	8.38 ± 1.2
20 days	8.96 ± 0.8	8.44 ± 1.4	12.38 ± 1.6	9.16 ± 0.6
30 days	9.48 ± 0.6	9.82 ± 0.4	14.40 ± 0.4	10.04 ± 0.4
40 days	9.88 ± 0.6	10.16 ± 0.6	14.48 ± 1.0	10.60 ± 0.6
50 days	10.26 ± 0.4	10.50 ± 0.6	16.20 ± 1.1	12.38 ± 0.8
Left Side A ♂				
New Born	3.82 ± 0.6	3.26 ± 0.6	4.26 ± 0.4	5.02 ± 0.5
5 days	5.52 ± 0.6	5.60 ± 0.8	7.50 ± 0.4	5.96 ± 1.2
10 days	6.54 ± 0.4	6.80 ± 0.6	9.32 ± 0.6	7.00 ± 0.8
15 days	7.94 ± 0.6	7.46 ± 0.6	11.82 ± 1.4	8.36 ± 0.6
20 days	8.54 ± 1.4	8.94 ± 1.0	12.76 ± 1.2	9.84 ± 0.8
30 days	8.96 ± 1.0	9.02 ± 0.6	14.04 ± 1.2	10.58 ± 1.8
40 days	9.70 ± 1.4	10.40 ± 1.0	15.48 ± 3.0	11.12 ± 1.4
50 days	10.18 ± 0.6	10.14 ± 0.4	15.72 ± 0.8	12.44 ± 0.6

TABLE III

MEAN LENGTH OF THE LONG BONES FOR THE RIGHT SIDE MALE AND FEMALE STRONG POLYDACTYLOUS MICE AT BIRTH, 5, 10, 15, 20, 30, 40, 50 DAYS. ALL MEASUREMENTS IN MM.

Age	Radius	Humerus	Tibia	Femur
	Right Side Poly ♀			
New Born	2.95 ± 1.2	4.07 ± 0.8	4.45 ± 2.2	3.80 ± 0.7
5 days	5.44 ± 1.6	5.74 ± 1.6	6.16 ± 1.0	5.50 ± 0.6
10 days	7.20 ± 0.6	7.22 ± 1.2	9.42 ± 1.6	6.66 ± 0.6
15 days	8.56 ± 1.6	7.64 ± 2.0	10.92 ± 2.4	7.52 ± 1.4
20 days	8.74 ± 1.2	8.92 ± 0.6	13.38 ± 0.4	9.08 ± 0.2
30 days	10.16 ± 0.4	10.38 ± 1.6	15.30 ± 0.6	11.24 ± 0.6
40 days	11.40 ± 1.2	11.00 ± 0.6	16.74 ± 0.6	11.60 ± 1.2
50 days	10.48 ± 0.4	11.03 ± 0.8	15.76 ± 0.8	12.92 ± 0.6
	Right Side Poly ♂			
New Born	3.24 ± 2.4	4.76 ± 0.2	3.88 ± 0.1	3.18 ± 0.6
5 days	4.92 ± 1.0	5.92 ± 1.4	6.64 ± 1.6	5.12 ± 1.0
10 days	7.24 ± 1.6	7.12 ± 1.4	10.12 ± 1.6	6.60 ± 0.6
15 days	8.18 ± 3.0	7.88 ± 0.4	11.68 ± 1.6	8.48 ± 2.0
20 days	8.46 ± 0.6	9.28 ± 0.8	13.62 ± 1.0	9.64 ± 5.8
30 days	9.94 ± 0.4	10.38 ± 0.6	15.42 ± 0.6	10.76 ± 1.2
40 days	10.86 ± 0.6	10.80 ± 0.6	16.38 ± 0.6	11.78 ± 2.0
50 days	10.58 ± 0.2	11.10 ± 1.0	16.06 ± 0.6	11.50 ± 0.6

TABLE IV

MEAN LENGTH OF THE LONG BONES FOR THE LEFT SIDE MALE AND FEMALE STRONG POLYDACTYLOUS MICE AT BIRTH, 5, 10, 15, 20, 30, 40, 50 DAYS. ALL MEASUREMENTS IN MM.

Age	Radius	Humerus	Tibia	Femur
	Left Side Poly ♀			
New Born	3.40 ± 0.8	4.42 ± 0.6	4.20 ± 1.6	4.00 ± 1.6
5 days	5.22 ± 1.2	5.90 ± 1.6	6.16 ± 1.2	5.50 ± 1.0
10 days	7.42 ± 1.8	7.16 ± 0.8	9.88 ± 1.2	6.56 ± 0.6
15 days	8.64 ± 4.6	8.04 ± 0.8	11.36 ± 1.8	8.28 ± 0.8
20 days	8.62 ± 0.2	9.02 ± 0.3	13.60 ± 0.4	9.20 ± 1.0
30 days	10.02 ± 0.6	10.46 ± 1.2	15.48 ± 0.4	11.22 ± 0.6
40 days	10.54 ± 0.8	11.30 ± 0.8	16.04 ± 0.8	12.46 ± 1.8
50 days	10.48 ± 0.4	10.48 ± 0.8	16.06 ± 0.8	13.82 ± 0.6
	Left Side Poly ♂			
New Born	3.24 ± 0.4	4.20 ± 0.4	4.06 ± 0.6	3.34 ± 0.4
5 days	4.48 ± 4.6	5.56 ± 0.6	6.57 ± 0.8	4.95 ± 0.8
10 days	7.40 ± 1.2	7.76 ± 0.6	9.94 ± 1.2	7.02 ± 0.8
15 days	7.98 ± 1.0	7.86 ± 0.8	11.02 ± 1.2	8.72 ± 3.0
20 days	8.40 ± 0.6	8.82 ± 0.8	13.52 ± 1.2	8.84 ± 1.6
30 days	9.90 ± 0.6	10.06 ± 0.6	15.06 ± 0.6	10.50 ± 0.6
40 days	10.52 ± 0.4	10.64 ± 1.0	16.02 ± 0.8	11.62 ± 0.6
50 days	10.56 ± 0.6	11.08 ± 0.6	16.06 ± 0.6	11.78 ± 0.6

15.16 ± 2.0 right and 15.48 ± 3.0 left, but at 50 days the right is 16.18 ± 1.2 and the left is 15.72 ± 0.8. This shows that different parts of the body grow at different rates and different times.

Discussion

In strain A the radii, humeri, and femurs of the right and left appendages in males and females have approximately the same growth rates. However, the right and left tibias in both male and female grow at a much more rapid rate than the radii, humeri, and femurs. This difference in growth rates of these two groups of bones shows that osteogenesis is occuring at different rates in different parts of the body. In the Poly strain of mice it was also found that growth rates were reducible to the same groups as strain A.

By comparing growth rates of the radius, femur, humerus and tibia in the two strains investigated (A and Poly), with data reported by Green (1) it was found that the newborn C_{57}BL mice are distinguishably smaller than A or Poly and this difference remains distinct until approximately ten days of age. The trend in the growth rate of right and left radii of the male and female, right and left humeri female, left humerus male, and right and left femurs male of the Poly strain are consistent with the trends of the ulna, humerus and radius of the C_{57}BL mice.

The growth indices (Table 5) show for the most part that the growth ratios are in the order of tibia, femur, radius, and humerus. This is the order of their size as in the adult mouse.

TABLE V

Growth Indices for the Long Bones in the Strong A and Strong Polydactylous Strains of Mice. The Average for Each Strain.

	Growth Indices			
	A Strain		*Poly Strain*	
	Female	Male	Female	Male
Rt. Tibia	3.82	3.78	3.54	4.14
Lt. Tibia	3.68	3.69	3.82	3.96
Rt. Femur	3.19	3.24	3.40	3.62
Lt. Femur	3.06	2.48	3.46	3.53
Rt. Radius	2.65	3.01	3.55	3.27
Lt. Radius	2.85	2.66	3.08	3.26
Rt. Humerus	2.58	2.84	2.71	2.33
Lt. Humerus	2.45	3.11	2.37	2.64
Average each strain	3.08		3.29	

Summary

Measurements of the total lengths of the radii, humeri, tibiae and femurs in the Poly and A strains were made at newborn-5-10-15-20-30-40-50 days. Growth is not at the same rate for all bones and is not constant for any one bone. The results obtained show that there are at least three or four trends in the growth rates of the bones measured. Data also showed that there were slight insignificant differences in the length of bones in the right as compared to the left of both sexes. However, the sex differences are apparent only in some cases.

In combining the male and female growth indices 3.08 times newborn size was found in the A strain and 3.29 times newborn size in the Poly strain (Table 5).

References

1. Green, C. V., & Fekete, E. 1933. Differential growth in the mouse. *J. Exp. Zool.*, **66**, 351-370.
2. Henrici, A. T., & Ordal, E. J. 1948. The Biology of Bacteria. Boston: D. C. Heath and Co. Pp. 169-171.
3. Lyon, M. Inbred Strains of Mice #1, pp. 68, 70. Companion issue to *Mouse News Letter # 21*, July, 1959.
4. Robb, R. C. 1929. On the nature of hereditary size limitation. II. The growth of parts in relation to the whole. *Brit. J. Exptl. Biol.*, **6**, 311-324.
5. Strong, L. C., & Fuller, C. A. 1958. Maternal age at time of first litters in mice. *J. Geron.*, **13**, 236-240.
6. Thimann, K. V. 1945. Plant hormones, growth and respiration. *Biol. Bull.*, **96**, 296-306.
7. Williams, T. W. 1941. Staining bone and cartilage in toto. *Stain Technology*, **16**, 23.

Growth, 1960, **24**, 215-264.

CHANGES IN FORM OF THE HEAD AND FACE DURING CHILDHOOD*

HOWARD V. MEREDITH

State University of Iowa

(Received for publication June 6, 1960)

This paper pertains to eleven indices of somatic form.[1] Its data are index values at annual ages between 5 years and 11 years derived from longitudinal study of 60 white girls. The purpose, expressed in tripartition, is to investigate:

1. Individual and group trends for selected faciocephalic indices over a six-year period of human ontogeny.
2. Intra-individual similarities and dissimilarities at three ages (5 years, 8 years, and 11 years) with respect to the entire series of continua studied.
3. Variability of each index at seven childhood ages, and variability of change in each index during the sexennium beginning 5 years after birth.

Investigation of problems relating to the form of animal organisms is one of the major facets of somatology (27). Crude metric approaches to the description of human form antedate the nineteenth century (24). Although substantial advances have been made subsequently (29), research pertaining specifically to ontogenic change in form of the human head and face has progressed at a fairly slow pace (1, 2, 3, 4, 5, 25, 31).

The writer, in conjunction with several collaborators, has participated many times in studies on aspects of the body form of North American children. Findings previously published have dealt with form of the trunk (7, 10, 16, 17), form of the extremities (13, 20, 21, 28), relative components of stature (9, 18, 26), and one measure of facial form (19). The findings of the present paper extend knowl-

* Supported in part by a research grant, D-217, from the National Institute for Dental Research, of the National Institutes of Health, Public Health Service.

[1] Different writers make synonymous use of the terms somatic form, morphologic shape, structural configuration, anatomic build, physical constitution, physique, somatotype, and body proportions.

edge on the form of the head and face, especially knowledge of individual variation in form change during middle and late childhood.

Subjects

The subjects were 60 American-born white girls drawn from 52 families residing in or near Iowa City, Iowa. All were voluntary participants in a long-term research program begun in 1946 at the State University of Iowa. The sample included no children from multiple births.

For 78 per cent of the subjects, all four grandparents were of northwest European ancestry, and for 97 per cent of the subjects, two or more grandparents were of northwest European ancestry. Vocationally, 65 per cent of the fathers held professional or major managerial positions; 30 per cent owned small businesses, followed skilled trades or engaged in commercial occupations; and 5 per cent were semiskilled or unskilled employees.

Every subject was examined annually from age 5 years to age 11 years. With few omissions, a semiannual examination schedule was maintained extending between ages 4.5 years and 11.5 years. The examination dates were routinely on or near each girl's birthday and mid-birthday anniversaries.

Materials and Methods

Computation of the eleven indices investigated required measurement values for eight different dimensions of the head and face. Four of these dimensions (head depth, head width, face width, and nose width) were obtained directly on the child, and four (lower jaw width, face height, nose height, and face depth) were secured from facial roentgenograms.[2]

Identified with greater anatomic precision, the eight basic dimensions are glabella-occipital depth of the head, biparietal width of the head, bizygomatic width of the face, bialar width of the nose, bigonial width of the lower jaw, nasion-menton height of the face (dental arches in occlusion), nasion-TANS height of the nose (distance from nasion to the tip of the anterior nasal spine), and TANS-APOC depth of the face (distance from TANS to the middle of a line connecting the anteriormost points of the occipital condyles). Meticulous

[2] As utilized throughout this paper, "width" implies a transverse distance, "depth" an anteroposterior distance, and "height" a vertical distance.

care was taken to obtain valid data for each measurement. Chance error was reduced through rigorous controls in subject positioning, landmark location, and measurement procedure (see references 6, 11, 12, 14, 15, 22). Anatomic relevance of the roentgenographic measures was enhanced by correction for the systematic error accompanying radiography (22).

The series of *semiannual* measurements for a given dimension on a particular child were subjected to three-point smoothing. This procedure was followed for each of the eight dimensions on all of the 60 girls.[3] From here forward, only the smoothed values for each dimension at annual ages from 5 years to 11 years were utilized. These values, specific for age and subject, were used in computing the following indices:

1. Head Width × 100/Head Depth
2. Face Width × 100/Head Width
3. Face Depth × 100/Head Depth
4. Face Depth × 100/Face Width
5. Face Depth × 100/Face Height
6. Face Height × 100/Face Width
7. Lower Jaw Width × 100/Face Width
8. Nose Height × 100/Face Height
9. Nose Height × 100/Face Depth
10. Nose Height × 100/Face Width
11. Nose Width × 100/Face Width

It should be recognized that those diameters obtained by direct measurement have integumental termini and those derived through radiography have osseous termini. References 12, 14, and 23 provide some aid to those interested in approximating the amounts by which the magnitude of indices 3, 4, 6, 7, and 10 would be systematically changed on adjusting head width, head depth and face width to osseous diameters.

Tersely, the data subjected to analysis were values for eleven indices of somatic form secured on the same 60 girls at yearly intervals during a sexennium of childhood.

The bulk of the presentation of findings will deal with the indices

[3] Smoothing sets of measures ordered in time reduces random errors and short-term oscillations, thereby facilitating the exhibition of trends. As stated earlier, description and intercomparison of trends (i.e., depicting, contrasting and colligating the overall movements of indices with age) were central interests in the present study.

singly. For each index, the same quinquepartile schema will be used: trend for total sample, subgroup contrasts, trends for individuals, individual contrasts, and variability at selected ages. A concluding section will consider the indices as a colligated series, depicting the status and change of selected individuals in each of the eleven variables.

1. Head Width × 100/Head Depth

Trend for total sample. Values for biparietal diameter × 100/glabella-occipital diameter ("cephalic index") were obtained at age 5 years and at consecutive annual intervals to age 11 years. The second column of Table 1 lists arithmetic means for the seven series

TABLE 1

Central Tendency and Variability Statistics for Biparietal Diameter × 100/Glabella-Occipital Diameter. The Subjects Are 60 North American White Girls Examined at Yearly Intervals.

Age	Mean	S.D.	Minimum	Percentiles: 10	30	70	90	Maximum
(years)								
			Distribution of index at selected ages					
5	78.2	3.2	71.2	74.4	76.3	79.7	82.8	84.5
6	78.2	3.2						
7	78.1	3.2						
8	78.0	3.1	70.7	74.2	76.0	79.3	82.4	83.9
9	77.8	3.1						
10	77.7	3.1						
11	77.6	3.1	70.4	73.9	75.8	78.9	82.3	84.0
			Distribution of change-in-index between ages 5 and 11 years					
5–11	−0.6	0.8	−2.0	−1.6	−1.0	−0.2	0.5	1.1

of values, and the upper-left section of Figure 1 presents a curve drawn to these means. Finding: The group trend for the total sample of 60 girls descends from 78.2 per cent at age 5 years to 77.6 per cent at age 11 years. Generalization: On the average, North American girls of northwest European descent have heads that are slightly more elongated in late childhood than in middle childhood.

Subgroup contrasts. Two subgroups were formed, each based on a combination of direction and magnitude of change in the cephalic index during the sexennium under study. Subgroup A includes six subjects whose indices *increased* 0.5 or more; and subgroup B, 11 subjects whose indices *decreased* 1.5 or more. The middle-left and lower-left sections of Figure 1 depict the composite trends obtained.

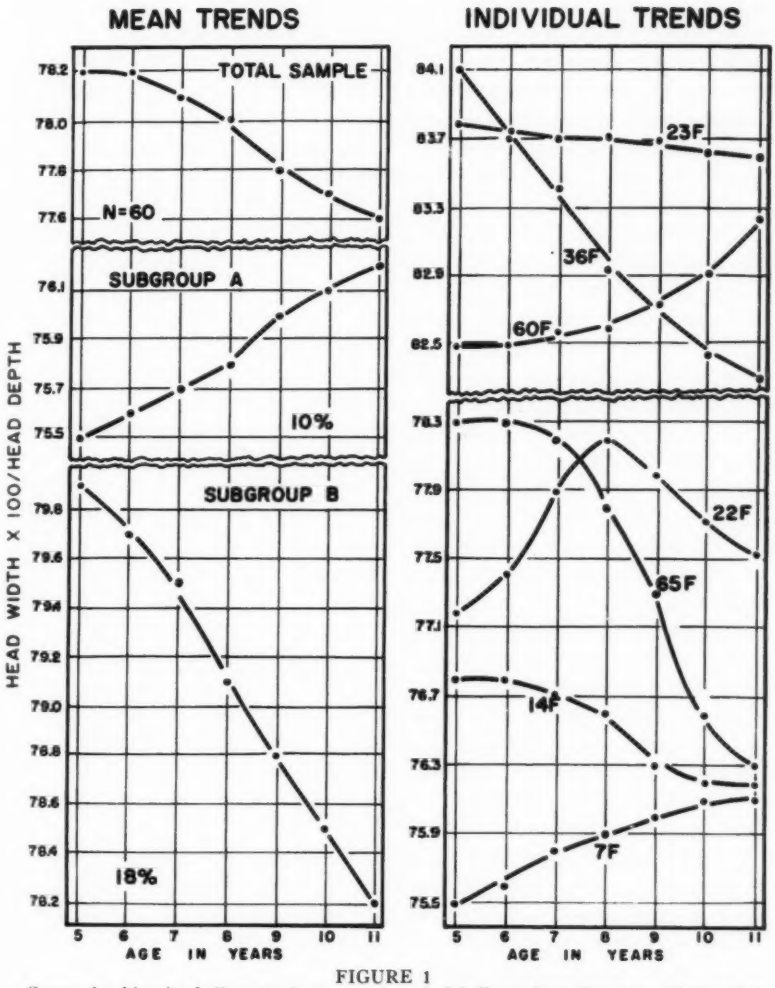

FIGURE 1

Curves for biparietal diameter in percentage of glabella-occiput diameter. Notice that the ordinate scale units in the left and right panels are not identical.

Finding: For the childhood period between ages 5 years and 11 years, subgroups of girls show divergent age trends in head shape, i.e., some girls become more brachycephalic with age and others become more dolichocephalic. Generalization: In regard to the cephalic index of North American white girls during middle and late childhood, despite a descending curve of means for the population, approximately one girl in ten has an index curve that ascends slightly.

Trends for individuals. A curve was drawn to the age and index data for each subject. From examination of the 60 individual curves for trend, it is found:

1. Forty-three per cent are falling trends for which, with similar frequency, the decline is concave to the chronologic base line, rectilinear, and convex to the base line. The curves for subjects 23F and 36F* in the upper-right section of Figure 1 illustrate the range of variation in amount of fall.

2. Eighteen per cent are falling trends concave to the chronologic base line during the first half of the age period studied, and convex to the base line after age 9 years. Curves 14F and 65F in the lower-right section of Figure 1 are examples. The aggregate for *descending* trends is 61 per cent (43 per cent plus 18 per cent).

3. Twelve per cent are *ascending* trends. In different subjects the ascent is convex to the chronologic base line, rectilinear, and concave to the base line. Figure 1 depicts one positively accelerated rising curve (60F) and one negatively accelerated rising curve (7F).

4. Twenty per cent are curves directed toward brachycephaly between ages 5 years and 8 years, and toward dolichocephaly between ages 8 years and 11 years. In other words, for one girl in five the cephalic index trend is *concave* to the chronologic base line; the curve for subject 22F in the lower-right section of Figure 1 is a representative illustration.

5. Seven per cent are trends *convex* to the chronologic base line. These curves register slight elongation of head form from age 5 years to ages 7 or 8 years, followed by gradual cancellation of this change in the interval between ages 8 years and 11 years.

Individual contrasts. Selected contrasts are portrayed in the upper-

* These are the identifications given at the time of enrollment in the program. The 60 females (F's) utilized in this investigation have numbers between 1 and 75. Missing numbers are those assigned to children withdrawing from the program before age 11 years.

right and lower-right sections of Figure 1. The cephalic indices for subjects 23F and 36 F are almost identical at age 6 years; at age 11 years, the indices for these subjects differ to the extent indicated by standard scores of +2.0 and +1.5, respectively. Compared with the head form of subject 36F, subject 60F's head is more elongated at age 5 years and less elongated at age 11 years. Subjects 22F and 65F, proceeding by different routes than 36F and 60F, show similar reversal of status. At 5 years of age, subjects 7F, 14F and 65F have percentile ranks of 20, 35, and 58, respectively; convergence occurs, so that by 11 years of age all three subjects have percentile ranks between 37 and 43.* The greatest index decline over the sexennium studied is that manifested by subject 65F; the curve for subject 60F depicts the second highest index rise.

Variability at selected ages. Columns 3 to 9 of Table 1 present statistics pertaining to the variability of the cephalic index among North American girls of northwest European ancestry. Selected findings are:

1. At each age during the childhood period from 5 years to 11 years, the estimated population standard deviation for the index approximates 3.1.

2. The obtained indices at age 8 years are distributed as follows: 10 per cent between 71.2 and 74.4, 20 per cent between 74.4 and 76.3, 40 per cent between 76.3 and 79.7, 20 per cent between 79.7 and 82.8, and 10 per cent between 82.8 and 84.5.

3. For the sexennium studied, the distribution of change-in-index has an obtained range of 3.1 (from −2.0 to +1.1) and an estimated population standard deviation of 0.8. The mean of the distribution differs significantly from zero at a high level of confidence ($t = 6.1$).

2. Face Width × 100/Head Width

Trend for total sample. Arithmetic means for bizygomatic diameter × 100/biparietal diameter at seven childhood ages are presented in the second column of Table 2. A Cartesian plot, using these means as ordinate values and ages as abscissa values, is reproduced in the upper-left section of Figure 2. Finding: The group trend for the total sample

* In contrasting individual trends, alternative use is made of standard scores and percentile ranks. This alternation will facilitate meaningful reading on the part of those more adept at interpreting comparisons presented in terms of one or the other of these transformations.

60 girls is an increasing, almost rectilinear, function of age. In relation to the obtained mean of 80.2 at age 5 years, the obtained mean at age 11 years is higher by 4.9. Generalization: Typically, the face width (bizygomatic diameter) of North American girls of northwest European ancestry approximates 80 per cent of head width at 5 years of age, and 85 per cent of head width at 11 years of age.

TABLE 2

CENTRAL TENDENCY AND VARIABILITY STATISTICS FOR BIZYGOMATIC DIAMETER × 100/ BIPARIETAL DIAMETER. THE SUBJECTS ARE 60 NORTH AMERICAN WHITE GIRLS EXAMINED AT YEARLY INTERVALS.

				Percentiles:				
Age	Mean	S.D.	Minimum	10	30	70	90	Maximum
(years)								
			Distribution of index at selected ages					
5	80.2	2.3	75.2	77.2	78.7	81.3	83.4	86.1
6	81.0	2.3						
7	81.8	2.2						
8	82.7	2.2	78.3	79.8	81.5	83.7	86.2	89.1
9	83.6	2.3						
10	84.4	2.3						
11	85.1	2.4	80.7	81.6	83.8	86.3	88.4	91.3
			Distribution of change-in-index between ages 5 and 11 years					
5–11	4.9	1.1	2.1	3.5	4.4	5.4	6.5	8.5

Subgroup contrasts. Over the six-year span from age 5 years to age 11 years, the index increases 6.5 or more in 10 per cent of the subjects, and 3.5 or less in another 10 per cent of the subjects. Central tendency statistics on both of these subgroups are graphed in the middle-left and lower-left sections of Figure 2. Finding: The trend of means for six girls showing "small" increases in bizygomatic diameter × 100/ biparietal diameter rises 3.2; that for six girls showing "large" increases in this index rises 7.2. Generalization: Within the population identified as North American white girls, subpopulations representing the two tails of an increment distribution for face width in percentage of head width differ throughout middle and late childhood with respect to the slope of mean curves for the index.

Trends for individuals. Graphs constructed from the successive age and index values for each subject are, without exception, *ascending* curves. This finding is interpretable in the form: between ages 5 years and 11 years, every subject increases more in face width than

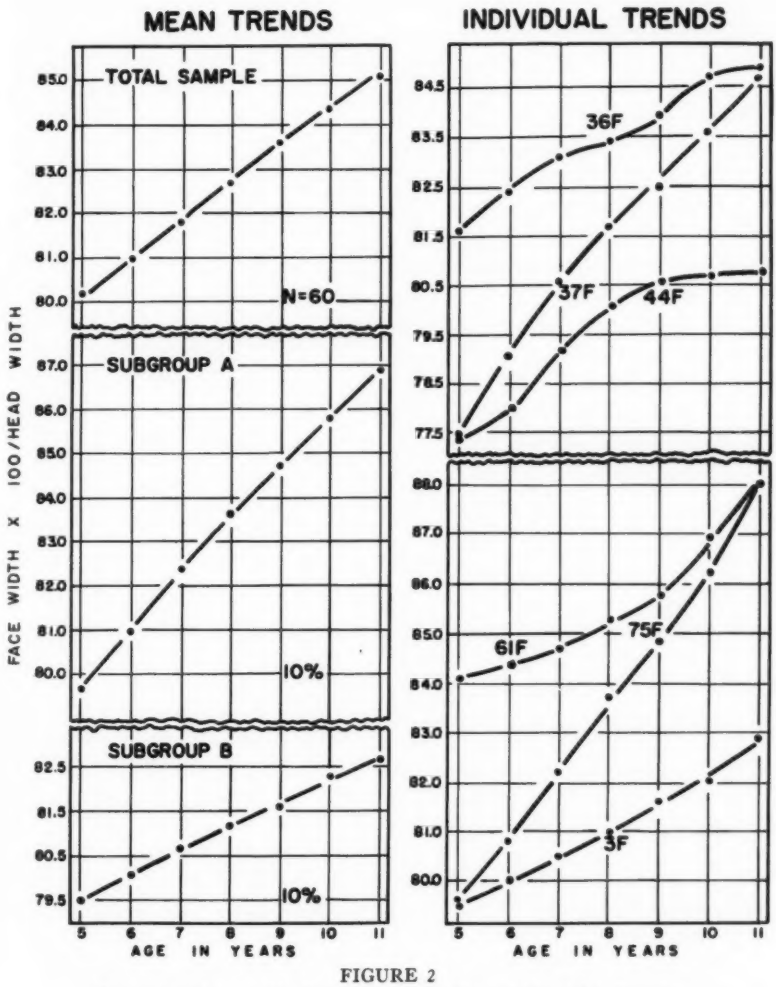

FIGURE 2
Curves for bizygomatic diameter in percentage of biparietal diameter.

in head width. More discriminate inspection of the 60 curves yields the following findings:

1. Twenty-five per cent are rising trends *concave* to the chronologic base line. The curve for subject 37F in the upper-right section of Figure 2 is a typical example.

2. Twelve per cent are rising *rectilinear* trends.

3. Twenty-seven per cent are rising trends *convex* to the chronologic base line. The range of variation among these positively accelerated increasing functions of age is illustrated in the lower-right section of Figure 2 by the curves for subjects 3F and 61F.

4. Twenty-three per cent are rising trends convex to the chronologic base line between age 5 years and ages 7 or 8 years, and concave to the base line thereafter. The curve for subject 44F in the upper-right section of Figure 2 depicts one member of this series.

5. Thirteen per cent are rising trends *concave-convex* to the base line from age 5 years to ages 10 or 11 years. These curves are negatively accelerated increasing functions of age during the period from 5 years to 7 or 8 years, and positively accelerated increasing functions of age from 7 or 8 years to 10 or 11 years. One of the more complex curves of this series (36F) is reproduced in the upper-right section of Figure 2.

Individual contrasts. Several contrasts among individual girls are displayed in the right-hand sections of Figure 2. For two pairs of curves, the ratios of face width to head width are similar at the beginning of the sexennium and show *divergence* with advance in age. Subjects 37F and 44F each have a standard score of —1.2 at age 5 years; at age 11 years, their standard scores are —0.2 and —1.8, respectively. Subjects 3F and 75F have percentile ranks of 38 and 40 at 5 years of age; at 11 years of age, their percentile ranks are 18 and 87. Two pairs of curves illustrate marked index dissimilarity at the beginning of the sexennium and *convergence* to practically identical indices at its termination. The percentile ranks for subjects 36F and 37F at age 5 years are 71 and 13, respectively; corresponding ranks for these subjects at age 11 years are 53 and 49. Comparably, at age 5 years subjects 61F and 75F have standard scores of +1.7 and —0.3; at age 11 years the standard scores of both subjects are +1.2. The girl whose index increases the most between ages 5 and

11 years climbs in percentile rank from 40 to 86; the girl manifesting the minimum index increase falls in percentile rank from 33 to 3.

Variability at selected ages. Statistics pertaining to the variability of bizygomatic diameter × 100/biparietal diameter are exhibited in columns 3 to 9 of Table 2. It will be seen:

1. At each age during middle and late childhood, the estimated standard deviation of the index for North American girls of northwest European lineage approximates 2.3.

2. Almost the same index value is obtained for percentiles 70 at age 5 years, 30 at age 8 years, and 10 at age 11 years. A confirmatory expression of the direction of movement and overlapping of index distributions for successive ages is found in the numerical similarity of the maximum and percentiles 90 and 70 at ages 5 years, 8 years and 11 years, respectively.

3. For the sexennium between age 5 years and age 11 years, the distribution of change in face width expressed as a percentage of head width has an estimated population standard deviation of 1.1, an obtained range of 6.4 (8.5 minus 2.1), and an obtained distance between percentiles 10 and 90 of 3.0 (6.5 minus 3.5).

3. Face Depth × 100/Head Depth

Trend for total sample. Columns 1 and 2 of Table 3 list seven childhood ages and associated means for TANS-APOC diameter × 100/glabella-occipital diameter. Utilizing these paired values as successive coordinates in a Cartesian graph, the result shown in the upper-left section of Figure 3 is obtained. Finding: The composite trend for the entire sample of 60 girls is an increasing function of age with slight negative acceleration. In relation to the obtained mean at age 8 years(face depth 47.3 per cent of head depth), the mean at age 5 years is lower by 1.2 and the mean at age 11 years is higher by 1.0. Generalization: On the average, the anteroposterior face diameter of North American white girls increases continuously during middle and late childhood with respect to anteroposterior head diameter.

Subgroup contrasts. The index increment for the period from age 5 years to age 11 years is 3.0 or more for 10 per cent of the girls in the sample (Subgroup A). For another 10 per cent, it is 1.5 or less (Subgroup B). Curves drawn to means for each of these subgroups

are presented in the middle-left and lower-left sections of Figure 3. Finding: The curve for subgroup A ascends 3.4 (from 46.8 at age 5 years to 50.2 at age 11 years) in a path weakly concave to the chronologic base line; the curve for subgroup B ascends 1.1 (44.7 to 45.8) in a path weakly concave to the base line prior to age 8 years and weakly convex to the base line after this age. Generalization: Within the population specified as North American girls of northwest European ancestry, subpopulations selected to represent terminal segments of a sexennial increment distribution for face depth in percentage of head depth have composite index curves of dissimilar slope for all comparable childhood ages from 5 years to 11 years.

TABLE 3

CENTRAL TENDENCY AND VARIABILITY STATISTICS FOR TANS-APOC FACE DEPTH × 100/GLABELLA-OCCIPITAL HEAD DEPTH. THE SUBJECTS ARE 60 NORTH AMERICAN WHITE GIRLS EXAMINED AT YEARLY INTERVALS.

Age	Mean	S.D.	Minimum	Percentiles: 10	30	70	90	Maximum
(years)			*Distribution of index at selected ages*					
5	46.1	1.8	42.3	43.8	45.1	47.1	48.4	49.5
6	46.5	1.8						
7	47.0	1.9						
8	47.3	1.9	42.9	44.9	46.1	48.4	49.7	50.7
9	47.6	1.9						
10	47.9	2.0						
11	48.3	2.0	43.6	45.7	47.2	49.4	51.0	51.9
			Distribution of change-in-index between ages 5 and 11 years					
5–11	2.2	0.6	0.5	1.4	1.9	2.5	3.0	3.8

Trends for individuals. A separate curve for each subject was drawn to her sequential paired values for age and TANS-APOC face depth × 100/glabella ad maximum head depth. By inspection and intercomparison of these 60 curves, it is found:

1. Forty per cent are rising trends concave to the chronologic base line. Variation in the concavity and rise of these curves is revealed on comparing 57F in the upper-right section of Figure 3 and 8F in the lower-right section of Figure 3.

2. Twelve per cent are rising rectilinear trends. The curve for subject 64F in the lower-right section of Figure 3 is an example.

3. Twenty per cent are trends convex to the chronologic base line. All of these trends ascend during the interval between ages 8 years

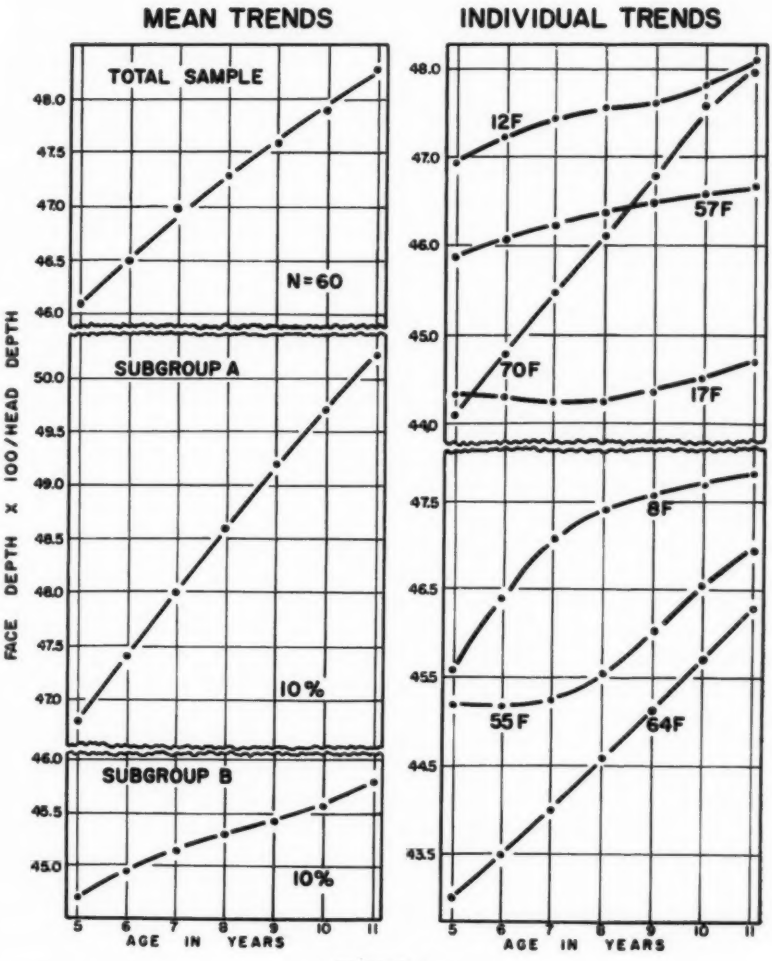

FIGURE 3

Curves for distance between the tip of the anterior nasal spine and the midpoint of a line connecting the anteriormost points on the occipital condyles in percentage of glabella-occiput diameter.

and 11 years; some ascend from age 5 years, some from ages 6 years or 7 years (e.g., subject 55F in the lower-right section of Figure 3), and one from age 8 years (subject 17F in the upper-right section of Figure 3).

4. Twenty-eight per cent are rising trends concave to the chronologic base line in the early part of the sexennium studied and convex to the base line in the later part. The curve for subject 12F in the upper-right section of Figure 3 is illustrative.

Individual contrasts. It will suffice to discuss two of the contrasts depicted in the right half of Figure 3, leaving the reader opportunity to observe others. Subjects 17F and 70F represent minimum and maximum change in the ratio of face depth to head depth between ages 5 years and 11 years; compared by means of percentile ranks at the beginning and end of the sexennium, 17F falls from 17 to 3 and 70F rises from 13 to 45. Subjects 57F and 70F are alike with respect to face depth in percentage of head depth at age 8.5 years; at age 5 years the standard score of 70F is 1.0 lower than that of 57F, whereas at age 11 years the standard score of 70F is 0.6 higher than that of 57F.

Variability at selected ages. Statistics describing the dispersion of TANS-APOC face depth $\times$ 100/glabella ad maximum head depth are assembled in columns 3 to 9 of Table 3. Selected findings are:

1. In the population identified as North American girls of northwest European descent, estimated standard deviations for the index are 1.8 at age 5 years and 2.0 at age 11 years. From application of a statistical test appropriate for comparing variances based on related measures (30), the hypothesis that the difference is due solely to chance may be rejected at a high level of confidence ($t = 2.9$, df 58). This finding, supported by the intermediate values listed in column 3 of Table 3, makes it reasonable to generalize that during middle and late childhood variability of the index increases slightly with age.

2. The obtained indices at age 5 years are spread between 42.3 and 49.5. Face depth equals or exceeds one-half of head depth in 7 per cent of the subjects at age 8 years, and 25 per cent of the subjects at age 11 years.

3. For the sexennium between age 5 years and age 11 years, the distribution of change in face depth expressed as a percentage of head depth has an estimated population standard deviation of 0.6, an

obtained range of 3.3 (3.8 minus 0.5), and an obtained distance between percentiles 10 and 90 of 1.6 (3.0 minus 1.4).

4. Face Depth × 100/Face Width

Trend for total sample. Arithmetic means for TANS-APOC diameter × 100/bizygomatic diameter at seven childhood ages are displayed in the second column of Table 4. A curve drawn to these values is shown in the upper-left section of Figure 4. Although the obtained curve will be seen to fall slightly with time, this cannot be interpreted as substantial support for the hypothesis of a descending index trend in the population. Application of an appropriate statistical test to the mean difference for the period from age 5 years to age 11 years yields a non-significant result ($t = 1.8$). Finding: Means for the total sample of 60 girls show TANS-APOC face depth to approximate 73.4 per cent of bizygomatic face width at all ages during middle and later childhood. Generalization: In North American girls of northwest European descent, the average ratio of dimensions representing the width and depth of the upper face remains practically constant during the childhood sexennium between ages 5 years and 11 years. These results make it necessary to modify the widespread view that throughout childhood the face increases "back-to-front . . . more than it does . . . side-to-side" (8, see also, 4, 5).

Subgroup contrasts. Two subgroups were constituted, each defined by a combination of direction and magnitude of change in the index during the age interval under study. Subjects whose indices *decreased* 2.0 or more were placed in subgroup A; those whose indices *increased* 1.5 or more in subgroup B. The middle-left and lower-left sections of Figure 4 portray the mean trends for A and B, respectively. Finding: Over the ontogenic span from age 5 years to age 11 years, TANS-APOC face depth × 100/bizygomatic face width shows an average decline of 2.5 in 13 per cent of the sample and an average rise of 2.2 in 7 per cent of the sample. Generalization: During middle and late childhood, the upper face of North American white girls becomes substantially deeper relative to its width in some children, and substantially wider relative to its depth in other children.

Trends for individuals. Employing the age and index values for each subject, 60 graphs were prepared. Classification of these curves for individual girls reveals:

1. Twenty-eight per cent are *descending* trends convex, rectilinear, or slightly concave to the chronologic base line. The curve for subject 43F in the upper-right section of Figure 4 is one of the convex descending trends.

2. Seventeen per cent are *ascending* trends concave, rectilinear, or convex to the chronologic base line. The curves for subjects 32F and 72F in the upper-right section of Figure 4 illustrate the concave and rectilinear varieties of this class.

TABLE 4

CENTRAL TENDENCY AND VARIABILITY STATISTICS FOR TANS-APOC FACE DEPTH × 100/ BIZYGOMATIC FACE WIDTH. THE SUBJECTS ARE 60 NORTH AMERICAN WHITE GIRLS EXAMINED AT YEARLY INTERVALS.

Age	Mean	S.D.	Minimum	Percentiles: 10	30	70	90	Maximum
(years)			*Distribution of index at selected ages*					
5	73.5	3.7	66.3	68.7	71.5	75.6	78.7	81.1
6	73.6	3.7						
7	73.5	3.7						
8	73.4	3.6	67.3	68.4	71.1	75.5	78.4	80.4
9	73.2	3.6						
10	73.2	3.7						
11	73.2	3.7	66.0	68.4	71.1	75.3	78.6	80.4
			Distribution of change-in-index between ages 5 and 11 years					
5–11	−0.3	1.3	−3.3	−2.2	−1.0	0.4	1.2	3.1

3. Twenty-five per cent are trends *concave* to the chronologic base line. The curve for subject 23F in the lower-right section of Figure 4 is an example.

4. Eighteen per cent are trends *convex* to the base line. The curve for subject 41F in the lower-right section of Figure 4 typifies this class. Some individuals show an index decline to age 9 years, and others an index rise from age 7 years.

5. Ten per cent are trends concave to the base line during the first half of the period studied, and convex to the base line thereafter. An example is the curve for subject 15F in Figure 4.

6. The remaining 2 per cent is represented by one trend (that for subject 55F in Figure 4) which runs parallel with the chronologic base line.

Individual contrasts. A selected assortment of developmental contrasts is depicted in the upper-right and lower-right sections of Figure

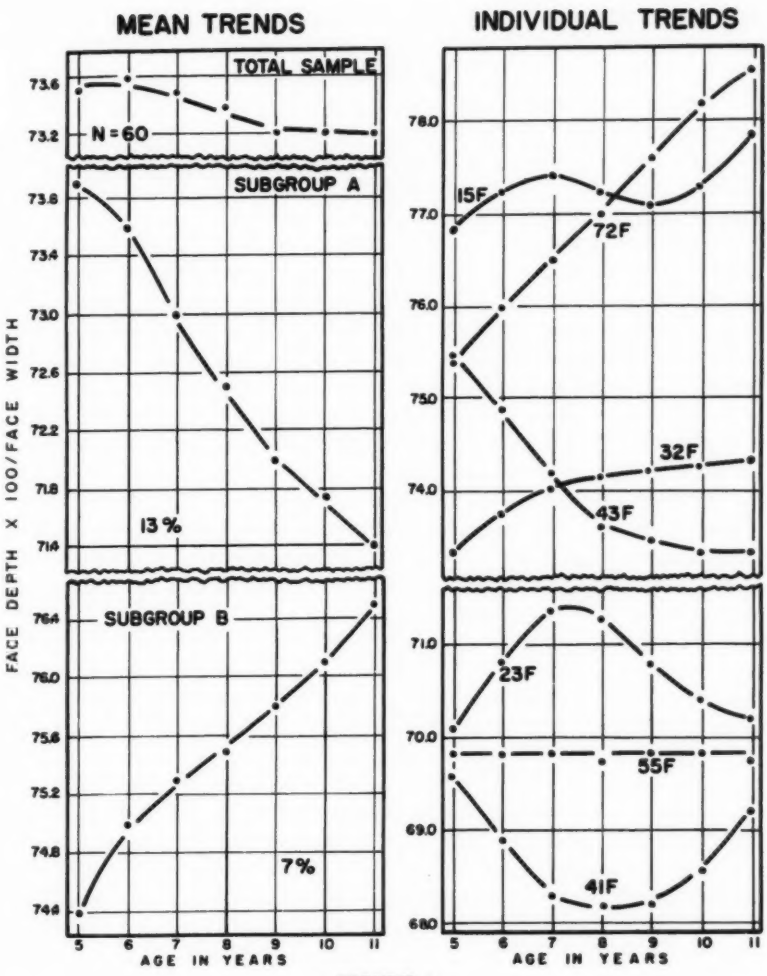

FIGURE 4

Curves for distance between the tip of the anterior nasal spine and the midpoint of a line connecting the anteriormost points on the occipital condyles in percentage of bizygomatic diameter.

4. Attention is called to the divergence of curves 43F and 72F, the early divergence and later convergence of curves 23F and 41F, and the crossing of curves 32F and 43F. Standard scores for subjects 43F and 72F at age 5 years are +0.5 in each instance; at age 11 years, comparable scores are 0 and +1.5, respectively. At ages 5 years, 8 years, and 11 years, the percentile ranks on subject 23F are 18, 37 and 25, respectively; corresponding ranks on subject 41F are lower by 3, 29 and 8, respectively.

Variability at selected ages. Columns 3 to 9 of Table 4 carry statistics which characterize the dispersion of TANS-APOC face depth × 100/bizygomatic face width. Selected findings are as follows:

1. The estimated standard deviation of the index for North American girls of northwest European descent approximates 3.7 at each age during middle and late childhood.

2. There is almost complete overlapping of the obtained index distributions for different ages. Inspection of columns 5 to 8 in Table 4 indicates that about 40 per cent of the frequencies at any given age lie between 71.3 and 75.5, and about 80 per cent between 68.5 and 78.5. Assuming the index were normally distributed, with a mean of 73.4 and a standard deviation of 3.7, 40 per cent of the population would have indices dispersed from 71.5 to 75.3, and 80 per cent indices scattered from 68.7 to 78.1.

3. The distribution of change in index during the interval between age 5 years and age 11 years has an estimated population standard deviation of 1.3, an obtained range of 6.4, and an obtained distance from percentile 30 to percentile 70 of 1.4.

5. Face Depth × 100/Face Height

Trend for total sample. Columns 1 and 2 of Table 5 present seven childhood ages and associated means for TANS-APOC diameter × 100/nasion-menton diameter. A graph constructed by use of these paired values as consecutive coordinates is shown in the upper-left section of Figure 4. Finding: The mean index curve for the entire sample of 60 girls declines 1.9 from age 5 years to age 7 years, 1.1 from age 7 years to age 9 years, and 0.9 from age 9 years to age 11 years. With respect to the mean difference of 3.9 between ages 5 years and 11 years, rejection of the null hypothesis is tenable statistically at a high confidence level ($t = 13.5$). Generalization: During

middle and late childhood, the mean trend of North American white girls for face depth in percentage of face height is a negatively accelerated decreasing function of age. Obviously, acceptance of the results obtained for this index requires qualification of the position that throughout childhood the face increases "back-to-front . . . more than it does . . . up-and-down" (8).

Subgroup contrasts. The middle-left and lower-left sections of Figure 5 each display a subgroup mean trend extending from age 5 years to age 11 years. Subgroup A includes those girls whose indices decreased 7.0 or more; subgroup B, those girls whose indices showed no change, decreased slightly (not more than 1.0), or increased slightly (less than 2.0). Finding: The means for subgroups A and B are almost alike at age 5 years and become increasingly different with age. Those for subgroup B cluster about 88.5 and yield a trend mildly convex to the chronologic base line. Those for subgroup A decline 4.8 during the triennium following age 5 years, and 3.3 during the succeeding triennium. Generalization: Between middle and late childhood, in the population identified as North American girls of northwest European ancestry, the ratio of upper face depth to total face height remains practically constant in a few children and declines appreciably in others.

Trends for individuals. A curve was drawn to the age and index data for each subject. By inspection and intercomparison of these 60 curves, it is found:

1. Forty-five per cent are falling trends convex to the chronologic base line. The variation in convexity among this series is illustrated in Figure 5 by the curves for subjects 50F and 62F.

2. Thirteen per cent are falling rectilinear trends, or falling trends slightly concave to the chronologic base line. The curve for subject 1F in Figure 5 is an example of the latter.

3. Twenty-two per cent are trends convex to the chronologic base line during the early part of the period studied, and concave to the base line during the later part of the period. Ten of this series descend with age, e.g., subject 45F's curve in Figure 5. The remainder register no overall descent (see the curve for subject 64F in Figure 5); subject 33F's curve, also reproduced in Figure 5, is included here.

4. Thirteen per cent are convex trends similar to that for subject 72F in Figure 5. In comparison with 72F, some of the curves in this

class show greater fall from age 5 years to age 8 years, and less rise from age 8 years to age 11 years.

5. Seven per cent are falling trends concave to the chronologic base line in the early portion of the sexennium studied, and convex to the base line in the later portion. An example is the curve for subject 8F in Figure 5.

TABLE 5

CENTRAL TENDENCY AND VARIABILITY STATISTICS FOR TANS-APOC FACE DEPTH × 100/NASION-MENTON FACE HEIGHT. THE SUBJECTS ARE 60 NORTH AMERICAN WHITE GIRLS EXAMINED AT YEARLY INTERVALS.

Age	Mean	S.D.	Minimum	Percentiles: 10	30	70	90	Maximum
(years)			*Distribution of index at selected ages*					
5	88.9	4.1	78.6	84.0	86.2	91.4	94.2	98.3
6	87.9	4.2						
7	87.0	4.3						
8	86.4	4.5	77.6	80.4	83.9	88.9	92.7	95.9
9	85.9	4.6						
10	85.4	4.7						
11	85.0	4.8	75.7	77.9	82.6	87.9	91.7	93.8
			Distribution of change-in-index between ages 5 and 11 years					
5–11	–3.9	2.3	–9.1	–7.0	–4.8	–2.9	–1.2	1.2

Individual contrasts. A varied group of inter-individual comparisons are assembled in the right-hand sections of Figure 5. Attention is directed to the index similarities of subjects 1F and 62F at age 5 years, 45F and 50F at age 6.5 years, 62F and 72F at age 9 years, and 8F and 50F at age 10.5 years. For each pair of these subjects, observe the index dissimilarities at younger or older ages. Percentile ranks are 72 at age 5 years and 95 at age 11 years for subject 72F, and 97 at both ages for subject 1F. Subject 64F has standard scores of +1.2 at age 5 years, and +1.8 at age 11 years; standard scores for subject 50F at these ages are +1.1 and —0.1, respectively. The index remains practically constant at 84.5 in subject 33F, and changes from 93.5 to 84.5 in subject 50F.

Variability at selected ages. Statistics pertaining to the variability of TANS-APOC face depth × 100/nasion-menton face height are presented in columns 3 to 9 of Table 5. It will be seen:

1. During the segment of ontogeny investigated, standard deviation estimates for the population identified as North American white

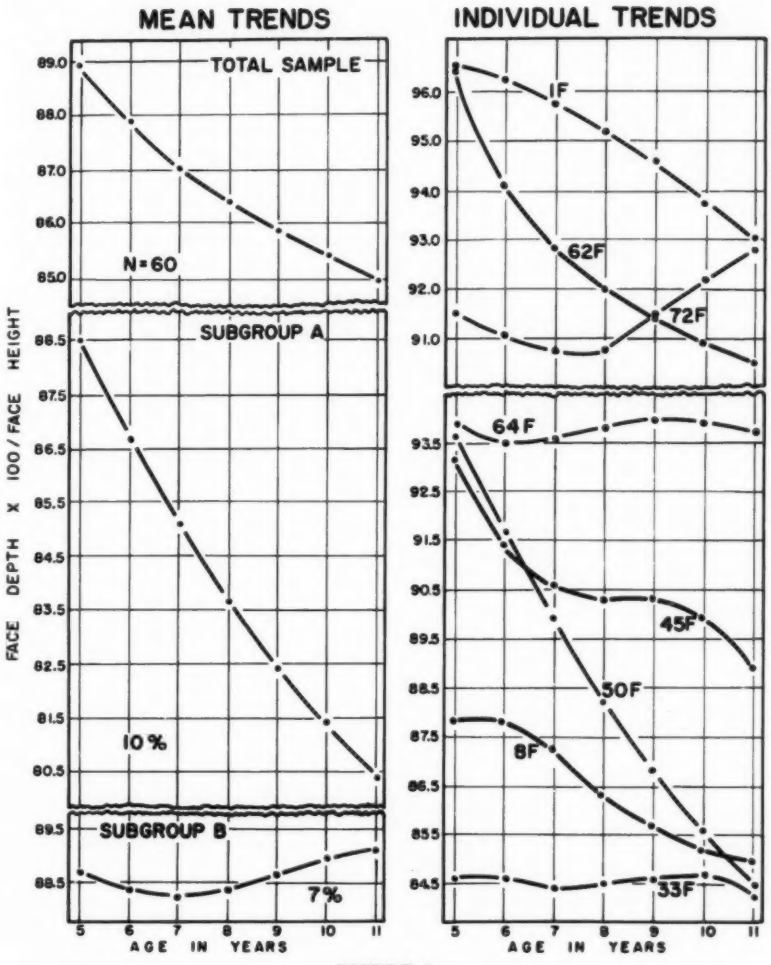

FIGURE 5

Curves for distance between the tip of the anterior nasal spine and the midpoint of a line connecting the anteriormost points on the occipital condyles in percentage of nasion-menton diameter (dental arches occluded).

girls climb from 4.1 to 4.8. The inference of increasing variability with age is tenable statistically. Using a test for comparison of two variances based on related measures (30), the hypothesis that no systematic change occurs can be rejected at a high level of confidence ($t = 2.6$, df 58).

2. The direction of movement and amount of superimposition of index distributions for successive ages is indicated by the equivalence of the tenth percentile at age 5 years and the thirtieth percentile at age 8 years, also by the similarity of the seventieth and ninetieth percentiles at ages 5 years and 11 years, respectively.

3. Values obtained by subtracting the index on each subject at age 5 years from her index at age 11 years are spread as follows: 10 per cent between —9.1 and —7.0, 20 per cent between —7.0 and —4.8, 40 per cent between —4.8 and —2.9, 20 per cent between —2.9 and —1.2, and 10 per cent between —1.2 and +1.2.

6. Face Height × 100/Face Width

Trend for total sample. Arithmetic means for nasion-menton diameter × 100/bizygomatic diameter at seven childhood ages are listed in the second column of Table 6. A curve obtained by using the means as ordinate values and the corresponding ages as abscissa values is shown in the upper-left section of Figure 6. Finding: The central tendency trend for the total sample of 60 girls is an increasing

TABLE 6

Central Tendency and Variability Statistics for Nasion-Menton Diameter × 100/Bizygomatic Diameter. The Subjects Are 60 North American White Girls Examined at Yearly Intervals.

Age	Mean	S.D.	Minimum	Percentiles: 10	30	70	90	Maximum
(years)			*Distribution of index at selected ages*					
5	82.2	4.8	66.0	75.9	80.1	84.9	87.4	90.1
6	83.3	4.8						
7	84.1	4.8						
8	84.5	4.8	70.3	78.2	82.1	87.2	89.9	91.8
9	84.9	4.8						
10	85.4	4.9						
11	85.8	5.0	73.3	78.9	83.6	88.7	91.6	95.3
			Distribution of change-in-index between ages 5 and 11 years					
5–11	3.6	2.1	−1.4	0.8	2.6	4.4	6.6	8.6

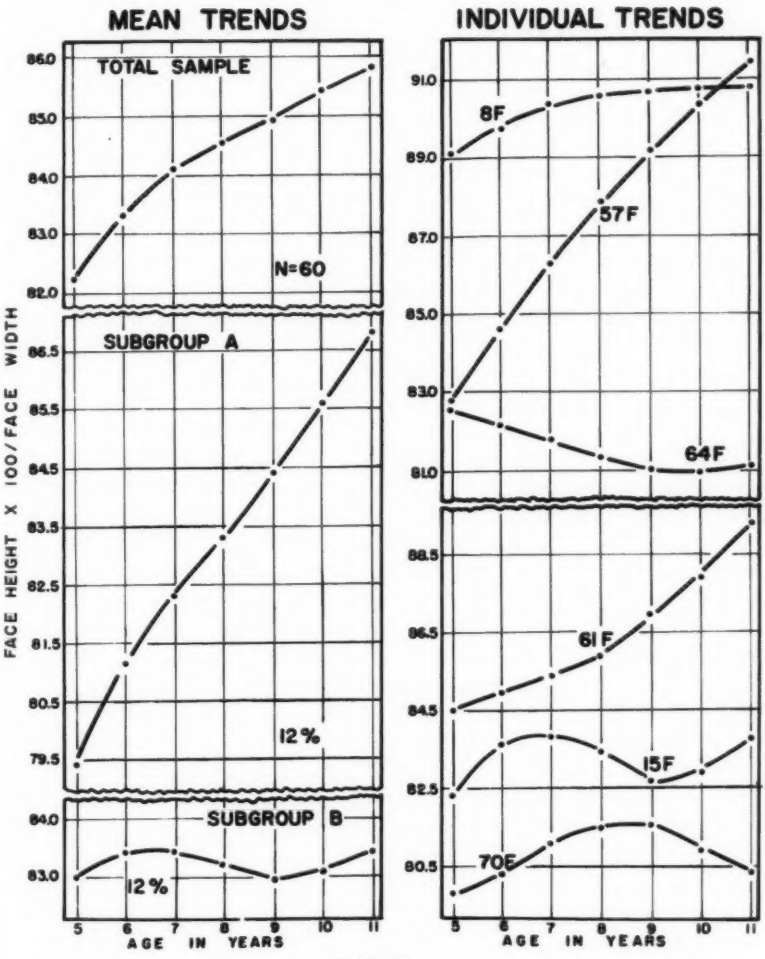

FIGURE 6

Curves for nasion-menton diameter (dental arches occluded) in percentage of bizygomatic diameter. Observe that different ordinate scale units are used in the left and right panels.

function of age, with the amount of increase in the biennium from age 5 years to age 7 years equaling that in the quadrennium from age 7 years to age 11 years. Generalization: During middle and late childhood, in the average North American girl of northwest European descent, nasion-menton face height becomes greater relative to bizygomatic face width.

Subgroup contrasts. Twelve per cent of the girls in the sample have indices that are higher at age 11 years than at age 5 years by 6.5 or more (Subgroup A). For another 12 per cent, index variations during the same ontogenic sexennium are between ± 1.5 (Subgroup B). Curves drawn to index means for each of these subgroups at annual ages are presented in the middle-left and lower-left sections of Figure 6. Finding: The means for subgroup B fluctuate between 83.0 and 83.4, those for subgroup A ascend from 79.4 to 86.8. Generalization: Compared with the population mean trend for face height in percentage of face width on North American white girls, mean trends for defined subdivisions of the population differ markedly, particularly during the period between ages 7 years and 11 years. By reference to the left half of Figure 6, notice that the mean index at age 11 years is 1.7 above that at age 7 years in the total sample, 4.5 above that at age 7 years in subgroup A, and the same as that at age 7 years in subgroup B.

Trends for individuals. A separate curve for each subject was drawn to her paired seriate values for age and nasion-menton diameter $\times$ 100/bizygomatic diameter. Classification of these 60 graphs for individuals shows:

1. Fifty-three per cent are rising trends concave to the chronologic base line. Variations in rise and concavity among these curves is illustrated in Figure 6 by subjects 8F and 57F.

2. Fifteen per cent are rising rectilinear trends, or rising trends convex to the chronologic base line. For an example of the latter, see the curve of subject 61F in Figure 6.

3. Twenty per cent are trends concave to the base line from age 5 years to ages 8 or 9 years, and then convex to the base line. In relation to the curve for subject 15F in Figure 6, most of the curves in this group show a smaller drop from age 7 years to age 9 years, and a greater rise from age 9 years to age 11 years.

4. Twelve per cent are trends concave to the base line, parallel

with the base line, or convex to the base line. Figure 6 depicts two of the curves included in this series; the curve for subject 70F is concave, that for subject 64F descends more than any other among the 60 studied.

Concisely, 80 per cent of the subjects have single-cycle trends (classes 1, 2, 4) and 20 per cent more complex trends (class 3). Sixty-eight per cent of the former ascend continuously (classes 1, 2) and all of the latter exhibit a course concave-convex to the base line.

Individual contrasts. Selected contrasts are portrayed in the upper-right and lower-right sections of Figure 6. The indices for subjects 57F and 64F at age 5 years transform to standard scores of +0.1; at age 11 years, the indices for these subjects differ to the extent indicated by standard scores of +1.1 and —0.9, respectively. This amount of divergence is not exceeded in any other pairing among the 60 curves. The curves for subjects 8F and 57F illustrate marked convergence. From percentile ranks of 95 and 55 at age 5 years, they move to tied ranks near 85 between ages 10 years and 11 years.

Variability at selected ages. Columns 3 to 9 of Table 6 present statistics to describe the dispersion of nasion-menton diameter × 100/ bizygomatic diameter. Selected findings are as follows:

1. At each age during middle childhood, the estimated parameter for the standard deviation of the index in North American girls of northwest European lineage approximates 4.8.

2. Individual differences at age 5 years spread from a child with face height two-thirds of face width to a child with face height nine-tenths of face width. The positional relation of the index distributions with age is indicated by the approximate equivalence of percentiles 90 and 70 at ages 5 and 8 years, respectively.

3. The distribution of change in index during the interval between age 5 years and age 11 years has an estimated population standard deviation of 2.1, an obtained range of 10.0, and an obtained distance from the tenth percentile to the ninetieth percentile of 5.8.

7. Lower Jaw Width × 100/Face Width

Trend for total sample. Columns 1 and 2 of Table 7 carry series of childhood ages and corresponding means for bigonial diameter × 100/bizygomatic diameter. Employing these paired values as consecutive coordinates in a Cartesian graph, the result portrayed in the

upper-left section of Figure 7 is obtained. Finding: The mean index trend for the entire sample of 60 girls is a negatively accelerated increasing function of age. In differential terms, the declining rate of change in facial form is shown by mean increments for successive bienniums of 1.2, 0.5, and 0.3, respectively. Generalization: For North American white girls, the mean ratio of lower face width to upper face width increases at a falling rate throughout middle and late childhood.

TABLE 7

CENTRAL TENDENCY AND VARIABILITY STATISTICS FOR BIGONIAL DIAMETER × 100/BIZYGOMATIC DIAMETER. THE SUBJECTS ARE 60 NORTH AMERICAN WHITE GIRLS EXAMINED AT YEARLY INTERVALS.

				Percentiles:				
Age	Mean	S.D.	Minimum	10	30	70	90	Maximum
(years)								
			Distribution of index at selected ages					
5	68.0	2.8	61.2	64.3	66.9	69.2	71.4	72.9
6	68.7	2.9						
7	69.2	2.9						
8	69.6	3.0	63.0	65.0	68.3	70.9	73.8	74.9
9	69.7	2.9						
10	69.9	2.9						
11	70.0	2.9	63.1	65.8	68.9	71.4	73.8	75.7
			Distribution of change-in-index between ages 5 and 11 years					
5–11	2.0	1.0	−0.3	0.7	1.4	2.7	3.4	4.2

Subgroup contrasts. The middle-left and lower-left sections of Figure 7 display mean trends for two subgroups. Subgroup A includes girls whose indices increase 3.5 or more between age 5 years and age 11 years; subgroup B, girls whose indices differ no more than 1.0 at any two ages within the sexennium. Finding: The means for subgroups A and B are similar at age 5 years and differ progressivly with age. Those for subgroup B are 70.3 at ages 6 years, 7 years and 11 years, varying slightly below or above this value at the other ages. Those for subgroup A give a curve that ascends from 69.7 to 73.6 in a path concave to the chronologic base line. Generalization: With explicit reference to the age period from 5 years to 11 years, and to the population identified as North American girls of northwest European ancestry, lower face width relative to upper face width remains almost constant in some children and broadens as much as 5 per cent in others, e.g., 5 per cent of 70.0 = 3.5.

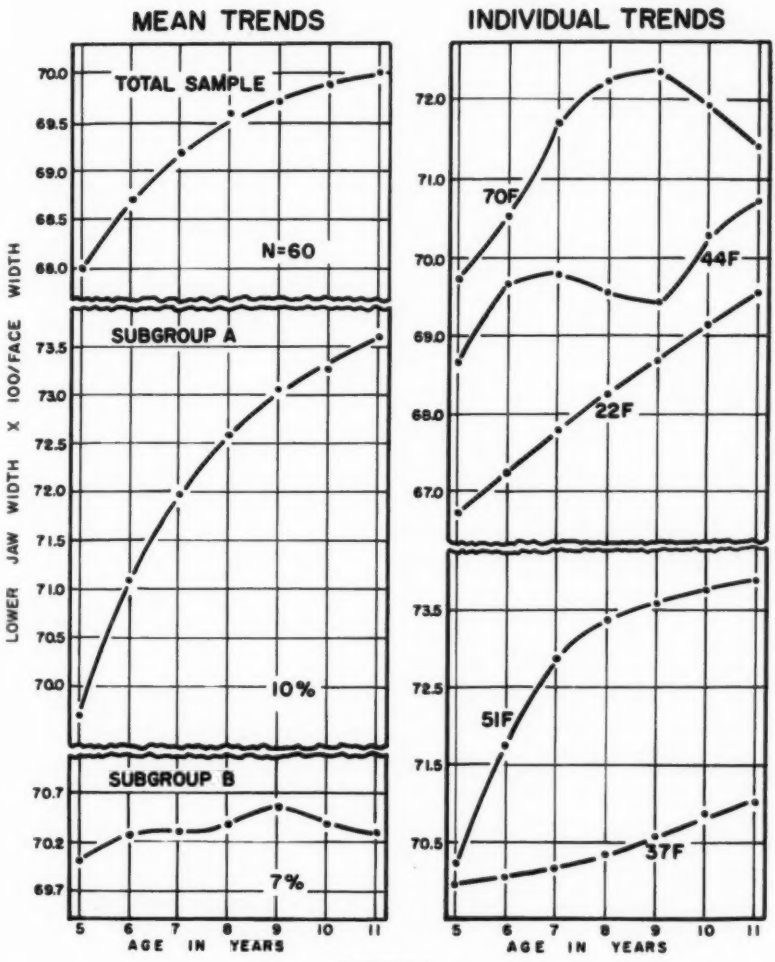

FIGURE 7
Curves for bigonial diameter in percentage of bizygomatic diameter.

Trends for individuals. Curves were drawn to each of the 60 sets of paired values for age and bigonial diameter × 100/bizygomatic diameter. By inspection and intercomparison of these curves, it is found:

1. Fifty per cent are ascending trends concave to the chronologic base line. Variation among these curves is from the strong concavity depicted in the lower-right section of Figure 7 for subject 51F to almost the rectilinearity shown in the upper-right section of Figure 7 for subject 22F.

2. Fifteen per cent are rising rectilinear trends, or rising trends convex to the chronologic base line. The curves for subjects 22F and 37F in Figure 7 illustrate each variety. Differences in slope within the rectilinear variety vary from that portrayed by subject 22F to that portrayed over the period between ages 5 years and 8 years by subject 37F. It follows that 65 per cent of the subjects (50 per cent plus 15 per cent) have continuously ascending trends.

3. Twenty per cent are trends concave to the base line from age 5 years to ages 8 years or 9 years, and convex to the base line thereafter. An example is the curve for subject 44F in Figure 7.

4. Fifteen per cent are concave trends similar to that shown in Figure 7 for subject 70F. Most of the curves in this series are more mildly concave than the one reproduced.

Individual contrasts. The right-hand sections of Figure 7 depict an assortment of dissimilarities in the course of development of bigonial diameter × 100/bizygomatic diameter. Subject 37F has standard scores of +0.7 at age 5 years, +0.2 at age 8 years, and +0.3 at age 11 years. The standard scores of subject 51F at these ages are higher by 0.1, 1.0 and 1.0, respectively. Clearly, there is divergence during the first half of the sexennium and parallelism during the second half. A different series of ontogenic relations is obtained from comparison of the curves for subjects 44F and 70F. Percentile ranks for subject 70F are 72 at age 5 years, 82 at age 8 years, and 70 at age 11 years. Corresponding ranks for subject 44F are lower by 10, 32 and 10, respectively. The reader is left to employ Figure 7 in observing other contrasts of change in facial form.

Variability at selected ages. Statistics pertaining to the dispersion of lower face width in percentage of upper face width are presented in columns 3 to 9 of Table 7. It will be seen:

1. The estimated standard deviation of the index for the population identified as North American girls of northwest European descent is approximately 2.9 at each age throughout middle and late childhood.

2. Comparison of the two girls at the extremes of the index distribution for age 8 years shows that bigonial diameter is 63 per cent of bizygomatic diameter in one instance and 75 per cent of bizygomatic diameter in the other.

3. Values obtained by subtracting the index on each subject at age 5 years from her index at age 11 years are spread as follows: 10 per cent between —0.3 and 0.7, 20 per cent between 0.7 and 1.4, 40 per cent between 1.4 and 2.7, 20 per cent between 2.7 and 3.4, and 10 per cent between 3.4 and 4.2.

8. Nose Height × 100/Face Height

Trend for total sample. Arithmetic means for nasion-TANS diameter × 100/nasion-menton diameter at seven successive childhood ages are listed in the second column of Table 8, and a curve drawn to these values is presented in the upper-left section of Figure 8. Finding: The composite index trend for the entire sample of 60 girls ascends with age at a declining rate. In relation to the obtained mean at age 8 years (nose height 44.4 per cent of face height), the mean at age 5 years is lower by 1.3 and the mean at age 11 years is higher by 0.7. Generalization: During middle and late childhood, osseous nose height in the average North American white girl increases more rapidly than overall height of the osseous face (cf. 19).

Subgroup contrasts. Twelve per cent of the girls in the sample have indices that are higher at age 11 years than at age 5 years by 3.0 or more (Subgroup A). Over the same ontogenic sexennium, 18 per cent of the girls show index variation between the limits of ±1.0 (Subgroup B). Curves representing each of these subgroups are portrayed in the middle-left and lower-left sections of Figure 8. Finding: The curve for subgroup A ascends in a path that is almost rectilinear, whereas the curve for subgroup B is concave to the chronologic base line. Generalization: The population identified as North American girls of northwest European lineage yields subsamples, drawn as the two tails of a distribution for change in facial form during childhood, having mean trends for nose height in percentage of face height that differ in slope over the period from age 5 years to age 8 years,

and diverge in direction over the period from age 8 years to age 11 years.

Trends for individuals. Separate graphs were plotted from each subject's paired seriate values for age and nasion-TANS diameter × 100/nasion-menton diameter. Examination of the resulting curves shows:

1. Forty-eight per cent are rising trends concave to the chronologic base line. The variation in ascent among these curves is illustrated in the right-hand panel of Figure 8 by subjects 3F and 60F.

TABLE 8

CENTRAL TENDENCY AND VARIABILITY STATISTICS FOR NASION-TANS DIAMETER × 100/NASION-MENTON DIAMETER. THE SUBJECTS ARE 60 NORTH AMERICAN WHITE GIRLS EXAMINED AT YEARLY INTERVALS.

Age	Mean	S.D.	Minimum	Percentiles: 10	30	70	90	Maximum
(years)			*Distribution of index at selected ages*					
5	43.1	1.5	39.7	41.1	42.4	43.9	45.1	46.5
6	43.6	1.5						
7	44.1	1.6						
8	44.4	1.6	40.7	42.1	43.5	45.3	46.3	47.7
9	44.7	1.7						
10	44.9	1.7						
11	45.1	1.8	41.2	42.8	44.1	45.9	47.5	49.5
			Distribution of change-in-index between ages 5 and 11 years					
5–11	2.0	1.1	–0.2	0.6	1.5	2.5	3.2	5.7

2. Twelve per cent are rising rectilinear trends. Curves 4F and 57F in the lower-right section of Figure 8 depict differences in slope within this series.

3. Fifteen per cent are trends convex to the chronologic base line. With one exception, these curves ascend with age. The upper-right section of Figure 8 presents the exception (28F), and the curve registering the greatest rise (18F).

4. Twelve per cent are trends concave to the chronologic base line. An example is the curve for subject 75F in the upper-right section of Figure 8.

5. Thirteen per cent are rising convex-concave trends or rising concave-convex trends. The curves for subjects 21F and 52F in the the lower-right section of Figure 8 depict each variety.

Classified somewhat differently, 73 per cent of the subjects have

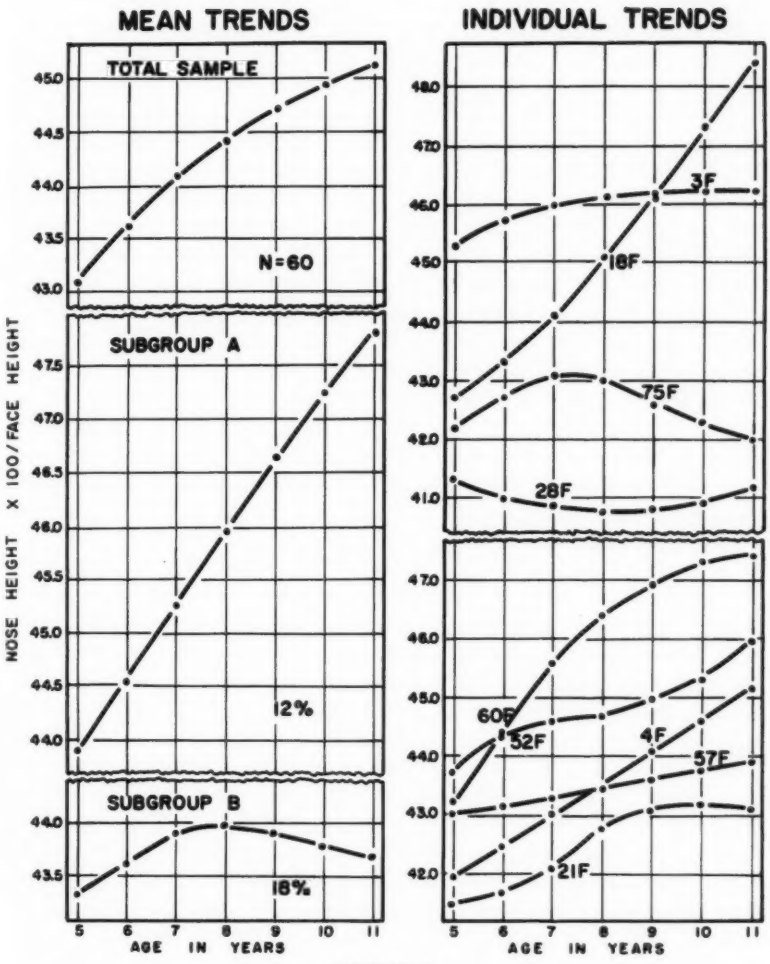

FIGURE 8

Curves for distance from nasion to the tip of the anterior nasal spine in percentage of nasion-menton diameter.

single-cycle, continuously ascending trends; 14 per cent single-cycle trends that do not ascend continuously (12 per cent concave and 2 per cent convex to the base line); and 13 per cent more complex ascending trends.

Individual contrasts. A selected assortment of developmental comparisons is portrayed in the right-hand portion of Figure 8. Notice the early convergence and later divergence of curves 4F and 57F, the early divergence and later convergence of curves 28F and 75F, the crossing of curves 52F and 6OF at age 6 years, and the crossing of curves 3F and 18F at age 9 years. For subject 18F, nose height is approximately 43 per cent of face height at age 5 years and 48 per cent of face height at age 11 years. In contrast, the ratio of nose height to face height is no greater at age 11 years than at age 5 years for subject 28F. The percentile ranks of subjects 18F and 28F at age 5 years are 32 and 12, respectively. By age 11 years, the percentile rank of the latter has fallen to 2 and that of the former has risen to 95.

Variability at selected ages. Columns 3 to 9 of Table 8 carry statistics which characterize the dispersion of nasion-TANS diameter $\times$ 100/nasion-menton diameter. Selected findings are as follows:

1. During the segment of ontogeny investigated, parameter estimates for the standard deviation of the index ascend from 1.5 to 1.8. It is tenable to claim increasing variability with age within the population identified as white girls of northwest European ancestry. By a test of statistical significance derived for comparing two variances based on related measures (30), the hypothesis that no systematic change occurs can be rejected at a high level of confidence ($t = 2.8$, df 58).

2. Near the lower end of the distribution representing age 5 years there are girls with osseous nose height 40 per cent of osseous face height. Osseous nose height near 50 per cent of osseous face height is found at the upper end of the distribution representing age 11 years. The direction of movement and overlapping of successive index distributions is indicated by the similarity of the seventieth percentile at age 5 years and the ninetieth percentile at age 11 years.

3. For the six-year period from age 5 years to age 11 years, the distribution of change in nose height expressed as a percentage of face height has an estimated population standard deviation of 1.1, an

obtained range of 5.9, and an obtained distance between percentiles 10 and 90 of 2.6.

9. Nose Height × 100/Face Depth

Trend for total sample. Columns 1 and 2 of Table 9 carry series of ordered ages and corresponding means for nasion-TANS diameter × 100/TANS-APOC diameter. A curve drawn with the aid of these paired values as successive coordinates is shown in the upper-left section of Figure 9. Finding: The mean index trend for the entire sample of 60 girls is a negatively accelerated increasing function of age. Expressed another way, there is a slowing advance of nose height in percentage of face depth as reflected in mean increments for consecutive bienniums of 2.1, 1.5, and 1.0, respectively. Generalization: In North American girls of northwest European descent, the average ratio of nose height to face depth increases at a falling rate throughout middle and late childhood.

Subgroup contrasts. The middle-left and lower-left sections of Figure 9 display mean trends for two subgroups. Subgroup A includes girls whose indices increase 7.0 or more between age 5 years and age 11 years; subgroup B, girls whose indices increase 3.0 or less during the same sexennium. Finding: Starting from a similar level at age 5 years, the trend for the rapidly changing subgroup ascends along an almost rectilinear path and that for the slowly changing subgroup ascends along a path strongly concave to the chronologic base line. Generalization: Central tendency trends for selected subgroups from the population of North American white girls show that nose height relative to face depth increases less in some children during the triennium between ages 8 years and 11 years (Subgroup B) than in other children during any annual period within the triennium (Subgroup A).

Trends for individuals. Curves were drawn to each of the 60 sets of paired values for age and nasion-TANS nose height × 100/TANS-APOC face depth. By inspection and intercomparison of these curves, it is found:

1. Sixty-five per cent are ascending trends concave to the chronologic base line. The variation in ascent among these curves is illustrated in the upper-right section of Figure 9 by subjects 13F and 72F.

2. Fifteen per cent are rising rectilinear trends, or rising trends

convex to the chronologic base line. An illustration of each variety is portrayed in the lower-right section of Figure 9 by the curves for subjects 44F and 28F, respectively.

3. Twelve per cent are trends convex to the chronologic base line in the period from 5 years to 8 years, and concave to the base line in the period from 8 years to 11 years. The curve for subject 7F, reproduced in the upper-right section of Figure 9, is an example.

TABLE 9

CENTRAL TENDENCY AND VARIABILITY STATISTICS FOR NASION-TANS NOSE HEIGHT × 100/TANS-APOC FACE DEPTH. THE SUBJECTS ARE 60 NORTH AMERICAN WHITE GIRLS EXAMINED AT YEARLY INTERVALS.

Age	Mean	S.D.	Minimum	Percentiles: 10	30	70	90	Maximum
(years)								
			Distribution of index at selected ages					
5	48.6	2.1	43.0	45.6	47.4	50.0	51.7	52.5
6	49.7	2.2						
7	50.7	2.3						
8	51.5	2.4	45.4	47.9	49.9	52.9	54.5	56.5
9	52.2	2.6						
10	52.7	2.7						
11	53.2	2.8	47.4	49.3	51.3	55.0	56.4	58.8
			Distribution of change-in-index between ages 5 and 11 years					
5–11	4.6	1.6	1.3	2.7	3.7	5.3	6.9	8.6

4. Eight per cent are concave trends similar to that shown in the lower-right section of Figure 9 for subject 67F. Some of these curves ascend until age 9 years before beginning to descend.

Individual contrasts. In the aggregate, the six trends comprising the right-hand portion of Figure 9 depict numerous differences among individual girls with respect to changes during childhood in the ratio of nose height to face depth. Subjects 13F and 72F each have standard scores near zero at 5.5 years of age; at age 11 years, the standard scores of these girls are +1.0 and —0.9, respectively. Percentile ranks for subject 28F are 17 at age 5 years, 5 at age 8 years, and 15 at age 11 years; comparable ranks for subject 67F are higher by 31, 33 and 2, respectively. The curves for subjects 7F and 13F show an early period of marked convergence; those for subjects 44F and 67F, a late period of marked divergence.

Variability at selected ages. Statistics pertaining to the dispersion

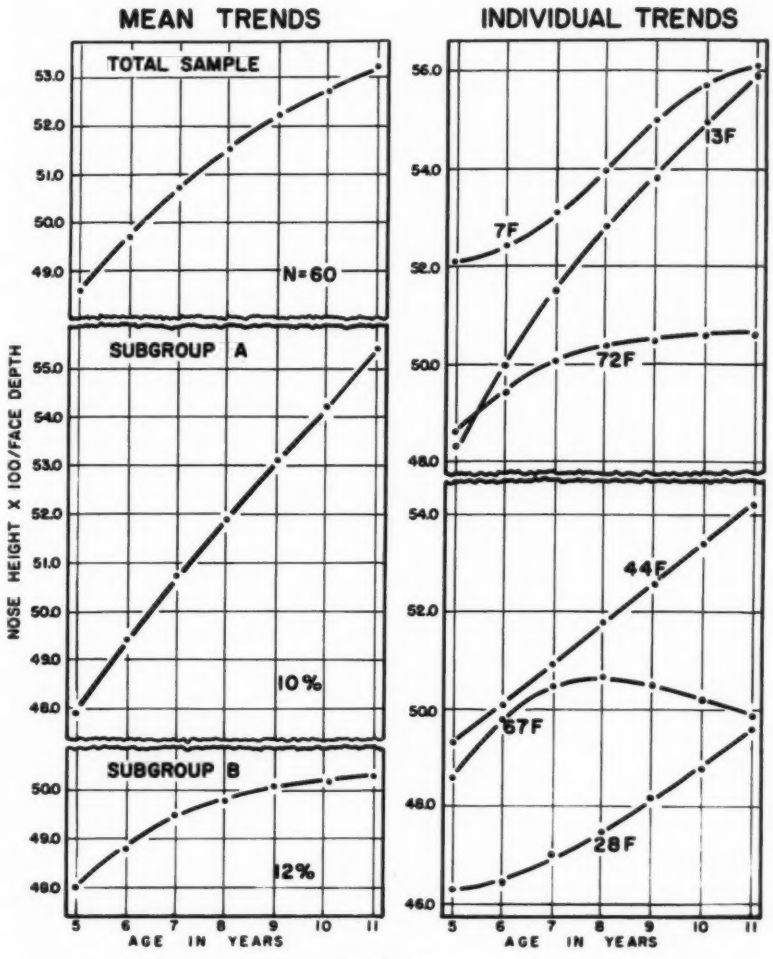

FIGURE 9

Curves for distance from nasion to the tip of the anterior nasal spine in percentage of distance between the tip of the anterior nasal spine and the midpoint of a line connecting the anteriormost points on the occipital condyles.

of nose height in percentage of face depth are presented in columns 3 to 9 of Table 9. It will be seen:

1. Estimated standard deviations of the index for the population defined as North American girls of northwest European lineage are 2.1 at age 5 years and 2.8 at age 11 years. A statistical test, appropriate for comparing variances based on related measures (30), allows rejection of the hypothesis that the difference at these two ages is due to chance alone ($t = 3.6$, df 58). With this foundation, supplemented by the progression of the series of values in column 3 of Table 9, it is reasonable to deduce that during middle and late childhood the index increases in variability with age.

2. Direction of movement and overlapping of the successive index distributions is indicated by the similarities of (a) percentiles 70 at age 5 years and 30 at age 8 years, and (b) percentiles 99 at age 8 years and 90 at age 11 years. Near the extremes of the distribution representing age 8 years there are girls with osseous nose heights 46 per cent and 56 per cent of their respective osseous face depths.

3. Values obtained by subtracting the index of each subject at age 5 years from her index at age 11 years are scattered between a minimum of 1.3 and a maximum of 8.6, the central 40 per cent being clustered within the limits of 3.7 and 5.3.

10. Nose Height × 100/Face Width

Trend for total sample. Arithmetic means for nasion-TANS diameter × 100/bizygomatic diameter at seven successive childhood ages are listed in the second column of Table 10. A Cartesian plot obtained by utilizing these means as ordinate values and their corresponding ages as abscissa values is presented in the upper-left section of Figure 10. Finding: The composite index trend for the entire sample of 60 girls ascends with age. The ascent is concave to the chronologic base line during the period from age 5 years to age 8 years and almost rectilinear during the succeeding triennium. Compared with the obtained mean at age 5 years (nose height 35.7 per cent of face width), the obtained means at ages 8 years and 11 years are higher by 2.1 and 3.2, respectively. Generalization: On the average North American white girls manifest ongoing increase throughout middle and late childhood in the ratio of nasion-TANS nose height to bizygomatic face width.

Subgroup contrasts. Twelve per cent of the girls in the sample have indices that are higher at age 11 years than at age 5 years by 4.5 or more (Subgroup A). Over the same sexennium of ontogeny, 12 per cent of the girls have indices that increase 2.0 or less (Subgroup B). Curves drawn to the index means of each subgroup are portrayed in the middle-left and lower-left sections of Figure 10. Finding: Both curves rise from practically the same level as the trend for the total sample; the curve on subgroup B is concave to the chronologic base line continuously, whereas that on subgroup A is rectilinear after age 7 years. Generalization: The population identified as North American girls of northwest European descent yields subsamples that differ more than expected from the procedure in subsample selection. This follows since groups made up of girls showing small and large changes in the ratio of nose height to face width exhibit mean trends for the index that, between ages 7 years and 11 years, are represented best by parabolic and linear equations, respectively.

Trends for individuals. Separate graphs were plotted from each subject's paired seriate values for age and nasion-TANS diameter $\times$ 100/bizygomatic diameter. Examination of the resulting curves shows:

1. Sixty-two per cent are rising trends concave to the chronologic base line. The variation in concavity among this series is illustrated in the right-hand portion of Figure 10 by subjects 14F and 40F.

2. Fifteen per cent are rising rectilinear trends. The curves for subjects 25F and 30F in the lower-right section of Figure 10 depict the range in slope for this series.

3. Five per cent are rising trends convex to the chronologic base line. An example is the curve for subject 29F in the upper-right section of Figure 10.

4. Thirteen per cent are rising trends concave to the base line from age 5 years to age 8 years, and convex to the base line during the interval between ages 8 years and 11 years. The curve for subject 45F in the lower-right section of Figure 10 is representative of this series.

5. Five per cent are concave trends similar to that for subject 67F reproduced in the upper-right section of Figure 10. One of this series rises until age 9 years before beginning to fall.

Individual contrasts. A selected assortment of developmental com-

parisons is portrayed in the right-hand panel of Figure 10. Notice the early convergence and later divergence of curves 29F and 67F, the continuous divergence of curves 14F and 25F, the convergence of curves 25F and 30F, and so forth. Percentile ranks for subject 67F are 46 at age 5 years, 46 at age 8 years, and 23 at age 11 years. Comparable ranks for subject 29F are higher by 38, 21 and 63, respectively. Standard scores at ages 5 years and 11 years are +0.7 and +1.7 for subject 14F, +0.9 and zero for subject 25F, —0.4 and —0.1 for subject 30F.

TABLE 10

CENTRAL TENDENCY AND VARIABILITY STATISTICS FOR NASION-TANS NOSE HEIGHT × 100/BIZYGOMATIC FACE WIDTH. THE SUBJECTS ARE 60 NORTH AMERICAN WHITE GIRLS EXAMINED AT YEARLY INTERVALS.

Age	Mean	S.D.	Minimum	Percentiles: 10	30	70	90	Maximum
(years)			*Distribution of index at selected ages*					
5	35.7	2.0	31.2	32.8	34.6	37.0	38.2	39.1
6	36.6	2.1						
7	37.3	2.1						
8	37.8	2.1	33.2	35.1	36.6	39.1	40.4	41.7
9	38.2	2.2						
10	38.6	2.2						
11	38.9	2.3	33.4	35.9	37.6	40.2	41.6	43.8
			Distribution of change-in-index between ages 5 and 11 years					
5–11	3.2	1.0	0.4	1.9	2.8	3.6	4.5	5.6

Variability at selected ages. Columns 3 to 9 of Table 10 carry statistics that describe the dispersion of nasion-TANS diameter × 100/bizygomatic diameter. Selected findings are as follows:

1. At each age during middle childhood, the estimated parameter for the standard deviation of the index in North American girls of northwest European ancestry approximates 2.1.

2. The direction of movement and overlapping of successive index distributions is depicted by the correspondence of the maximum value at age 5 years with the 70 percentile at age 8 years, also by the similarity of percentiles 90 and 70 at ages 8 years and 11 years, respectively. Near the lower end of the distribution representing age 5 years there are girls whose nasion-TANS nose height is 32 per cent of their bizygomatic face width. Girls near the upper end of the distribution representing age 11 years have indices 11 points higher.

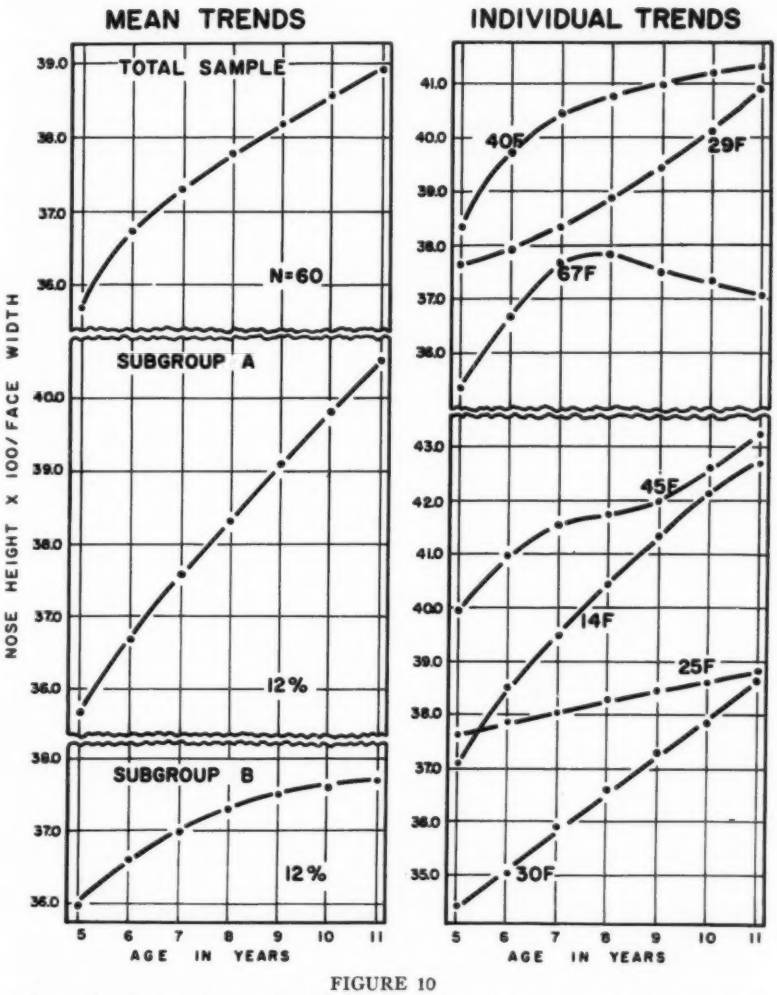

FIGURE 10

Curves for distance from nasion to the tip of the anterior nasal spine in percentage of bizygomatic diameter.

3. For the sexennium from age 5 years to age 11 years, the dispersion of change in nose height × 100/face width has an estimated population standard deviation of 1.0, an obtained range of 5.2, and an obtained distance between the tenth and ninetieth percentiles of 2.6. Nose height increases in percentage of face width by 0.4 to 3.2 for one-half of the subjects, and by 3.2 to 5.6 for the other one-half.

11. Nose Width × 100/Face Width

Trend for total sample. Columns 1 and 2 of Table 11 carry series of ordered ages and corresponding means for bialar diameter × 100/bizygomatic diameter. A curve drawn to these values is presented in

TABLE 11

Central Tendency and Variability Statistics for Bialar Nose Width × 100/Bizygomatic Face Width. The Subjects Are 60 North American White Girls Examined at Yearly Intervals.

Age	Mean	S.D.	Minimum	Percentiles: 10	30	70	90	Maximum
(years)			*Distribution of index at selected ages*					
5	24.7	1.3	22.4	23.0	24.0	25.3	26.3	28.2
6	24.7	1.2						
7	24.7	1.2						
8	24.7	1.3	22.0	23.0	24.1	25.3	26.3	28.3
9	24.7	1.3						
10	24.8	1.4						
11	24.9	1.4	21.4	23.0	24.3	25.5	26.5	28.9
			Distribution of change-in-index between ages 5 and 11 years					
5–11	0.2	0.6	−1.2	−0.5	−0.2	0.5	1.2	1.7

the upper-left section of Figure 11. Finding: The mean index trend for the entire sample of 60 girls parallels the chronologic base line from age 5 years to age 9 years and ascends slightly in the ensuing biennium. The ascent, although slight, is significant statistically (difference in means at age 9 years and 11 years = 0.2, $t = 2.7$). Generalization: In the typical North American girl of northwest European lineage, integumental nose width closely approximates 25 per cent of integumental face width at each age during middle and late childhood.

Subgroup contrasts. The middle-left and lower-left sections of Figure 11 depict mean trends for two subgroups. Subgroup A includes girls whose indices *increase* 1.0 or more between ages 5 years and 11

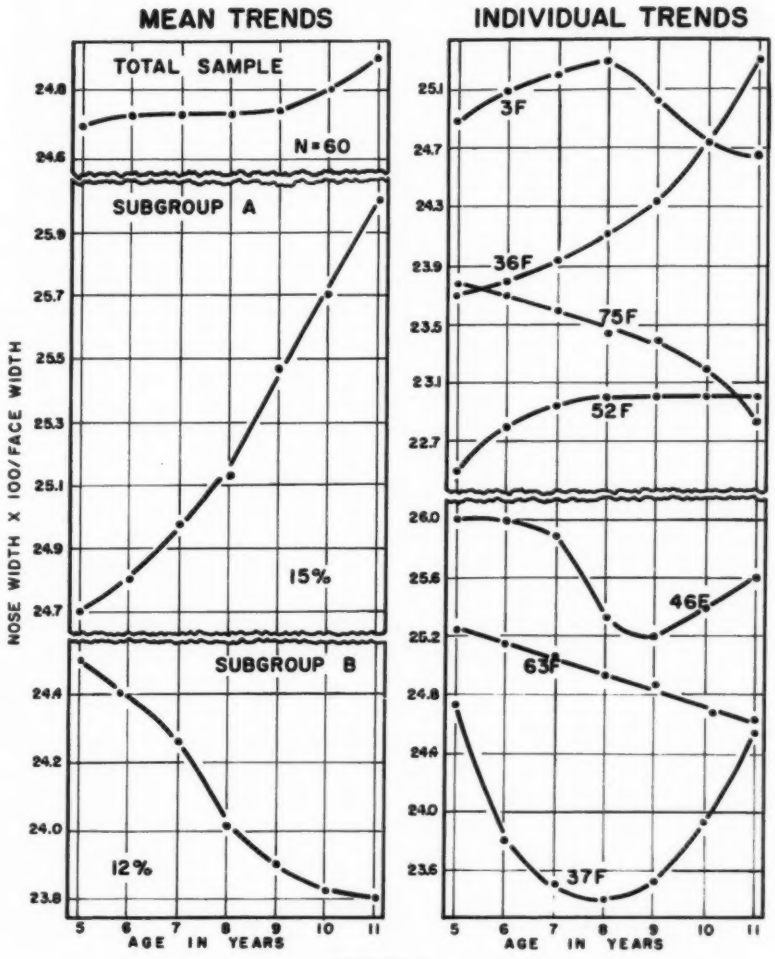

FIGURE 11

Curves for distance from nasion to the tip of the anterior nasal spine in percentage of distance between the lateralmost points of the alae nasi.

years; subgroup B, girls whose indices *decrease* 0.5 or more during the same sexennium of ontogeny. Finding: Starting from a similar level near 24.6 at age 5 years, the trend for subgroup A rises to 26.0 at age 11 years, while that for subgroup B declines to 23.8 at age 11 years. Generalization: In the population of North American white girls, the ratio of nose width to face width becomes greater with age in some children and less with age in others.

Trends for individuals. Curves were drawn to each of the 60 sets of paired values for age and bialar nose width × 100/bizygomatic face width. From inspection and intercomparison of these curves, it is found:

1. Thirty-two per cent are *ascending* trends concave, rectilinear, or convex to the chronologic base line. The curves for subjects 36F and 52F in the upper-right section of Figure 11 are examples of the convex and concave varieties, respectively.
2. Seventeen per cent are *descending* trends concave, rectilinear, or convex to the chronologic base line. Illustrations of the rectilinear and concave varieties are provided in the right-hand panel of Figure 11 by the curves for subjects 63F and 75F, respectively.
3. Eighteen per cent are trends *convex* to the base line. An example is the curve for subject 37F in the lower-right section of Figure 11.
4. Fifteen per cent are trends *concave* to the base line. The curve for subject 3F, reproduced in the upper-right section of Figure 11, is illustrative.
5. Ten per cent are trends concave to the base line during the early years of the sexennium studied, and convex to the base line during the later years. This series is represented by the curve for subject 46F in the lower-right section of Figure 11.
6. Eight per cent are trends *parallel* with the base line, or trends convex to the base line in the first part of the period and concave thereafter.

Individual contrasts. In the aggregate, the curves displayed in the right-hand portion of Figure 11 reveal numerous differences among individual girls with regard to change during childhood in the ratio of nose width to face width. Between ages 5 years and 8 years, there is movement of 46F toward 63F, and movement of 37F away from 63F. Between ages 8 years and 11 years, there is index decrease for

3F, index constancy for 52F, and index increase for 37F. Throughout the sexennium, there are divergencies and convergencies that result in the crossing of curves 3F and 36F at age 10 years, and of curves 52F and 75F between ages 10 years and 11 years. Standard scores for subject 36F are —0.8 at age 5 years and +0.3 at age 11 years; corresponding scores for subject 75F are higher by 0.1 and lower by 1.2 at ages 5 years and 11 years, respectively. Subject 63F has percentile ranks of 69 at age 5 years, 58 at age 8 years, and 41 at age 11 years; the percentile ranks for subject 37F at these ages are lower by 19, 44 and 2, successively.

Variability at selected ages. Statistics pertaining to the dispersion of nose width in percentage of face width are presented in columns 3 to 9 of Table 11. It will be seen:

1. The estimated standard deviation of the index for the population defined as North American girls of northwest European descent approximates 1.3 at each age throughout middle childhood.

2. There is almost complete overlapping of the index distributions for successive ages. The obtained percentiles at ages 5 years and 8 years are practically identical, while those at age 11 years are only slightly higher. Collapsing for age, nose width in percentage of face width lies between 24.0 and 25.5 on two-fifths of the girls studied, and between 23.0 and 26.5 on fourth-fifths of them.

3. Values obtained by subtracting the index of each subject at age 5 years from her index at age 11 years are dispersed from —1.2 to +1.7, the central two-fifths falling between —0.2 and +0.5.

Intra-individual Similarities and Differences

Having reported on the eleven indices singly, it is appropriate to present findings from considering them jointly. Table 12 displays the percentile ranks of nine selected individuals for all eleven indices at three childhood ages. One subject was chosen to satisfy each three-facet requirement specified below:

Age 5 years, percentile rank 50, index 1.
Age 8 years, percentile rank 50, index 6.
Age 11 years, percentile rank 50, index 10.
Age 5 years, percentile rank 10, index 2.
Age 8 years, percentile rank 10, index 9.
Age 11 years, percentile rank 10, index 5.

Age 5 years, percentile rank 90, index 3.
Age 8 years, percentile rank 90, index 4.
Age 11 years, percentile rank 90, index 7.

The subjects meeting these selection criteria will be discussed in turn. Discussions will not be exhaustive; the intent is to start the

TABLE 12
NINE GIRLS EACH DESCRIBED AT THREE CHILDHOOD AGES WITH RESPECT TO PERCENTILE RANK FOR ELEVEN INDICES OF FACIO-CEPHALIC FORM.

	Age in years								
Index	5	8	11	5	8	11	5	8	11
	39F-5-50-1*			5F-8-50-6			68F-11-50-10		
1	50	42	39	62	55	53	82	85	82
2	78	85	85	85	76	67	46	57	56
3	7	8	8	48	43	40	72	70	73
4	7	10	10	22	28	31	35	36	37
5	61	62	61	12	20	28	43	33	38
6	7	8	12	54	50	49	38	44	43
7	17	18	19	18	17	12	8	8	7
8	46	84	56	3	5	8	52	52	68
9	35	62	48	29	33	31	62	69	66
10	8	18	12	23	15	15	45	47	50
11	17	33	45	86	94	83	25	12	4
	47F-5-10-2			59F-8-10-9			13F-11-10-5		
1	71	63	60	29	24	22	8	10	13
2	10	18	17	8	18	18	92	92	95
3	20	20	28	31	23	32	4	3	2
4	39	42	47	79	70	75	14	8	2
5	15	18	22	63	68	73	33	13	10
6	73	73	73	78	47	45	28	35	41
7	32	37	57	53	45	44	5	3	4
8	63	46	32	10	13	18	21	18	20
9	92	83	57	8	10	5	47	65	80
10	69	65	55	40	24	23	18	18	19
11	3	7	7	91	81	90	39	18	22
	38F-5-90-3			71F-8-90-4			56F-11-90-7		
1	86	82	85	27	18	18	64	53	60
2	56	63	70	2	2	2	15	5	8
3	90	82	85	28	28	18	93	92	92
4	51	47	42	92	90	82	95	99	99
5	83	78	75	50	40	23	93	95	91
6	18	22	20	93	98	98	58	52	56
7	28	30	34	21	21	19	86	87	90
8	87	66	56	73	74	72	90	97	93
9	37	32	28	66	78	88	33	40	37
10	34	27	17	99	99	97	84	93	93
11	14	10	4	58	75	63	99	99	99

* Identification of subjects and basis of selection, e.g. subject 39F at age 5 years with percentile rank 50 for index 1; subject 5F at age 8 years with percentile rank 50 for index 6; and so forth.

reader on a thorough study of the intra-individual findings included in Table 12. To facilitate such study, the anatomic identifications of the indices are repeated:

1. Head width × 100/head depth.
2. Face width × 100/head width.
3. Face depth × 100/head depth.
4. Face depth × 100/face width.
5. Face depth × 100/face height.
6. Face height × 100/face width.
7. Lower jaw width × 100/face width.
8. Nose height × 100/face height.
9. Nose height × 100/face depth.
10. Nose height × 100/face width.
11. Nose width × 100/face width.

Beginning with the upper-left segment of Table 12, it will be seen:

Subject 39F. Small face depth relative to head depth (3); small face depth, face height, and lower jaw width relative to face width (4, 6, 7); above average face depth relative to face height (5); large face width relative to head width (2); decrease in the ratio of head width to head depth from average to below average (1); increase in the ratio of nose width to face width from small to average (11); and marked increase followed by decrease in the ratios of nose height to face height and depth (8, 9).

Subject 5F. Large nose width relative to face width (11), average face height to face width (6), and moderately small face depth to face width (4); moderately small nose height relative to face depth (9); small nose height relative to face height (8); increase in the ratio of face depth to face height from small to moderately small (5); and decrease in the ratio of face width to head width from large to moderately large (2).

Subject 68F. Small lower jaw width relative to face width (7); moderately small face depth relative to face width and height (4, 5); average face width relative to head width (2) and nose height to face width (10); moderately large head width and face depth relative to head depth (1, 3); decrease in the ratio of nose width to face width from moderately small to small (11); and increase in nose height to face height from average to moderately large (8).

Subject 47F. Moderately large face height relative to face width (6), and head width to head depth (1); average face depth to face width (4); moderately small face depth to head depth (3); small nose width to face width (11) and face width to head width (2); increase in the ratio of lower jaw width to face width from moderately small to average (7); decrease in nose height to face height from moderately large to moderately small (8); and decrease in nose height to face depth from large to average (9).*

Subject 59F. Small nose height relative to face height and depth (8, 9); moderately small face depth to head depth (3); average lower jaw width to face width (7); moderately large face depth to face width and height (4, 5); large nose width to face width (11); decrease in the ratio of face height to face width from large to average (6); and decrease in nose height to face width from average to moderately small (10).

Subject 13F. Large face width relative to head width (2), and small lower jaw width to face width (7); small face depth to head depth (3); increase in the ratio of nose height to face depth from average to moderately large (9); and decrease in face depth to face height from moderately small to small (5). Percentile ranks below 25 at each age are obtained on this subject for head width to head depth (1), face depth to head depth and face width (3, 4), lower jaw width to face width (7), and nose height to face height and width (8, 10).

Subject 38F. Small nose width relative to face width (11); moderately small lower jaw width to face width (7); average face depth to face width (4); moderately large face depth to face height (5); large head width and face depth to head depth (1, 3); decrease in the ratio of nose height to face height from large to average (8); and increase in face width to head width from average to moderately large (2).

Subject 71F. Large face depth, face height, and nose height relative to face width (4, 6, 10); moderately large nose height to face height (8); moderately small lower jaw width to face width (7); small

* By this time, the reader will be curious to know whether there is any systematic relation between the magnitude of an index at age 5 years and its change during the ensuing sexennium of childhood. For each index, the Pearson *r* method of correlation was employed. The eleven coefficients obtained lie between —.30 and +.20, none differing dependably from zero at the 1 per cent confidence level.

face width to head width (2); increase in the ratio of nose height to face depth from moderately large to large (9); and decrease in face depth to face height from average to moderately small (5).

Subject 56F. Small face width relative to head width (2); moderately small nose height to face depth (9); and average face height to face width (6). Percentile ranks above 80 at each age are obtained on this subject for face depth to head depth, face width and face height (3, 4, 5); nose height to face height and width (8, 10); nose width to face width (11); and lower jaw width to face width (7).

Summary

Eleven indices of facio-cephalic form are investigated within the sexennium of human ontogeny between ages 5 years and 11 years. For the indices jointly, intra-individual similarities and differences are examined; and for the indices singly, study is made of central tendency and variability at selected ages, mean trends on the total sample and subgroups, and trends of individual subjects.

A sample of 60 American-born white girls is utilized. Its members are predominantly of northwest European ancestry and above average socioeconomic status. Each subject provides data for computation of the eleven indices at consecutive annual ages from 5 years to 11 years.

The basic materials are time series for eight diameters of the head and face. Four of these diameters are obtained by direct measurement of the child (glabella-occipital head depth, biparietal head width, bizygomatic face width, and bialar nose width), and four are derived from measurement of roentgenograms (bigonial jaw width, nasion-menton face height, nose height from nasion to the tip of the anterior nasal spine, and face depth from the tip of the anterior nasal spine to the midpoint of a transverse line connecting the most anterior points on the occipital condyles).

For the total sample, mean trends on age show:

1. Relative to face width, lower jaw width increases, nose width remains almost constant, and head width decreases.
2. Face depth decreases relative to face height, remains almost constant to face width, and increases relative to head depth.
3. Relative to face width, face depth and face height, there is increase in nose height.

4. Face height increases relative to face width, and head width decreases relative to head depth.

From selective subgrouping, it is found:

1. Mean trends for the ratios head width/head depth, face depth/face width, and nose width/face width ascend continuously in one subgroup, and decline continuously in another.

2. The ratios face height/face width and lower jaw width/face width yield continuously rising mean trends on one subgroup, and mean trends roughly parallel to the age base line on another. Comparable subgroup trends for face depth/face height are descending, and roughly parallel, respectively.

3. For nose height/face height, one subgroup gives an ascending rectilinear mean trend, and another a mean trend that is concave to the age base line.

Trends of individuals reveal:

1. Variation among subjects is pronounced. Some individual trends are negatively accelerated, others positively accelerated; some are increasing functions of age, others decreasing functions of age; some are best expressed by rectilinear or parabolic equations, others by more complex equations.

2. Of the eleven indices studied, the fairly homogeneous trends on individuals are those for face width/head width, face depth/head depth, and nose height/face depth. Face width/head width increases with age in every subject, despite varied inter- and intra-individual differences in rate of increase.

3. Markedly heterogeneous individual trends are found for nose width relative to face width, face depth relative to face width, and head width relative to head depth.

Standard deviations at annual ages from 5 years to 11 years indicate:

1. Variability remains practically constant for face depth/face width, lower jaw width/face width, face width/head width, and head width/head depth.

2. Variability increases with age for face depth relative to head depth, face depth relative to face height, nose height relative to face height, and nose height relative to face depth.

References

1. Bayley, N. 1936. Growth changes in the cephalic index during the first five years of life. *Human Biology,* **8**, 1-18.
2. Davenport, C. B. 1940. Post-natal development of the head. *Proc. Am. Philos. Soc.,* 83, No. 1, 127 pp.
3. Gray, H. & Ayres, J. G. 1931. Growth in private school children. Univ. Chicago Press, Chicago, 282 pp.
4. Goldstein, M. S. 1936. Changes in dimensions and form of the face and head with age. *Am. J. Phys. Anthrop.,* **22**, 37-89.
5. Hellman, M., 1935. The face in its developmental career. *Dental Cosmos,* **77**, 685-699, 777-787.
6. Knott, V. B. 1941. Physical measurement of young children. *Univ. Iowa Stud. Child Welf.,* **18**, No. 3, 99 pp.
7. Knott, V. B. & Meredith, H. V. 1937. Changes in body proportions during infancy and the preschool years: II. Width of hips in relation to shoulder width, chest width, stem length and leg length. *Child Develop.* **8**, 311-327.
8. Krogman, W. M. 1960. The Philadelphia center for research in child growth. Univ. Pennsylvania, Philadelphia, 32 pp.
9. Meredith, H. V. 1939. Length of head and neck, trunk, and lower extremities on Iowa City children aged 7 to 17 years. *Child Develop.,* **10**, 129-144.
10. ———. 1951. Size and form of boys of U. S. A.—North American ancestry born and reared in Oregon. *Growth,* **15**, 39-55.
11. ———. 1953. Growth in head width during the first twelve years of life. *Pediatrics,* **12**, 411-429.
12. ———. 1954. Growth in bizygomatic face breadth during childhood. *Growth,* **18**, 111-134.
13. ———. 1955. A longitudinal study of change in size and form of the lower limbs on North American white schooboys. *Growth,* **19**, 89-106.
14. ———. 1958. A time series analysis of growth in nose height during childhood. *Child Develop.,* 29, 19-34.
15. ———. 1959. A longitudinal study of growth in face depth during childhood. *Am. J. Phys. Anthrop.,* 17 n.s., 125-135.
16. Meredith, H. V., & Culp, S. S. 1951. Body form in childhood: Ratios quantitatively describing four slender-to-stocky continua on boys 4 to 8 years of age. *Child Develop.,* **22**, 3-14.
17. Meredith, H. V., & Knott, V. B. 1937. Changes in body proportions during infancy and the preschool years: I. The thoracic index. *Child Develop.,* **8**, 173-190.
18. ———. 1938. Changes in body proportions during infancy and the preschool years: III. The skelic index. *Child Develop.,* **9**, 49-62.
19. Meredith, H. V., Knott, V. B., & Hixon, E. H. 1958. Relation of the nasal and subnasal components of facial height in childhood. *Am. J. Orthodont.,* **44**, 285-294.
20. Meredith, H. V., & Meredith, E. M. 1953. The body size and form of present-day elementary school children residing in west-central Oregon. *Child Develop.,* **24**, 83-102.
21. Meredith, H. V., & Sherbina, P. R. 1951. Body form in childhood: Ratios quantitatively describing three slender-to-stocky continua on girls 4 to 8 years of age. *Child Develop.,* **22**, 275-283.
22. Newman, K. J., & Meredith, H. V. 1956. Individual growth in skeletal bigonial diameter during the childhood period from 5 to 11 years of age. *Am. J. Anat.,* **99**, 157-187.
23. Potter, J. W., & Meredith, H. V. 1948. A comparison of two methods of obtaining biparietal and bigonial measurements. *J. Dent. Res.,* **27**, 459-466.

24. SEAVER, J. W. 1909. Anthropometry and the physical examination. By author, New Haven, 191 pp.
25. SCHULTZ, A. H. 1926. Fetal growth in man and other primates. *Quart. Rev. Biol.*, **1**, 465-521.
26. SPURGEON, J. H., YOUNG, N. D., and MEREDITH, H. V. 1959. Body size and form of American-born boys of Dutch ancestry residing in Michigan. *Growth*, **23**, 55-71.
27. THOMPSON, D. W. 1917. On growth and form. Cambridge Univ. Press, Cambridge, 793 pp.
28. TRIM, P. T., & MEREDITH, H. V. 1952. Body form in Homo sapiens: A study of five anthropometric ratios on white boys fifteen years of age. *Growth*, **16**, 1-14.
29. TUCKER, W. B., & LESSA, W. A. 1940. Man: A constitutional investigation. *Quart Rev. Biol.*, **15**, 265-289, 411-455.
30. WALKER, H. M., & LEV, J. 1953. Statistical inference. Holt, New York, 510 pp.
31. WALLIS, W. D., & WALLIS, R. S. 1946. Sex differences in cephalic index during growth. *Southwestern J. Anthrop.*, **2**, 56-83.

Growth, 1960, **24**, 265-323.

OOGENESIS IN ADULT *DROSOPHILA MELANOGASTER*. IX. STUDIES ON THE CYTOCHEMISTRY AND ULTRASTRUCTURE OF DEVELOPING OOCYTES[1]

ROBERT C. KING

Northwestern University, Evanston, Illinois and
The Rockefeller Institute, N. Y. C., N. Y.

(Received for publication June 9, 1960)

INTRODUCTION

Previous studies have shown that vitellogenesis is retarded or abolished in the ovaries of 1) female *Drosophila melanogaster* homozygous for certain recessive genes (King and Burnett, 1957), 2) wild type females fed upon diets deficient in certain essential nutrients (Sang and King, 1959), and 3) wild type females poisoned with certain antimetabolites (King and Sang, 1958, 1959). Little information exists concerning the distribution of polysaccharides, lipids, proteins and ribonucleic acids in developing oocytes of normal *Drosophila*, and clearly such information must be obtained before the previously mentioned abnormalities of oogenesis can be studied and interpreted further. This paper reports investigations which provide a foundation for such future studies.

MATERIAL AND METHODS

Preparation of Sections:

One day old, female *Drosophila melanogaster* belonging to an Oregon-S wild type strain reared at 25° C were used. The ovaries were dissected from etherized flies immersed in *Drosophila* Ringer solution (the formula for this is given in *Growth* **20**:121) and left for one hour in fixative at 0° C. The fixative was Caulfield's modification of Palade's fluid. However, twice the concentration of OsO_4 shown in Caulfield's recipe (J. B. B. C. **3**:828 column 1) was used.

[1] Research supported by a U. S. Public Health Service Training Program Grant (No. 2G-70) to Drs. D. H. Moore and K. R. Porter of the Rockefeller Institute, and by funds provided R. C. King by the U. S. Atomic Energy Commission and the National Science Foundation (contract AT(11-1), project 12 and NSF-G 11710, respectively).

Tissue was passed through 50%, 70%, and 90% ethanol (5 minutes in each solution) and then through 2 changes of absolute ethanol (15 minutes in each). After dehydration the ovaries were soaked for one hour in two changes of methacrylate monomer (supplied by Rohm and Haas, Philadelphia, Pa.) A mixture of 80 parts butyl:20 parts methyl methacrylate monomer was used. The tissue was then left at 0° C for two hours in a mixture of monomer and initiator. Methacrylate monomer containing 4% 2, 4-dichlorobenzoyl peroxide with dibutyl phthalate (supplied under the name Luperco CDB by Novadel-Agene Corporation, 1740 Military Road, Buffalo, N. Y.) was employed. The methacrylate used in the steps referred to above had had the hydroquinone inhibitor, contaminating water and dissolved gases removed using the methods worked out by Moore and Grimley (1957). Subsequently, each ovary was placed in a dry, #2, gelatin, pill capsule containing syrupy, partially polymerized methacrylate and the initiator. The capsules were left overnight under an ultraviolet lamp where polymerization was completed.

The blocks were trimmed, and sections 2 micra in thickness were cut using a Servall, Porter-Blum microtome or a Leitz-Fernandez-Moran microtome with a glass knife. Sections floating on a 10% acetone solution in the microtome trough were transferred with a camel's hair brush to water drops on albumenized microscope slides. The slides were left on a 60° C hot plate until the fluid had evaporated and the sections were firmly attached to the slides.

Next, each slide was examined under dark field illumination, and the position of the section recorded using a Field Finder (supplied by the Lovins Company, Silver Spring, Md.). In certain cases sections were coated with immersion oil of 1.460 refractive index, covered by a No. 0 cover slip and viewed with a high-power phase contrast objective with immersion oil of 1.515 refractive index. The detail observed was far superior to that seen in paraffin-embedded material. Such preparations last several months. Note that the embedding medium is not removed and, therefore, that the only compounds extracted from tissue would be those which after osmium fixation are soluble in water, ethanol, or monomeric methacrylate. Towards the end of the study some use was made of Vestopal W as the embedding material following the instructions of the manufacturer (Martin Jaeger, Vesenaz, Geneva, Switzerland). For electron microscopy of *Drosophila* oocytes Vestopal gives superior results.

Cytochemical Procedures and Rationale

In the cytochemical studies to be described, the following stains were used: azure B bromide, orange G, fast green FCF, basic fuchsin, Nile blue A, acetylated Sudan black B, oil red O (all supplied by National Aniline Division, N. Y., N. Y.), alcian blue 8GX300 (Arnold, Hoffman and Company, Providence, R. I.), and bromphenol blue (Amend Drug Company, N. Y., N. Y.). Determinations of the pH of the dye solutions were made with a Beckman Model G ph meter.

In the case of dyes used in aqueous solution such as fast green (0.1% at pH 1.2), orange G (1% at pH 1.6), azure B bromide (0.025% at pH 4 or 9), and mercuric bromphenol blue (1 mg. bromphenol blue and 100 mg. $HgCl_2$ per ml., pH 2.2) a very rapid, simple procedure was found which gave excellent results. A drop of stain was pipetted over the section, and the slide was left on a hot plate set at 200° C. As soon as the solution started to bubble the slide was allowed to cool and was then rinsed in distilled water, passed through three changes of tertiary butyl alcohol and two changes of toluene. The preparation was completed by covering the section with Permount and adding a coverslip. The preparations obtained were similar to those stained in the conventional manner (for 2-3 hours at room temperature or 40° C) and dehydrated more slowly. The stains were brought to the desired pH with 0.1 N HCl or NaOH.

Procedures for proteins: The acidic dyes fast green and orange G form compounds with positively charged molecules. Under the acidic conditions employed almost all the groups capable of being positively charged in all proteins are ionized, and consequently, all proteins should bind the dyes. However, some non-proteinaceous compounds may also bind these dyes. The basic group of choline, for example, has a pK value which is higher than that given by groups from any of the basic amino acids found in polypeptide chains (Oncley, 1959). Choline and ethanolamine-containing lipids would bind the dyes, unless previously extracted. Amino-sugar-containing (PA/S-reactive) glycolipids might also bind acidic dyes (Stacey, 1946). However, sections extracted by various lipid solvents (including hot pyridine) showed a similar distribution of bound dye. Therefore, under these conditions and in this material the fast green and orange G-staining procedures are useful for visualizing the relative concentration of

protein in various cytological structures. The mercuric bromphenol blue technique of Mazia, Brewer and Alfert (1953) for proteins yields a similar cytological picture. Positively charged groups (ionized amino, imidazole, and guanidine groups) bind the dye under the conditions of the method, and other groups (such as sulfhydryls) may bind dye by coupling through mercury.

Methacrylate sections were stained with ammoniacal silver nitrate (Fontana's reagent; see Pearse, p. 475) to demonstrate reducing groups. Prior to staining, adjacent sections were placed for 72 hours in 80% ethanol saturated with phenylmercuric chloride (a treatment which blocks sulfhydryl groups; Pearse, p. 76). A decrease in the reduction of ammoniacal silver nitrate by tissue brought about by phenylmercuric chloride demonstrates the presence of protein sulfhydryl groups.

Procedures for acid mucopolysaccharides: Alcian blue was used to demonstrate the location of acid mucopolysaccharides. The mechanism whereby alcian blue combines with acid groups remains unclear (Spicer, 1960). In this case it was found necessary to remove the methacrylate from the sections. After removal of the methacrylate (by dipping the slides about 15 times in xylene), sections were rehydrated by passage through 100%, 85%, 70%, 50% and 30% ethanol to water. 1% alcian blue in 0.01N HCl (pH 2.3) was used as suggested by Zugibe, Brown and Last (1959). After staining for 15 minutes at 30° C, excess stain was rinsed off with water, followed by 0.01 N HCl for 1 minute. The tissue was then dehydrated through the alcohol series, dealcoholized in xylene and mounted in Permount.

Procedures for nucleic acids: The azure B bromide method was developed by Flax and Himes, and under the conditions specified (0.025% at pH 4) this basic dye stains RNA metachromatically (purple) and DNA orthochromatically (greenish blue). This differential chromotropic activity may result from differences between the two nucleic acids in the density distribution of available phosphate groups. A 15 minute extraction at 90° C in 5% aqueous trichloracetic acid (TCA) (pH 0.9) removes RNA and many carbohydrates from ovarian sections.

Schiff reagent was prepared from basic fuchsin by the method of Swift (1955). In studies involving the Schiff reagent the methacrylate was removed and sections were rehydrated. In the case of the Feul-

gen-Rossenbeck procedure for DNA (hereafter abbreviated as HCl/S), sections were hydrolized in 1 N HCl at 60° C for 15 minutes prior to staining in the Schiff reagent. The hydrolysis splits purine-deoxyribose bonds, removes the purine bases, and exposes the deoxyribose. This sugar, unlike ribose, exists largely in a non-cyclic form with a terminal aldehyde group. Such groups couple with the colorless Schiff reagent to form a colored aldehyde-Schiff complex. The deoxyribose components thus revealed are still attached in the main chain of the nucleic acid through phosphate linkages (Overend and Stacey, 1949).

Procedures for carbohydrates: The localization of carbohydrates required prior oxidation at 21° C with aqueous 1% periodic acid (pH 1.8) for 10 minutes or with 1% lead tetra-acetate in glacial acetic acid for 4 hours at 21° C or 60° C. In the H_5IO_6-Schiff technique (hereafter abbreviated as PA/S) the oxidant cleaves C-C bonds where these carbon atoms have adjacent hydroxyl groups or adjacent hydroxyl and amino groups, or hydroxyl and acylated amino groups and converts them to dialdehydes which combine subsequently with the Schiff reagent. Phosphatides (such as cardiolipin and those containing inositol or sphingosine), cerebrosides and gangliosides will be PA/S-positive (Deuel, 1951; Hale, 1957; Lovern, 1957) but at least some of these are removed during the xylene treatment and rehydration. The most common compounds which survive the procedures required to produce a rehydrated, methacrylate-free section and which contain sufficient numbers of the appropriate groups to produce a distinct coloration are polymers containing glucose, galactose, or glucosamine units. Such polymers include glycogens, mucopolysaccharides (including chitin; Richards, 1952), mucoproteins, and glycoproteins (including collagen; Bangle and Alford, 1954). Chondroitin sulphuric acid and hyaluronic acid are generally PA/S-negative, and whether or not heparin is PA/S-reactive depends on the degree to which it is sulfated (Hale, 1957).

Glegg, Clermont and Leblond (1952) have demonstrated that certain PA/S-positive carbohydrates can be distinguished from one another if lead tetra-acetate in non-aqueous solvent is used as the oxidant in place of periodic acid. The oxidation was carried out at room temperature or at elevated temperatures. Certain polysaccharides were found to stain intensely if oxidation was carried out at 70° C,

but not at all at 21° C. The reverse situation held for other PA/S-positive carbohydrates. The lead tetra-acetate-Schiff technique is hereafter abbreviated to LT/S. According to Casselman (1959, pg. 45) glycogen does not give a positive LT/S test under the above conditions.

In certain cases sections were brominated subsequent to the removal of the methacrylate by leaving the slides for 1 hour at 21° C in a 2% solution of bromine in chloroform. Bromination failed to reduce the amount of PA/S-positive material in the ovary, demonstrating that ethylenic groups play no role in the reaction.

In all procedures involving Schiff's reagent (HCl/S, PA/S, LT/S) subsequent to the hydrolysis or oxidation the sections were washed in running water, stained 30 minutes, immersed 2 minutes in each of three successive sulfurous acid rinses, washed 5 minutes in running water, dehydrated through an alcohol series, dealcoholized in xylene, and mounted in Permount. In the LT/S procedure a 5 minute immersion in glacial acetic acid was inserted after the oxidation.

Procedures for lipids: For coloring lipids the lysochromes Sudan black B (the acetylated derivative) or oil red O were used (both at 1% in 60% triethyl phosphate). The methacrylate was removed from the section with chloroform heated to 56° C, the slide was transferred to triethyl phosphate and next to the dye solution at 21° C or 60° C for 5 minutes. Excess dye was rinsed off in 60% triethyl phosphate, and after two rinses in distilled water the sections were mounted in Farrant's medium. Such preparations fade very quickly. Sudan black B colors all lipids indiscriminately; whereas oil red O colors triglycerides and fatty acids a much darker shade than phospholipids (Gomori, 1952).

Aqueous 1% Nile blue (pH 2.5) was used to distinguish acidic and non-acidic lipids. It was found that the methacrylate could be left in the section in this case, and staining of certain structures took place instantaneously at room temperature. Subsequently, other structures could be stained by heating the slide on a hot plate as described previously. After excess stain was rinsed off, the sections were transferred directly to toluene and mounted in Permount. Occasionally, sections were stained with aqueous Nile blue and orange G (both at 1% concentration) simultaneously at pH 1.6.

The water soluble, oxazine, basic dye, Nile blue A, always contains

a small amount of its red oxazone (formed through spontaneous oxidation). The oxazone, which is soluble both in oils and in aqueous Nile blue, dissolves in all lipids liquid at the prevailing temperature, coloring them red. However, only in the case of the non-acidic triglycerides and glycolipids is this red color observed, since it is masked by the blue coloration imparted by oxazine when it dissolves in or forms salts with acidic lipids (Lillie, 1956; Casselman, 1959). Lecithin (and perhaps all phosphatides) stain intensely with concentrated Nile blue even when solid (Pearse, 1954). In addition, Nile blue binds to any non-lipid which is negatively charged at the prevailing pH, and depending on the density distribution of negative charges on the polymer Nile blue may stain orthochromatically (blue) or metachromatically (pink) (Baker, 1958). However, such Nile blue-positive compounds will be insoluble in lipid solvents and therefore can be distinguished from lipids. The lipid solvents employed for such extractions were: chloroform, acetone, toluene, pyridine, or ethanol (either at 21° C or 56° C). If a one hour extraction is employed, the methacrylate is also removed from the sections at the same time in the case of the first four solvents (if used at 56° C). Nile blue is soluble in ethanol and acetone.

Structural lipids which are conjugated with proteins often fail to color with lysochromes. The formation of a complex between protein and lipid need not invariably involve chemical linkage; rather, lipid and protein molecules may be sandwiched together in such a way that the hydrophilic groups of both lipids and proteins point toward and bind the water solvent and so prevent lipid solvents and lysochromes from reaching the lipids (see Macheboeuf, 1937; Stoeckenius, 1959). Mild protein hydrolysis with phenol (1% aqueous, pH 4.5) as described by Gupta (1958) often "unmasks" bound lipids. I have used this method without success; but I have noted that heat alone or hot chloroform treatment may result in an increased uptake of lipid colorants. According to Nath, Gupta and Lal (1958), extraction with hot acetone unmasks mitochondrial lipids in the oocytes of *Periplaneta americana*.

Enzyme Extractions

In these studies the ovaries were dissected from etherized flies immersed in *Drosophila* Ringer solution, left for one hour in Carnoy's

(6:3:1) fluid, embedded in methacrylate, and sectioned at 2 micra. The methacrylate was removed with xylene, and following rehydration the sections were extracted with various enzymes at concentrations of 1 mg/ml for one hour at 37° C. Suitable controls were run with buffer solutions. The enzymes used were trypsin (at pH7), pepsin (in 0.01N HC1), and ribonuclease (at pH6). All enzymes were obtained from the Sigma Chemical Company, St. Louis, Missouri. Subsequently, the sections were stained using the PA/S, fast green, Feulgen, Nile blue, or azure B procedures.

Electron Microscopy

On frequent occasions observations were made of thin sections (giving gray interference patterns) cut from the same blocks which provided thick sections for cytochemical studies. The sections were stretched using the xylene vapor method of Satir and Peachey. Sections were picked up on 200 mesh copper grids. The surface of each grid had been previously covered by a carbon-coated collodion film. To enhance contrast some sections were stained with lead hydroxide according to the method of Watson (1958). Electron micrographs were taken with an RCA EMU 2 electron microscope.

Oogenesis: General Aspects

The developing egg of *Drosophila melanogaster* consists of a 16 cell nest surrounded by an envelope of follicle cells (see King and Devine, 158, their figure 1). The 16 cells are daughters which arise from four consecutive divisions of an oogonium. Fifteen of the daughter germ cells differentiate into nurse cells and nourish the most posterior, daughter germ cell which becomes the oocyte. Intercommunication of cytoplasm between all members of the 16 cell cyst is made possible by large pores in the walls separating adjacent cells (King and Devine, 1958). Intercellular cytoplasmic bridges connect the oocyte with the three or four most posterior nurse cells, and these in turn are connected to their neighbors in the same fashion. A molecule formed in the most anterior nurse cell will generally have to pass through two intervening nurse cells before entering the oocyte. Thus the 16 cells form a syncytium, and this presumably results from incomplete cytoplasmic division. Fawcett, Ito and Slatterback (1959) have described in many species situations where groups of simul-

taneously formed daughter cells are connected by sizeable intercellular bridges. These bridges are formed in telophase when the advancing margin of the cleavage furrow is arrested by the spindle remnant. With the subsequent dissolution of the spindle filaments, an open communication is established between the daughter cells.

The development of the nest of 16 cells in the *Drosophila* ovariole may be subdivided into a series of consecutive stages, ending with stage 14, the mature, ovarian, primary oocyte. (King, Rubinson, and Smith, 1956). During the first seven stages all 16 germ cells grow at roughly identical rates. During stages 8 through 11 vitellogenesis occurs, and the oocyte grows at a rate approximately 10 times faster than previously and at the expense of the nurse cells which shrink and eventually degenerate (King, 1957). The follicular epithelium and oocyte interact during stages 8-11 to produce the vitelline membrane. During stages 11 through 13 the chorion is formed by the follicular epithelium.

During stages 12-14 no further increase in the volume of the oocyte takes place. However, as will be demonstrated in this paper, great changes occur in the yolk organelles. Between stage 1 and 14 the oocyte increases in volume by a factor of over 100,000 times, and under optimum conditions it takes 3 days for the completion of this process.

Observations

The dimensions given in the following account refer to those measured in methacrylate-embedded material. However, considerable shrinkage occurs during dehydration and polymerization. A methacrylate-embedded, stage 14 egg, for example, has linear dimensions 70% those seen in the living state. A similar amount of shrinkage occurs in Feulgen-stained whole mounts or in paraffin-embedded material.

The Cytochemistry and Ultrastructure of the Nurse Cells

The nucleus: The nurse cell nuclei are generally spherical until vitellogenesis begins. Subsequently, the surface of the nuclei of posterior nurse cells becomes undulate and later lobate (see figure 1).

The nurse cell nuclear envelope stains with fast green, hot Nile blue, and contains PA/S-reactive material. In pre-yolk stages of development the nuclear envelope becomes thickened in localized areas (King and Devine, their figure 8, 1958). These thickened areas

stain in a fashion similar to the rest of the envelope. Since the nuclear envelope at later stages appears to be of uniform thickness, the thickened areas may be sloughed off into the cytoplasm subsequent to their formation. The scattered endoplasmic reticulum may arise in this fashion.

5 μ

FIGURE 1

An electron micrograph of a portion of posterior, early stage 10 nurse cell. Note the lobate nucleus (n). The cytoplasm (c) contains dense ellipsoidal mitochondria, pale vacuoles (which probably represent extracted fat droplets), and scattered filaments of endoplasmic reticulum.

In electron micrographs, the surface of the nuclear envelope is seen to be studded with myriads of annuli (each about 40 millimicra in diameter). The annuli are so closely packed that they lie almost side by side. Within each annulus the nuclear membrane is presumed to be exceedingly thin. The large number of annuli per unit area of the nurse cell nuclear envelope presumably bears some relation to the intense metabolic activity of these nuclei.

The nucleoplasm stains pale green with fast green and fails to stain with any of the other dyes employed in this study.

The behavior of the nurse cell chromosomes as a function of developmental stage has been worked out recently in considerable detail (King, Rubinson and Smith, 1956; Jacob and Sirlin, 1958). It is clear that these chromosomes elongate by uncoiling and concurrently undergo a series of 8 or 9 endomitotic doublings which produce polytene chromosomes whose multiple strands become more and more loosely associated as the nucleus grows. The few slides prepared from Carnoy-fixed, methacrylate-embedded ovaries stained by the Feulgen procedure for DNA showed nuclear detail identical to that seen in Feulgen-stained, ovarian whole mounts (see King, Burnett and Staley (1957) for a description of the whole mount procedure). The DNA-protein complex of the chromosomes is not extracted by trypsin or pepsin.

Great differences were noted between osmium- and Carnoy-fixed ovarian tissues. The differential staining by azure B (at pH4) of DNA and RNA is much more pronounced in Carnoy-fixed material, and Carnoy-fixed chromosomes stain much more intensely after the Feulgen procedure than do osmium-fixed chromosomes. These facts suggest that a chromosomal lipid which interferes with the Feulgen and azure B staining is retained after osmium fixation but extracted by Carnoy's fluid.

If the ovary is placed for 15 minutes in Ringer solution saturated with bromine and subsequently fixed in osmium and embedded as previously described, little osmium is taken up by the tissue. The addition of bromine takes place predominately at ethylenic groups of unsaturated fatty acids thus blocking sites which serve as the main reactive groups for OsO_4. According to Wigglesworth (1957) polymerization of lipids through osmium forms the basis of fixation by OsO_4, although osmium does react to some extent with proteins as

well (Bahr, 1954). Such brominated, osmium-fixed, methacrylate-embedded, ovarian sections fail to stain with cold or hot Nile blue (pH 2.5) or with cold azure B (pH 9) but do stain with hot azure B. Under these conditions the chromosomes stain an intense purple and the plasmosomes a paler purple. The chromosomal staining is more intense than in nonbrominated ovaries.

The nurse cell nucleus contains large amounts of RNA, not confined to a single structure (as in the case of the follicle cell), but rather localized in very dense, ribbon-like chains of blobs. This compound plasmosomal element presumably originates by the fusion of the numerous plasmosomes arising from the multiple chromosomal nucleolus organizers. Plasmosomal material stains with fast green, azure B and iron haematein. Plasmosomal RNA-proteins are removed by trypsin but not by pepsin. Plasmosomal RNA is removed by RNA-ase, but the plasmosomes continue to stain with fast green which indicates that protein remains. The plasmosomes are very osmiophilic; they color with acetylated Sudan black B and oil red O, fail to color with cold Nile blue, but color blue with hot Nile blue or with cold Nile blue after extraction with hot acetone, chloroform, toluene, or ethanol. Plasmosomes colored blue by Nile blue are immediately decolorized by cold ethanol. Following treatment with trypsin or pepsin, plasmosomes fail to stain with either hot or cold Nile blue. Plasmosomes contain large amounts of PA/S-reactive material (figure 2 left). When the LT/S-procedure is used, the plasmosomes stain more intensely if the oxidation is carried out at low than at high temperatures. Carnoy's fluid extracts the carbohydrate of the plasmosomes.

These data indicate that the plasmosomes contain an acidic lipid-protein complex which fails to stain with cold Nile blue when intact, which dissociates after being heated in water or organic solvents and which colors with Nile blue while dissociated. The lipid is not removed by extraction with hot organic solvents. The lysochrome readily diffuses out of the lipid into ethanol.

In addition to RNA, lipid and protein, the plasmosomes contain PA/S-reactive material which could be carbohydrate. However, the positive PA/S and Nile blue reactions could both be due to the same compound (an inositol-containing phospholipid, for example), or the positive fast green and PA/S reactions could be due to the same com-

pound (a hexosamine-containing glycolipid, for example). This is not the case, however, since extraction with hot TCA removes from the plasmosomes the material stainable with azure B and *also* that stainable by the PA/S procedure (figure 2 right). However, the Nile blue-stainable material remains and so does the fast green-positive material.

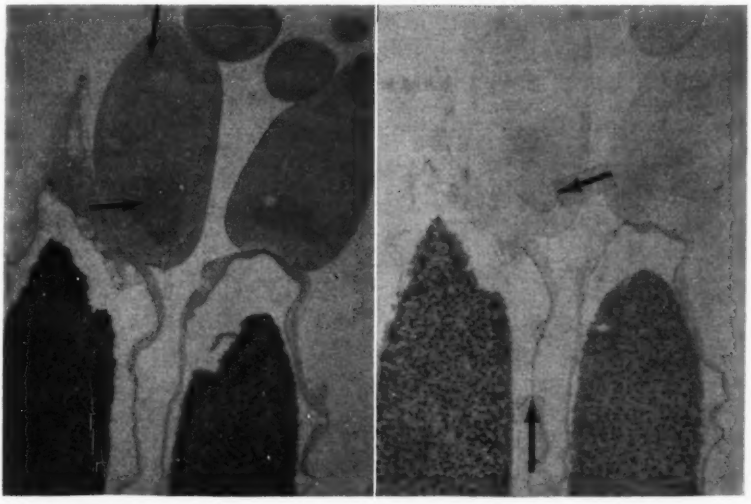

FIGURE 2

Left. A light micrograph of a portion of a section of an ovary stained by the PA/S-procedure. Horizontal and vertical arrows point to (1) the Schiff/-positive alpha spheres in the ooplasm and (2) the plasmosomes in a nurse cell nucleus of a stage 10 chamber. Myriads of intensely Schiff-positive beta spheres are seen in the two mature oocytes. *Right*. An adjacent section extracted with hot TCA prior to performing the PA/S-procedure. Vertical and horizontal arrows point to the endochorion and vitelline membrane which retain their stainability. Beta spheres also stain, but the background cytoplasm fails to stain. Alpha spheres and plasmosomes are PA/S-negative.

Electron micrographs of stage 8 nurse cell nuclei show nucleolar exudations. The plasmosomal element shown in figure 3 contains about 2 dozen spherical clusters of granules embedded in it. The clusters of granules are 0.3 to 0.7 micra in diameter and are less dense than the plasmosomal material but more dense than the nucleoplasm.

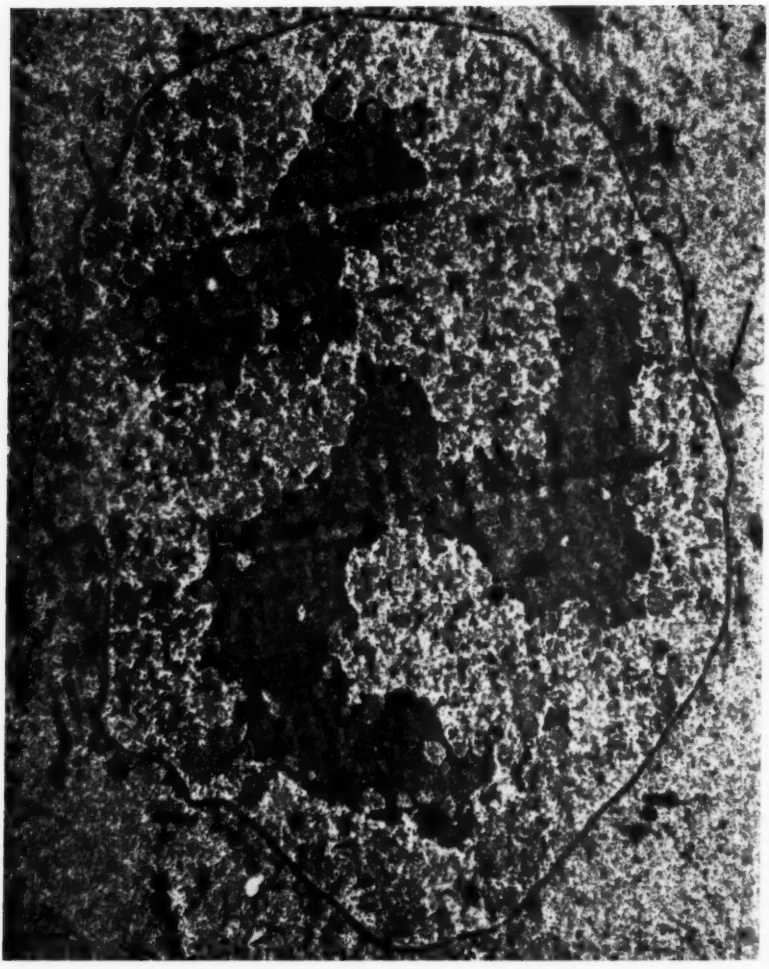

FIGURE 3

An electron micrograph of a stage 8 nurse cell nucleus containing two dense plasmosomal masses. The plasmosomes contain numerous pale clusters of granules. One such cluster is marked with an e. Similar clusters are seen in the nucleoplasm and cytoplasm (see arrows).

The granules themselves have diameters smaller than the annuli of the nuclear envelope. Similar clusters are found in the nucleoplasm and cytoplasm. Larger bodies (1-3 micra in diameter) were seen under the electron microscope in the nucleoplasm of nurse cells during early stages of vitellogenesis by King and Devine (their figures 13 and 14). These "emission bodies" are granular, are less dense than the plasmosomal material, and appear to pass intact into the cytoplasm through holes in the nuclear membrane. The emission bodies apparently break down rapidly once in the cytoplasm, since they are rarely observed there, and those that are are smaller than the ones found in the nucleus. PA/S-reactive bodies of similar size and distribution have been seen with the light microscope. The time interval during which these nucleolar emissions take place is about 5 hours. Subsequently (during stages 11 and 12), the nurse cell nuclei shrink and are eventually sloughed off as debris as the egg is laid.

The cytoplasm: The nurse cell cytoplasm contains relatively low concentrations of proteins. RNA and acid mucopolysaccharides are present in moderate amounts. There is evidence (King and Burnett, 1959; Zalokar, 1960) that at least some of the cytoplasmic RNA originates in the nucleus. Cytoplasmic RNA-proteins are removed by trypsin but not by pepsin. Cytoplasmic RNA is removed by RNA-ase, but the cytoplasm continues to stain with fast green which indicates that proteins remain.

In electron micrographs the cytoplasm is seen to be filled with dense granules each of which is about 5 millimicra in diameter. If these are ribonucleoprotein particles, they may be responsible for the cytoplasmic basophilia. Different nurse cells in the same chamber often differ in the concentration of azure B-positive material in their cytoplasms which probably indicates that they are out of phase with respect to cytoplasmic RNA synthesis. There is good evidence that adjacent nurse cells are out of phase with respect to DNA synthesis (King and Burnett, 1959).

The cytoplasm fails to stain with cold Nile blue, stains very faintly with hot Nile blue and stains pale blue with cold Nile blue after extraction with hot acetone. Thus, it is likely that some of the protein is associated with acidic lipids in the form of heat dissociable complexes. The cytoplasm contains myriads of non-staining vacuoles which are at or are just above the limit of resolution of the light

FIGURE 4

(Upper) An electron micrograph of a later stage 10 nurse cell nucleus and adjacent cytoplasm. Dense plasmosomal material (p) is scattered through the nucleoplasm. An arrow points to an invagination of the nuclear envelope. The cytoplasm including that within the invagination is filled with dense bodies.

(Lower) The ooplasm of the same developing egg. The ooplasm contains myriads of dense bodies (d), small clusters of denser mitochondria (m), and larger yolk spheres (y). Much (in some cases all) of the dense material in the yolk spheres has been extracted during the embedding procedure.

10 μ

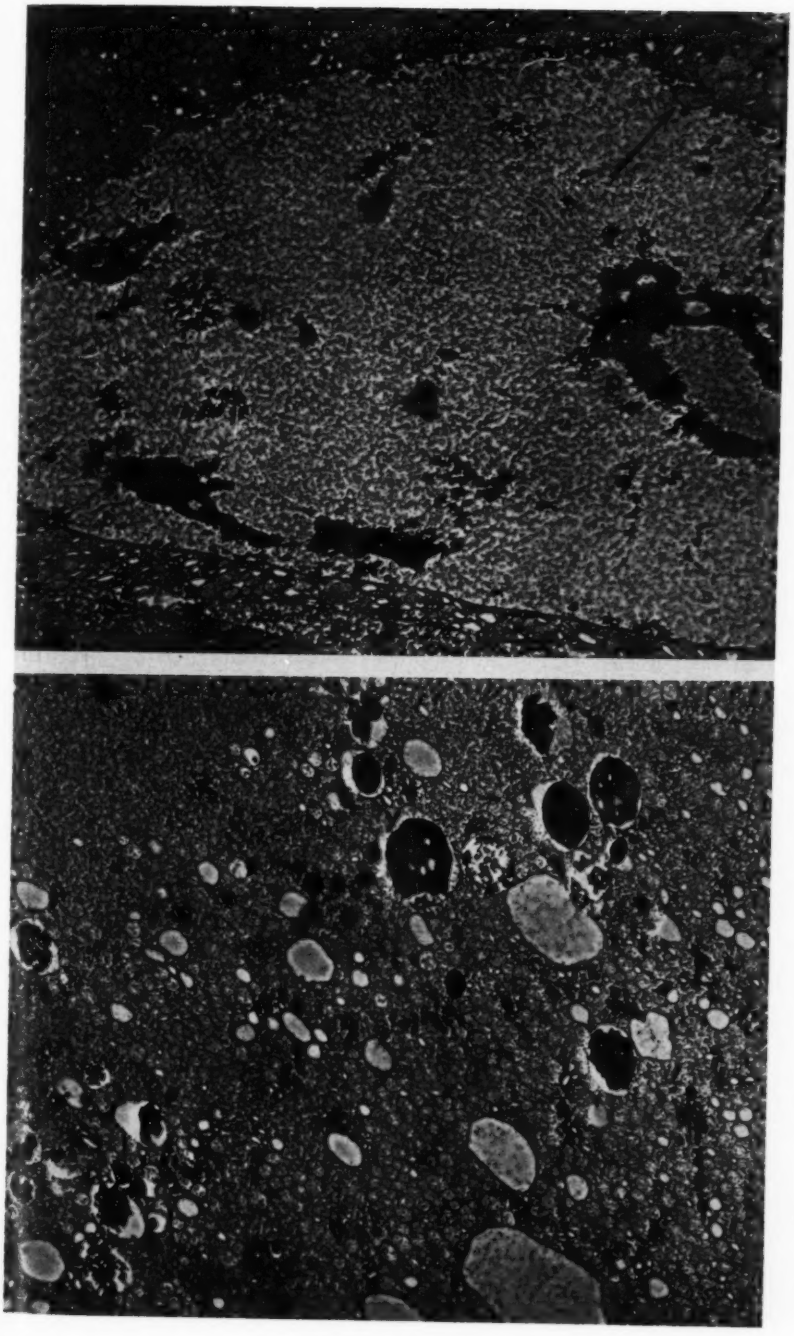

microscope (figure 1). These are probably the remains of fat droplets (see p. 313).

Mitochondria are present in the nurse cell cytoplasm from the earliest stages. Their distribution varies greatly. They may be dispersed homogeneously throughout the cytoplasm, or arranged in clumps, or located in a perinuclear fashion.

During vitellogenesis, dense bodies and lamellate bodies make their appearance (King and Devine, 1958). At the time that dense bodies are first seen, the nurse cell nuclear envelope contains peculiar invaginations (see figure 4 (upper) and King and Devine, their figure 19). Dense bodies are often found within these invaginations, and the possibility arises that these invaginations are the site of dense body manufacture. Both dense bodies and mitochondria stream into the developing oocyte. Here the dense bodies disappear, but at least some of the mitochondria remain intact. The dense bodies are the same size as mitochondria, and whereas they are readily distinguishable from them under the electron microscope (King and Devine, their figures 19 and 28), they both appear as tiny granules under phase contrast or bright field optics. Perhaps the two types of organelles eventually can be distinguished cytochemically. However, all cytoplasmic particles stain similarly with the procedures employed. In pre-yolk stages, mitochondria make up the majority of the population of particles; whereas during vitellogenesis the dense bodies predominate (see figures 4 (lower) and 5). Dense bodies presumably contribute their lipid to the ooplasm.

The particulate matter stains with fast green, iron haematein, Sudan black B, oil red O, fails to stain with cold Nile blue, but stains with hot Nile blue or with cold Nile blue after extraction with hot chloroform, toluene or ethanol. The Nile blue-stainable material is soluble in hot acetone, and the lysochrome readily diffuses out of the lipid into cold ethanol. The particles reduce ammoniacal silver nitrate. This is the sort of staining behavior expected from a phospholipid-protein complex. The particulate material is osmiophilic and cannot survive passage through ethanol and methacrylate unless fixed with osmium tetroxide. Extraction with hot TCA removes the particulate material from the cytoplasm. Carnoy's fluid removes the particulate material.

The large pores which connect adjacent nurse cells and the oocyte

have been mentioned previously. These pores have ring-shaped walls about 0.5 micron thick. The pore has a diameter of 4 microns. The pore wall stains with fast green, is sudanophilic and PA/S-reactive.

The cell walls are PA/S-reactive and stain with iron haematein. In electron micrographs one often notices that the nurse cell wall

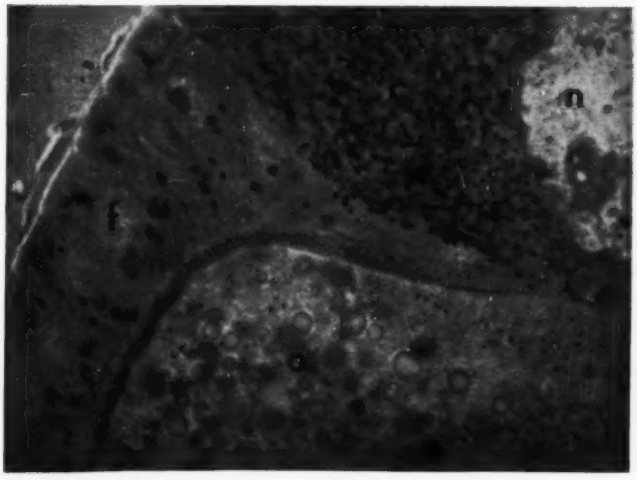

FIGURE 5

A light micrograph of a portion of a stage 10 chamber stained with Sudan black B. The nurse cytoplasm (c) contains myriads of sudanophilic particles (mostly dense bodies). The cytoplasm of the columnar follicle cells (f) contains sudanophilic epithelial bodies. The ooplasm (o) contains yolk spheres and paler dense bodies. The vitelline membrane is forming at the border between the oocyte and follicle cells. The nurse cell nucleus (n) contains a dense plasmosome.

sends out a nipple-like projection which fits into a socket-like invagination of the adjacent cell. Adjacent follicle cells are also held together in this manner (figure 6).

The Cytochemistry and Ultrastructure of the Follicle Cells

The mesodermal follicle cells congregate in the germarium to form an envelope of cuboidal cells about the stage 1, 16-cell cyst which subsequently pinches off the germarium. As the cyst grows in volume the enveloping follicle cells divide and so keep abreast of the increase

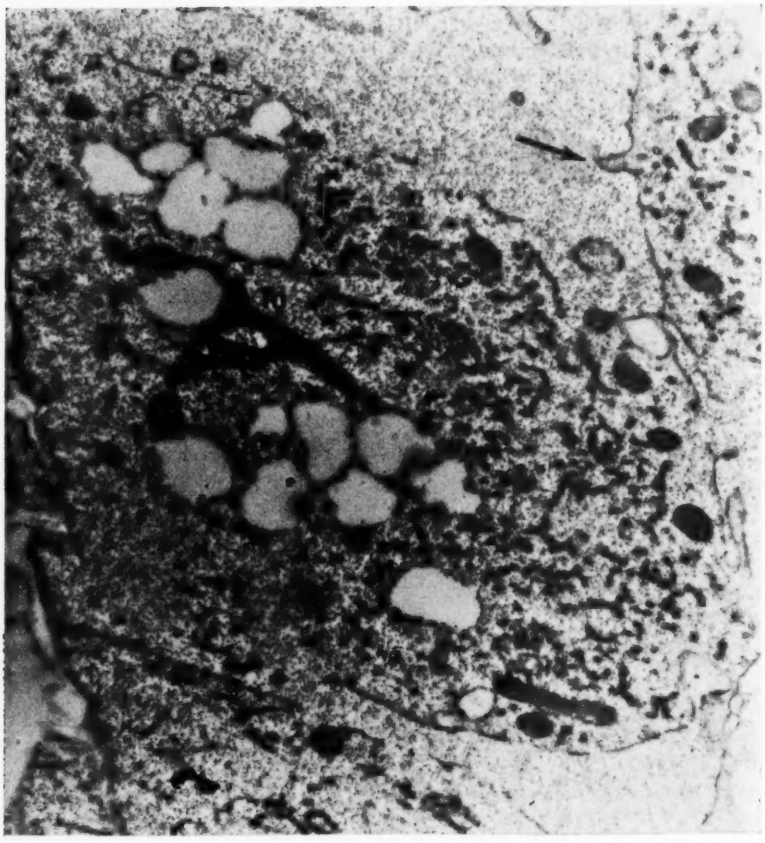

1μ

FIGURE 6

An electron micrograph of adjacent columnar follicle cells. An arrow points to a nipple-like projection of the wall of one cell which fits into an invagination in the wall of the adjacent cell. The large vacuoles may be the remains of large lipid droplets which have been completely extracted. A branching, filamentous mitochondrion (m) is in contact with one of these lipoidal epithelial bodies. The cytoplasm also contains ellipsoidal mitochondria and tubular endoplasmic reticulum.

in surface area. However, during stage 6 the follicle cells stop dividing. Subsequently increases in chamber volume are accompanied by increases in the surface area of the follicle cells. During stage 8 some follicle cells migrate posteriorly over the surface of the chamber to a position above the oocyte (King and Vanoucek, 1960). As yolk formation commences those follicle cells above the oocyte differentiate into type A, membranogenic cells; whereas those above the nurse cells differentiate into type B follicle cells which are incapable of forming membranes. The most anterior, type A, follicle cells migrate centripetally between the oocyte and adjacent nurse cells during stage 10 (see pg. 301) and during stages 12 and 13 form the chorionic appendages (see pg. 305). The other type A cells remain stationary and differentiate into a columnar epithelium. Type A cells are involved in the formation of the vitelline membrane and chorion. A small group of type B cells differentiate into the migratory border cells (see pg. 316); whereas the rest differentiate into squamous cells during stage 9 and during stage 12 degenerate.

The follicle cell cytoplasm contains mitochondria from the earliest stage. Some of these are filamentous forms which reach lengths of 3 micra and may branch several times (see figure 6). Mitochondria of this type are seldom observed in other ovarian tissues. The dense bodies which form in such huge numbers in the nurse cell cytoplasm during vitellogenesis are not seen in the cytoplasm of the follicle cells from the same chamber.

The cytoplasm of columnar follicle cells contains small populations of ellipsoidal, sudanophilic bodies which are roughly a micron in diameter (figure 5). These epithelial bodies are larger than dense mitochondria or the dense bodies, and under the electron microscope are seen as spheres which are surrounded by a husk of concentric, granular lamellae (figures 7 and 8). The spheres (which are either empty or contain clusters of granules) may be the remains of large lipid droplets which have been extracted completely or in such a way as to produce artifacts of the type described by Wigglesworth (see p. 313). Mitochondria are also often found intimately associated with these droplets (figure 6). The epithelial bodies presumably play some role in the fabrication of the lipoidal components of the vitelline membrane or endochorion.

The background cytoplasm stains with alcian blue, fast green, azure

FIGURE 7

An electron micrograph of four cells of the columnar epithelium. The section cuts through 4 nulei (n) and 8 epithelial bodies (e). These are surrounded by husks of endoplasmic reticulum. m, mitochondrion; p, plasmosome; s, epithelial sheath.

n
m
e

B, oil red O, cold Nile blue (after extraction with hot chloroform for one hour) and contains PA/S-reactive material (extractable by hot TCA). Extraction with hot TCA removes the fast green-positive material (which suggests the presence of hexosamine glycolipids). The concentration of carbohydrate, protein, and RNA is greater in

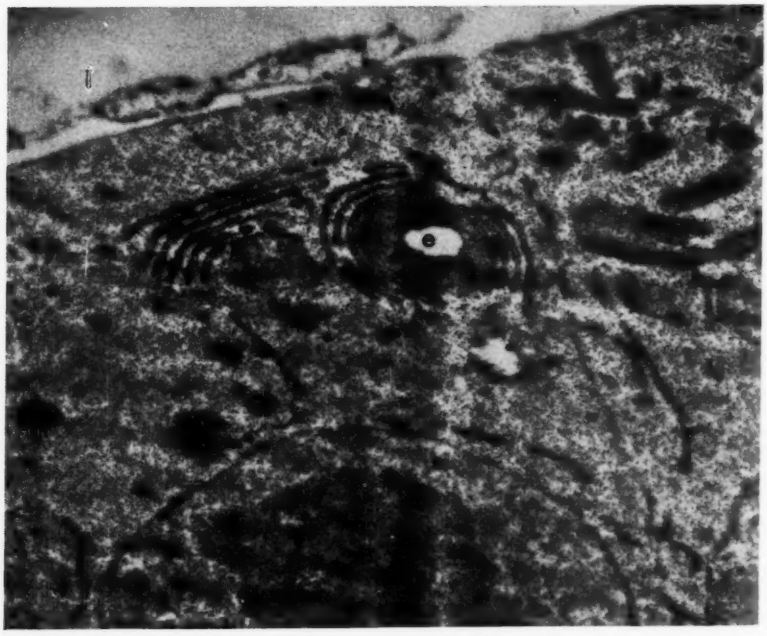

1μ

FIGURE 8

An electron micrograph of an epithelial body which has been only partially extracted. It is surrounded by a husk of concentric granular lamellae.

the cytoplasm of the columnar follicle cells than in the nurse cell cytoplasm or ooplasm at the same stage (figure 9). The cytoplasm of these follicle cells contains an endoplasmic reticulum at the time the vitelline membrane is synthesized. This endoplasmic reticulum becomes more extensive during chorion formation. In the follicular

epithelium of *Drosophilia* cells are occasionally seen which contain far greater concentrations of RNA and protein than their neighbors. These cells appear denser than their neighbors under phase contrast, and they fail to stain blue with alcian blue (unlike their neighbors). The cortex of the follicle cells is intensely PA/S-positive. After

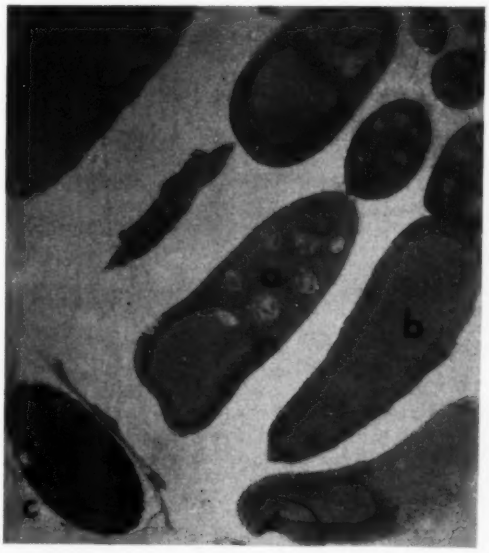

FIGURE 9

A light micrograph of a section of a portion of an ovary stained with azure B at pH 4 to demonstrate RNA. Oocytes in various stages of development include: (a) late stage 10, (b) stage 13, and (c) stage 14. The late stage 10 chamber is cut through the oocyte nucleus and six nurse cell nuclei. Note the azure B-positive nurse cell plasmosomes and the intense staining of the cytoplasm of the columnar follicle cells which surround the oocyte. Contrast the staining of the ooplasm in stages 13 and 14.

hydrolysis with trypsin or pepsin the only PA/S-positive areas remaining in the ovarioles are the cortical regions of the follicle cells.

The Cytochemistry and Ultrastructure of the Epithelial Sheath

The epithelial sheath also contains high concentrations of protein and carbohydrate. The PA/S-positive material of the epithelial sheath

is extracted by hot TCA. Bonhag has reported large amounts of PA/S-reactive material in the epithelial sheaths of *Anisolabis, Periplaneta* and *Oncopeltus*. The epithelial sheath is a contractile structure, and it contains numerous smooth muscle fibrils (figure 10). The epithelial sheath cylinder appears to be a highly specialized, tubular, multinucleate muscle cell. In the apical region where the germarial cortex and the epithelial sheath are adherent, numerous radially arranged fibrils are observed (King and Devine, 1958) both in the

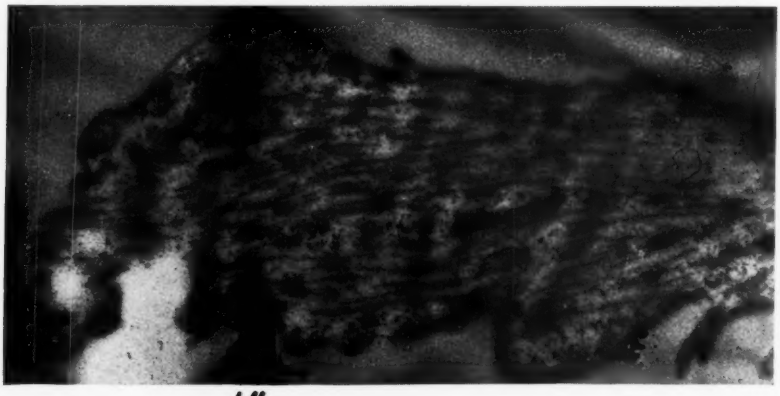

FIGURE 10
An electron micrograph of a portion of the epithelial sheath showing numerous smooth muscle fibrils.

germarial cortex and the sheath. These fibrils have dimensions similar to tonofibrils which are thought to function in maintaining a firm cohesion between adjacent cells (see Porter, 1954).

The Cytochemistry and Ultrastructure of the Oocyte during Vitellogenesis

Alpha yolk spheres: Yolk spheres which first appear in the ooplasm during stage 8 are seen under the electron microscope as homogeneous, electron-dense bodies between 1 and 3 micra in diameter which appear to arise by the growth of smaller, dense bodies a few hundred millimicra in diameter (figures 11 and 16). These early yolk spheres (hereafter called alpha spheres) and the bodies from which

they develop are surrounded by a double layered envelope. These yolk spheres stain with fast green, orange G, and mercuric bromphenol blue and are therefore proteinaceous. This protein is removed

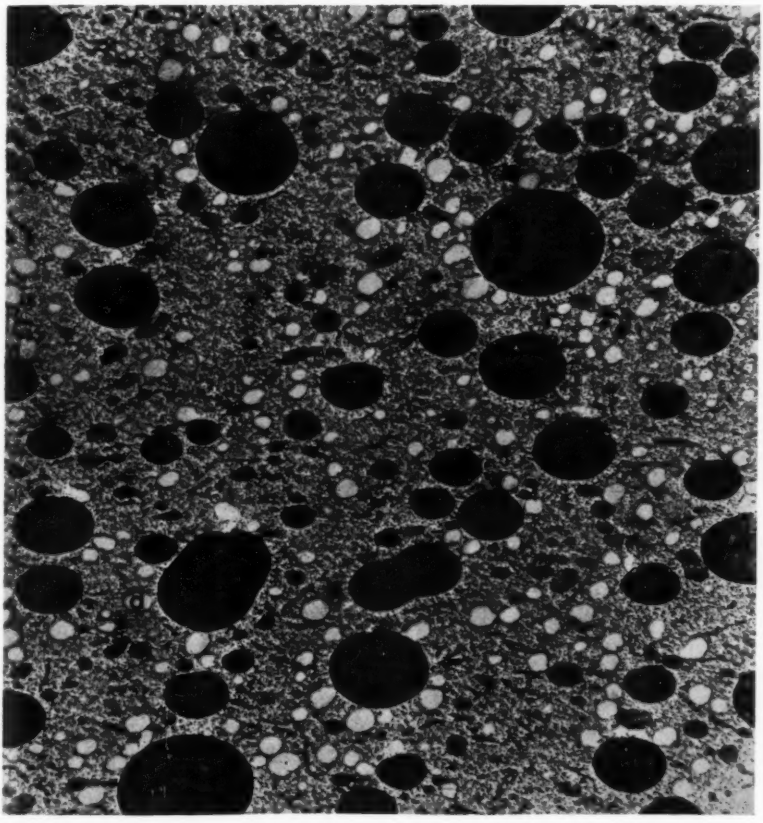

2μ

FIGURE 11

An electron micrograph of the ooplasm of an early stage 10 oocyte. Note the homogenous, electron dense, alpha yolk spheres (y), the dense, compartmented, ellipsoidal mitochondria (m), the pale vacuoles which presumably are extracted fat droplets (d), and the scattered filaments of endoplasmic reticulum. Contrast with Figure 1.

by both trypsin and pepsin. The phenylmercuric chloride-ammoniacal silver nitrate procedure demonstrates the presence of sulfhydryl groups in these spheres. Alpha spheres stain black with iron haematein and stain pale green and deep purple with azure B at pH 4 and 9, respectively.

At room temperature alpha spheres fail to color with Nile blue, but they color blue-green when the methacrylate-containing section

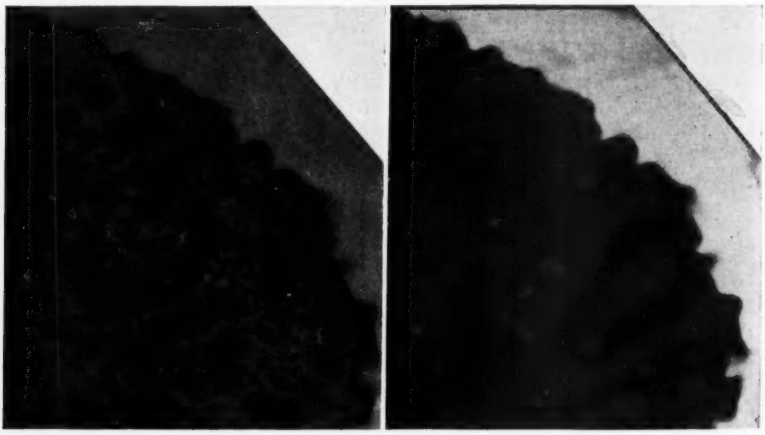

10μ

FIGURE 12

(Left) A light micrograph of a stage 14 oocyte stained with cold Nile blue. Dye is taken up by the beta spheres and the vitelline membrane.

(Right) As above—stained with hot Nile blue. Dye is taken up by the alpha spheres, the background ooplasm and the vitelline membrane.

is placed in hot stain (figure 12). If the section is placed in boiling water, transferred to water at 21° C and then to cool aqueous Nile blue, the alpha spheres fail to stain. However, if the section is soaked for 1 hour in chloroform at 56° C and subsequently cooled, the alpha spheres now stain with cold Nile blue. During stage 8 the spheres stain green, but as they increase in size, they take on a blue coloration. After extraction with hot acetone, ethanol or toluene, the spheres of varying sizes fail to stain with Nile blue at low temperatures but stain

green at high temperatures. To explain these observations it is postulated that as the alpha sphere matures it accumulates increasing amounts of an acidic lipid-protein complex which fails to stain with Nile blue while intact, which dissociates in hot aqueous solution (but is not washed out of the section) and reassociates when cooled, but which remains dissociated (but is not removed from the section) after being heated in chloroform and then cooled. The dissociated acidic lipid colors blue with Nile blue and is soluble in hot acetone, ethanol or toluene. In electron micrographs (figure 16) vacuoles are often noted in the smaller alpha spheres but not in the mature ones which suggests that the lipid component becomes more insoluble in organic solvents as the yolk sphere matures. A second compound which stains green with hot Nile blue and is insoluble in hot water, hot chloroform, or hot acetone, also occurs in the alpha sphere.

Alpha spheres contain relatively small amounts of PA/S-positive material (figure 2 left). If the LT/S procedure is used, the alpha sphere carbohydrates stain more intensely if the oxidation is carried out at low than at high temperature. Subsequent to the removal of the lipids, protein and carbohydrates can be demonstrated in the sphere. These carbohydrates can be removed by hot TCA, (figure 2 right), but the spheres retain their fast green stain-ability. PA/S-positive carbohydrates cannot be demonstrated in alpha spheres at stage 13 or 14, although the spheres still contain lipid and protein. At these stages, however, the ground ooplasm becomes PA/S-reactive suggesting that carbohydrate leaves the alpha spheres and enters the ooplasm. Carnoy's fluid extracts the carbohydrate and lipid of the alpha spheres.

Alpha spheres are dense (figure 13) and osmiophilic. This binding of osmium can be shown to an enhanced degree by using the ethyl gallate method of Wigglesworth (1957). However, if an ovary is placed for 15 minutes in Ringer solution saturated with bromine and subsequently fixed in osmium and embedded as previously described, alpha spheres are not found in the cytoplasm of oocytes at appropriate stages. Alpha spheres are found in ovaries fixed in permanganate according to the method of Luft (1956). $KMnO_4$ is known to be insoluble in fats and oils. It is clear that alpha spheres can survive passage through ethanol and butyl methacrylate if certain of the compounds which comprise them are bound to osmium or manganese. The

compounds linked through osmium are unsaturated lipids. Perhaps proteins are bound by manganese.

According to Ward (1959) yolk platelets of the mature egg of *Rana pipiens* arise from oocyte mitochondria. The alpha yolk spheres of *Drosophila* may also originate from mitochondria, since many of

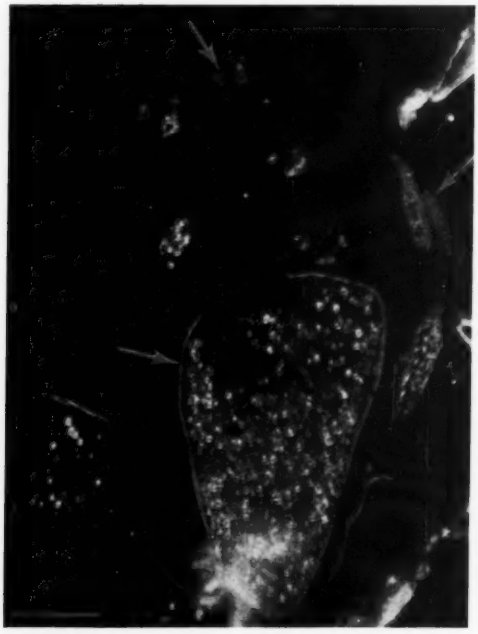

FIGURE 13

A late stage 10 chamber photographed with dark field illumination. Note the bright alpha spheres. Arrows point to the vitelline membrane, a nurse cell plasmosome, and to the chorionic appendages of an adjacent egg.

the smaller bodies from which alpha yolk spheres arise are the size of mitochondria and are surrounded by a double layered envelope. However, no typical cristae have been resolved as yet in these bodies.

Beta yolk spheres: The stage 14 oocyte contains alpha spheres which have reached their maximum size. During this stage a second type of yolk sphere (hereafter called a beta sphere) is seen which is about

the same size as the alpha sphere. At early stages there seems to be a size gradient of beta spheres, those at the micropylar end being the smallest. At late stages many beta spheres appear to coalesce. Unpublished observations by D. F. Poulson and the author indicate that

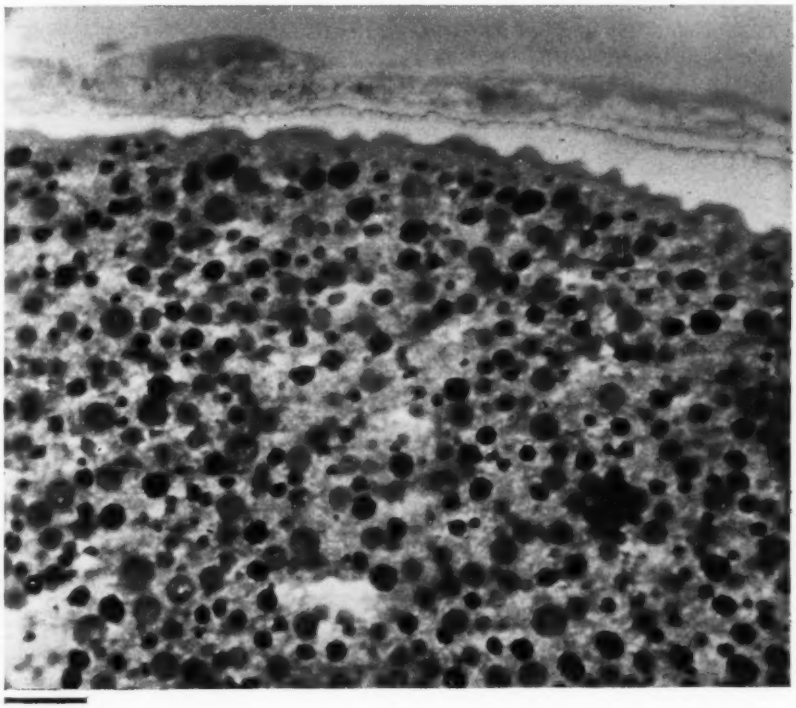

FIGURE 14

A light micrograph of a mature egg stained with the PA/S procedure and counterstained with fast green. Alpha spheres (which stain green) appear as large pale spheres; whereas beta spheres (which stain red) appear as large dense bodies. The vitelline membrane and chorion are out of focus.

in *D. willistoni* beta spheres arise from smaller bodies which are formed at the surface of alpha spheres. Beta spheres are protein free, but they contain very large amounts of PA/S-reactive material (figure 14). When the LT/S procedure is used, the beta sphere carbohy-

drates stain much more intensely if the oxidation is carried out at high than at low temperature. This polysaccharide is alcian blue-positive, stains metachromatically with Nile blue and is resistant to extraction by hot TCA. Thus, the beta sphere differs from the alpha sphere in the amount and type of carbohydrate it contains and in that it contains little or no protein. Beta spheres also contain a lipid which differs from the lipid of alpha spheres. The beta sphere lipid colors blue intensely and instantaneously with Nile blue at room temperature (figure 12 left) but is readily removed by toluene, acetone, chloroform, or ethanol (1 hr. at 56° C). PA/S-reactive material remains after extraction with lipid solvents. Beta spheres stain a pale, pinkish-green with azure B at pH 4 and pink with azure B at pH 9. Beta spheres which stain blue with cold Nile blue are found in permanganate-fixed ovaries. Carnoy's fluid removes the beta spheres.

In electron micrographs beta spheres appear as pale, spongy, plumbophilic masses which are often in close association with mitochondria (figures 15 and 16). Alpha and beta spheres are present in approximately equal numbers in the mature egg. There are approximately 85,000 spheres of each type in the mature oocyte, and together they take up about ¼th the volume of the egg.

Mitochondria: In *Drosophila,* dense mitochondria are found scattered throughout the ooplasm (figure 11). These mitochondria are demonstrated particularly effectively by staining sections with 1% Sudan black B (unacetylated) dissolved in acetone. A mature egg contains approximately $7x10^4$ mitochondria.

Tiny droplets: The ooplasm contains myriads of droplets (figure 11) which are at or are just above the limit of resolution of the light microscope. A mature egg contains $7x10^5$ droplets of this type which together make up about 1% of its total volume. Since these droplets fail to color with any of the staining procedures attempted, it appears that they represent vacuoles whose contents have been extracted. Under the electron microscope most droplets are devoid of external membranes, but a few are surrounded by limiting membranes, and in some cases the coverings of the vacuoles appear to be studded with granules (King and Devine, their figure 11) which are well below the resolving power of the light microscope. However, less complicated envelopes may be fixation artifacts (see p. 43).

The nucleus: A single, spherical plasmosome has been observed in

the nucleus of a stage 9 oocyte which stains with fast green and azure B.

The background cytoplasm: The background cytoplasm of osmium-fixed oocytes in stages 8-12 *fails* to color with Nile blue at room temperature but stains pale blue with hot Nile blue. Hower, the ooplasm will color intense blue with cold Nile blue, if the sections are soaked for 1 hour in hot chloroform, toluene or ethanol. The cyto-

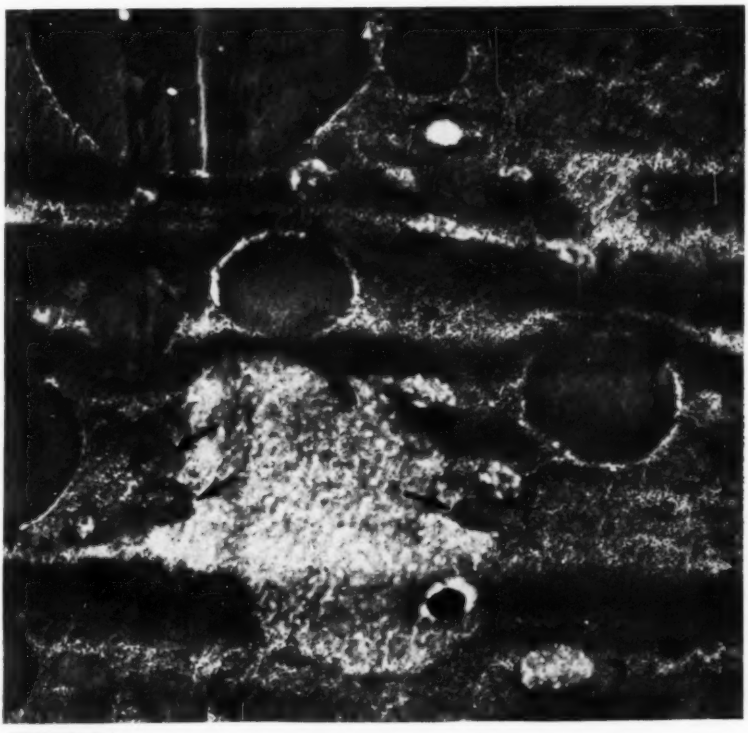

1μ

FIGURE 15

An electron micrograph of stage 14 ooplasm. Contrast the density of the background material with that in Figure 11. Note the homogenous, dense alpha spheres and the pale, spongy beta sphere. Arrows point to mitochondria embedded in the cortex of the beta sphere.

FIGURE 16

An electron micrograph of a section stained with lead hydroxide from a vestopal-embedded mature egg of *Drosophila willistoni*. The star marks a lead crystal in the center of a beta yolk sphere. The *m* marks one of the mitochondria which cluster about the sphere. The *y* marks a developing alpha sphere. Some of its contents have been extracted, and it is surrounded by a double layered membrane.

FIGURE 17

An electron micrograph of a section stained with lead hydroxide from a vestopal-embedded mature egg of *Drosophila willistoni*. The arrow points to a convoluted portion of the plasma membrane. Lead crystals bound to the vitelline membrane (v) give it a spotted appearance. A *c* marks the outer endochorion. Compare with figure 19.

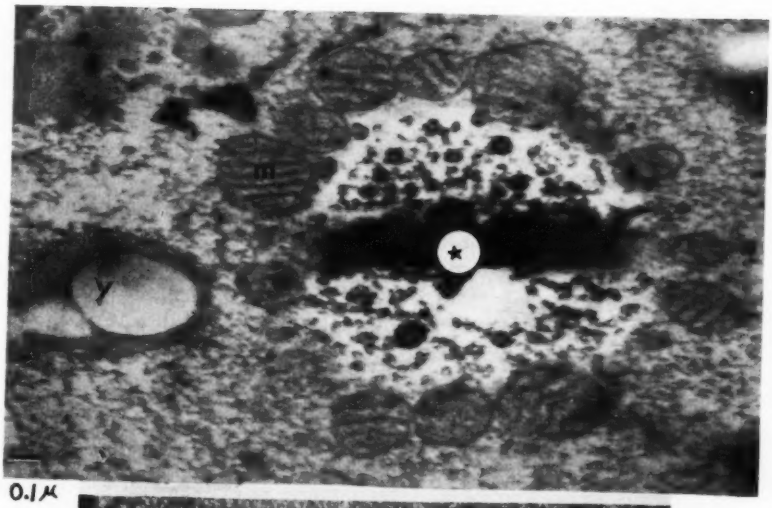
m
Y
0.1 μ

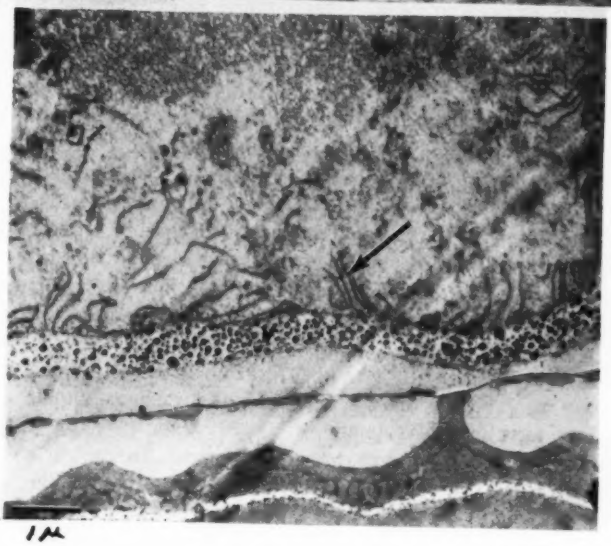
1 μ

plasmic material coloring with Nile blue is soluble in hot acetone. The lipoidal material found in the ooplasm thus has properties similar to the acidic lipid-protein complex of the dense bodies (see p. 282). Ooplasm from permanganate-fixed oocytes *does* stain with cold Nile blue. The lipoidal material of the ooplasm increases in concentration as the oocyte grows, but the maximum is reached during stage 14; i.e., after the oocyte has stopped growing.

The stage 14 ooplasm colors with oil red O and Sudan black B and is the most osmiophilic structure observed in ovaries. A 1-hour extraction at 56° C with acetone only removes a portion of the Nile blue-positive material present at this stage; whereas this procedure takes out all Nile blue-positive, cytoplasmic material from oocytes at earlier stages of development. Stage 14 ooplasm stains pinkish-brown with the Schiff reagent. The ground cytoplasm of oocytes in stages 8 through 12 stains pale purple with azure B, but deep purple during stage 14 (figure 9). Extraction with hot TCA removes the material which stains with azure B but fails to remove the material which stains with Nile blue. Thus, there is cytochemical evidence that RNA accumulates in the ooplasm during vitellogenesis. In *Drosophila* the vitelline membrane is completed by the beginning of stage 12, and therefore no further contribution of RNA to the ooplasm can be made by the nurse cells. Yet a great increase in the concentration of RNA obviously occurs between stage 12 and 14.

Electron micrographs demonstrate that the ooplasm of stage 10 oocytes contains scattered elements of endoplasmic reticulum (figure 11). The majority of these filaments presumably arise from the envelopes of nurse cell nuclei. Stage 14 ooplasm is much more electron dense (figure 15) and shows an extensive endoplasmic reticulum, especially in the cortex of the egg. It may be that this cortical endoplasmic reticulum arises from the plasma membrane which is thrown into folds (see figure 17). The proliferation of the endoplasmic reticulum does *not* require the presence of the nuclear envelope, since the nuclear envelope disappears previously (see p. 314). However, some endoplasmic reticulum may arise from filaments previously transferred from the nurse cell nuclei to the oocyte. The lamellar stacks of King and Devine (their figure 26) may represent instances of endoplasmic reticulum in the act of proliferation.

During stages 8 through 12 the back-ground ooplasm stains pale

yellow with orange G, pale green with fast green, and very pale pink following the PA/S procedure. The cytoplasm of stage 13 oocytes contains more PA/S-reactive material. If the LT/S procedure is used, these carbohydrates stain more intensely if the oxidation is carried out at low than at high temperature. The cytoplasm stains with fast green but fails to stain with Schiff's reagent after periodic oxidation if a hot TCA extraction is performed (figure 2 right). Carnoy's fluid extracts the carbohydrate of the alpha spheres, but PA/S-positive material remains in the ooplasm of mature, Carnoy-fixed oocytes which is removed by pepsin or trypsin. These facts suggest that the mature ooplasm contains a glycoprotein. Perhaps the polysaccharide lost from the alpha spheres enters the ooplasm and combines subsequently with protein. The early ooplasm stains with alcian blue, but the mature ooplasm is alcian-blue negative and contains alcian blue-positive beta spheres. Perhaps the acid mucopolysaccharides of the ooplasm are transferred to the beta spheres during stage 14.

Stage 14 ooplasm is fast green and PA/S-positive, but oocytes extracted with hot TCA are fast green and PA/S-negative. These findings suggest that there is also a hexosamine-containing polysaccharide present in the mature ooplasm.

The Cytochemistry and Ultrastructure of the Vitelline Membrane

The formation of the vitelline membrane takes about 3 hours and lasts from stage 8 through stage 11 (King and Devine, 1958). It is formed by the fusion of vitelline bodies which accumulate in the intercellular space between the follicle cells and the oocyte (figure 18). During the synthesis of the vitelline membrane the cell walls of both follicle cells and oocyte are thrown into numerous microvilli which project into the intercellular space. During stage 10 follicle cells migrate between the oocyte and the adjacent nurse cells, and the vitelline membrane is extended inwards concurrently. However, the vitelline membrane is not laid down across the intercellular bridges, and consequently material still can enter the oocyte from the nurse cells. However, these passages are blocked during stage 11. The vitelline membrane like the beta sphere is plumbophilic (see figure 17).

The vitelline membrane is osmiophilic and can survive passage through ethanol and butyl methacrylate if fixed with osmium tetrox-

ide. The membrane is leached out of brominated, osmium-fixed oocytes. The vitelline membrane (and the alpha spheres) withstand paraffin-embedding after fixation in Kahle's fluid. Carnoy's fluid removes the vitelline membrane of oocytes in early yolky stages. This membrane is one of the densest structures in the egg, and it shows

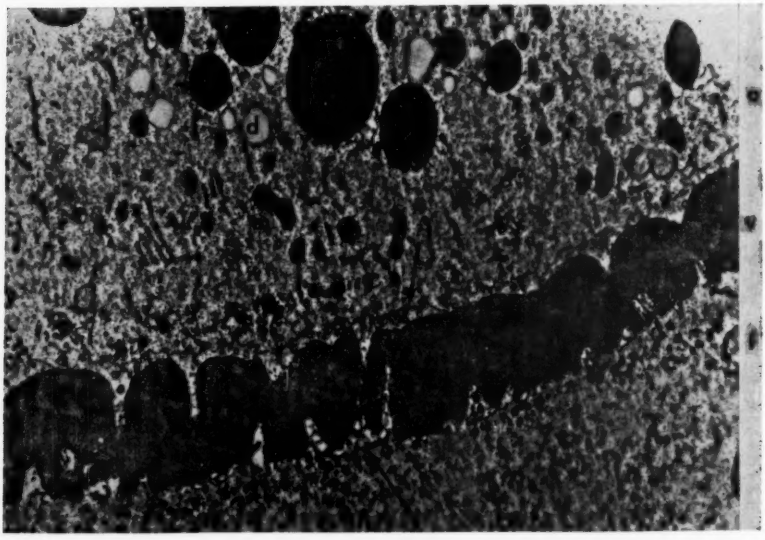

1A

FIGURE 18

An electron micrograph of the border between the follicular epithelium (f) and the oocyte (o). The vitelline membrane (v) is formed in the intercellular space. The cell walls of both the follicle cells and oocyte are thrown into numerous microvilli (see arrows) which project into the intercellular space. Mitochondria (m), fat droplets (d) and alpha yolk spheres (y) are seen in the ooplasm. Scattered filaments of endoplasmic reticulum are found in the ooplasm and follicle cell cytoplasm. Numerous dense spheres which are smaller than ellipsoidal mitochondria occur near the cell walls. The origin, fate and function of these particles is unknown.

up brilliantly under dark field or phase contrast illumination (figure 13).

If one observes a section while it is staining at room temperature in Nile blue or fast green, the vitelline membrane is the first structure to bind the dyes (figure 12 left) (second come the beta spheres and

third the chorion). The vitelline membrane stains most intensely during stage 10. A one hour extraction with hot chloroform, toluene, acetone or ethanol removes considerable lipid from the developing vitelline membrane in early stages (8 through 10). However, the integrity of the membrane is not impaired. Acetone and ethanol are more effective solvents than chloroform and toluene. A small amount of lipid is extracted by acetone or ethanol from the stage 12 vitelline membrane, but the stage 14 vitelline membrane resists the action of lipid solvents. The vitelline membrane colors with Sudan black B but not with oil red O.

The vitelline membranes of oocytes in stages 13 and 14 stain with fast green after attempted hydrolysis with either trypsin or pepsin. The protein of the vitelline membrane differs from all others observed in that it is sensitive to acid conditions. Thus, if a section is treated with warm 1 N HCl (as in the Feulgen procedure) or cold 1% periodic acid (as in the PA/S procedure), the vitelline membrane fails to bind fast green. However, the integrity of the membrane is not destroyed. The phenylmercuric chloride-ammoniacal silver nitrate procedure demonstrates the presence of sulfhydryl groups in this structure in greater concentration than in any other. The vitelline membrane of osmium-fixed oocytes stains with iron haematein.

The vitelline membrane contains large amounts of PA/S-reactive material. If the LT/S procedure is used, the *Drosophila* vitelline membrane stains intensely whether the oxidation is carried out at high or low temperatures. The vitelline membrane stains green with azure B at pH 4, but blue at pH 9. Carnoy's fluid extracts the carbohydrate of the mature vitelline membrane, but not the lipid.

The vitelline membrane forms a flexible, waterproof covering about the oocyte. The lipid material presumably functions as the waterproofing agent.

The Cytochemistry and Ultrastructure of the Chorion

The chorion, which forms a hard, dense protective covering about the oocyte, starts to be laid down by the follicular epithelium immediately after the vitelline membrane is finished. The mature chorion is seen in electron micrographs to consist of a dense endochorion which faces the vitelline membrane and a pale, outer exochorion (figure 19). The endochorion is made up of an inner layer (which

rests upon the basement membrane of the follicle cells) and an outer layer. The inner and outer layer are laid down during stages 12 and 13, respectively, and the exochorion is finished during stage 14. The two endochorionic layers are separated by an endochorionic space

1μ

FIGURE 19

An electron micrograph of the mature chorion. f, degenerating follicle cell; e, exochorion; x, outer endochorion; s, endochorionic space. The nearly vertical and horizontal arrows point to the inner endochorion and the basement membrane of the follicle cell, respectively.

which at first contains fluid, but this is replaced by air as the egg leaves the ovariole (Wigglesworth and Beament, 1950). The space is subdivided into open and closed compartments by endochorionic pillars and septa which connect the two endochorionic layers.

The mechanism by which air appears in the egg shell is not understood. The compartmented layer in the eggs of *Dixippus* and *Blattella* consists of lipoprotein, and Wigglesworth and Beament suggest that the lipid renders the layer hydrophobic. If a certain amount of fluid was subsequently actively absorbed by the oocyte, the dissolved gases in the remaining endochorionic fluid would be liberated. Whatever the mechanism, the air-filled chorion serves both as a protective covering and a respiratory surface. According to Wigglesworth and Beament the presence of an enclosed layer of air outside a waterproof membrane increases the impermeability of the system to water, while providing a large area across which diffusion can occur. According to Hinton (1959) the silvery, dorsal, chorionic appendages (figure 20) serve both for the extraction of oxygen dissolved in water and for atmospheric respiration. In situations where the egg is not emersed in some fluid the appendages do not involve water loss over an enormous surface, since the connexion between the appendage and the rest of the relatively impermeable chorion is small.

The chorion is modified at the anterior pole of the oocyte to provide for the fertilization of the egg. The endochorion forms a protuberance, the chorionic micropylar cone, which contains a tubular canal, the micropyle. In the region of the micropylar cone the endochorion is not compartmented. The ooplasm and its surrounding vitelline and plasma membranes protrude into the chorionic micropylar cone to form a nipple-like projection (figure 21). The micropyle appears to end at the vitelline membrane (Nonidez, 1920), and it is not known if the vitelline membrane is perforated near the base of the micropyle as in certain other dipterous eggs (Pantel, 1913). If perforations are not present, the spermatozoan must carry with it enzymes which can digest both the vitelline and plasma membranes which present barriers 500 and 20 millimicra thick, respectively (King and Devine, 1958). In *Rhodnius* a subendochorionic layer of waterproofing wax (250 mμ thick), which covers the inner openings of the micropyles, is penetrated by the fertilizing sperm. The perforation is repaired within a few hours after fertilization, and a fertilization membrane

2μ

FIGURE 20

An electron micrograph of the two developing chorionic appendages which are characterized by dense endochorionic pillars and septa. Four follicle cell nuclei are included in the section. The cytoplasm contains mitochondria, fat droplets and endoplasmic reticulum.

is produced immediately beneath the waxy layer (Beament, 1948, 1949).

In *Drosophila* the endochorion fails to color with oil red O, colors with Sudan black B, colors blue with cold Nile blue and dark blue with hot Nile blue. The Nile blue-positive lipid is extracted by hot

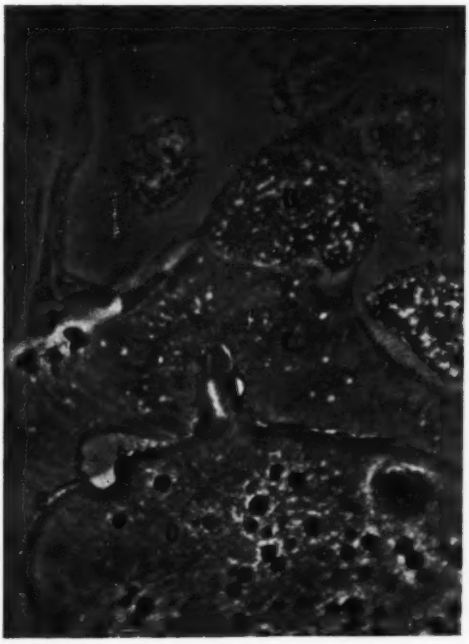

10μ

FIGURE 21

A phase contrast micrograph of the forming, nipple-shaped, micropylar apparatus. o, ooplasm; c, follicle cell cytoplasm; v, vitelline membrane; e, endochorion; n, degenerating nurse cell nucleus.

ethanol or acetone but not by hot chloroform. Hot toluene also extracts lipid but not as effectively as ethanol or acetone. Thus, the compartmented layer contains lipid in *Drosophila* as well as *Dixippus* and *Blattella*. The endochorion is present in oocytes which are brominated prior to osmium fixation.

The endochorion stains intensely with fast green, iron haematein and contains large amounts of PA/S-reactive material. If the LT/S procedure is used, the intensity of staining is similar whether high or low temperatures are used for the oxidation. The endochorion stains pale green with azure B at pH 4, but deep blue at pH 9. Carnoy's fluid extracts the lipid of the endochorion, but not the polysaccharide. The endochorion stains with fast green after attempted hydrolysis with trypsin or pepsin.

The exochorion contains large amounts of acid mucopolysaccharides and gives positive but weak reactions for lipid and protein. During the formation of the exochorion, the endoplasmic reticulum reaches its maximum development.

Summary of Cytochemical Findings

In the ovary deoxyribonucleoprotein is confined to the chromosomes and ribonucleoprotein to the plasmosomes and background cytoplasm. Four classes of protein can be demonstrated cytochemically, all of which stain with fast green. P_1 is extracted by both pepsin and trypsin; whereas P_2 resists both proteolytic enzymes. P_3 unlike the other proteins is sensitive to acidic conditions. P_4 unlike the others is PA/S-positive and is therefore a glycoprotein. Proteins belonging to the first class are found in the alpha spheres, and those of the second class are restricted to the endochorion. P_3 proteins occur in the mature vitelline membrane, and P_4 proteins in the mature ooplasm. DNA-proteins resist pepsin and trypsin; whereas RNA proteins are extracted by trypsin but not by pepsin.

Six classes of periodic acid-Schiff-positive carbohydrates are present in the ovary. C_1, found in the beta spheres, has the properties of a weakly sulfated mucopolysaccharide. It is alcian blue-positive, it stains metachromatically with Nile blue and is resistant to extraction by hot TCA. When the LT/S procedure is employed and the temperature at which the oxidation takes place is increased, the C_1 carbohydrates (unlike all others) stain *more* intensely. C_2, found in the exochorion, nurse cell cytoplasm, follicle cell cytoplasm, and early ooplasm is an acid mucopolysaccharide which stains with alcian blue and is readily extracted by hot TCA. C_3, found in the follicle cell cytoplasm and mature ooplasm, behaves like a hexosamine-containing polysaccharide. It is fast green-positive and readily extracted by hot

TCA. C_4, found in the plasmosomes and the young alpha spheres, can be removed by extraction with hot TCA. C_5, found in the mature vitelline membrane is resistant to extraction by hot TCA (figure 2 right), but is missing from Carnoy-fixed ovaries. C_6, found in the endochorion, is retained in Carnoy-fixed material and also resists TCA extraction. Since C_4, C_5 and C_6 carbohydrates stain with the LT/S procedure, they are not glycogens (see p. 270), and since they fail to bind acidic or basic dyes, they appear to be neutral mucopolysaccharides.

Six categories of acidic lipids are found in the ovary. These lipids are presumably phospholipids, since fatty acids would not be expected to survive the dehydration treatments to which the tissues were exposed. Furthermore fatty acids (unlike phospholipids) color very weakly with concentrated Nile blue solutions (Cain, 1947). Recent analyses of *Drosophila* by Wren and Mitchell (1959) have revealed an abundance of phospholipids. L_1, L_2 and L_3 lipids may or may not be bound to protein. They stain blue with cold Nile blue; whereas L_4, L_5 and L_6 are lipid-protein complexes of a type which stains with cold Nile blue only after certain "unmasking procedures". L_1 lipids are soluble in hot acetone, chloroform, ethanol or toluene, L_2 lipids are insoluble in hot chloroform, but soluble in hot acetone, ethanol, or toluene, and L_3 lipids are insoluble in all the hot organic solvents mentioned above. Beta yolk spheres contain lipids of the L_1 type, the endochorion contains the L_2 type, and the mature vitelline membrane contains type L_3 lipid. However, at early stages in its development the vitelline membrane contains acidic lipids which are soluble in hot organic solvents. Thus, maturation of the vitelline membrane involves changes in the lipid which confer upon it a resistance to extraction by organic solvents. L_4 lipids are insoluble in hot chloroform, but soluble in the other organic solvents; L_5 lipids are soluble in hot acetone, but insoluble in the other solvents; and L_6 lipids are insoluble in all solvents (but are sudanophilic). Alpha yolk spheres contain L_4 lipids, the cytoplasmic mitochondria and dense bodies and the early ooplasm contain L_5 lipids, and the mature ooplasm, the cytoplasm of the columnar follicle cells and the plasmosomes contain lipids of the L_6 type.

The dense bodies (which disappear once they enter the oocyte) and the ooplasm contain lipids of similar cytochemical properties.

These findings suggest that the ooplasm receives a lipid contribution from the dense bodies. The maturation of the ooplasm confers upon its lipids a resistance to extraction by organic solvents. Some of this information is summarized in Table 1.

The RNA which initially accumulates in the ooplasm arises from the nurse cell nuclei, but the subsequent build-up of ooplasmic RNA is independent of the nurse cells and the oocyte DNA.

Discussion

The plasmosomes: It has been shown in this paper that the plasmosomes of the nurse cell nuclei contain, in addition to RNA, a carbohydrate (which behaves like a neutral mucopolysaccharide) and a phospholipid-protein complex. Previous reports of carbohydrates in nucleoli have come from Monné and Slautterback (1950) and from Stich (1951), and Baker (1946) has demonstrated phospholipids in plasmosomes. More recently Wang, Mayer and Thomas (1953) have isolated lipoproteins from liver nuclei of rats.

The plasmosomes of the nurse cells may play an important role in the formation of yolk spheres. There exist in the literature numerous references to the occurrence of nucleolar emissions during vitellogenesis Buchner (1918), Chaudhry (1951), Srivastava (1953), Yosufzai (1953), Lewis and Walton (1958), and Bonhag (1958, 1959). Hsu (1952, 1953) reported that in *Drosophila melanogaster* the proteinaceous yolk (the alpha yolk) spheres originate from precursors embedded in the matrix material of flakes which are emitted by the plasmosomes of the nurse cells. The matrix material is considered to be lipoidal (since it is best preserved after prolonged chromation and is lost after acid fixation), and it contains little or no RNA or DNA. The flakes are the result of localized exudation by the plasmosomes at specific spots on their surfaces. The flakes and the plasmosomes stain intense purple and yellowish, respectively, after fixation in Champy's fluid and staining by Benda's alizarin S-iron alum-crystal violet technique. The flakes pass bodily from the nucleoplasm through the nuclear membrane into the cytoplasm where they release minute granules which in time develop into individual proteinaceous yolk spheres. That nucleolar material passes from the nurse nucleus to the cytoplasm is fairly certain from our studies. But whether these granules develope directly into alpha spheres is far from clear.

TABLE 1

	DNA Protein	RNA Protein	P_1	P_2	P_3	P_4	C_1	C_2	C_3	C_4	C_5	C_6	L_1	L_2	L_3	L_4	L_5	L_6
Nurse and follicle cell chromosomes	+																	
Nurse cell plasmosomes		+								+								+
Nurse cell cytoplasm		+						+										w
Columnar follicle cell cytoplasm		++						+	+									+
Cytoplasmic particles																	+	
Early ooplasm		w						+									+	
Mature ooplasm		++				+			+									+
Alpha yolk spheres			+							early + late −						+		
Beta yolk spheres							+						+					
Mature vitelline membrane					+						+				+			
Endochorion				+								+		+				
Exochorion								+										

w = weak reaction

The yolk spheres: The mature oocyte of *Drosophila* contains two types of yolk spheres: the alpha spheres which arise first and contain a phospholipid-protein complex and the beta spheres which contain mucopolysaccharides and phospholipids. This situation seems to be different from that encountered by workers in other insect species. In the oocytes of *Anacridium* (Columbo, 1955), *Oncopeltus* (Bonhag, 1956), *Periplaneta* (Nath, Gupta and Lal, 1958), and *Culex* (Nath, Gupta and Bains, 1958) large, PA/S-positive yolk spheres are observed which contain protein as well. Where tested, the PA/S-positive material has been shown *not* to be glycogen.

Mitochondria: The mitochondria of *Culex* and *Periplaneta* have been shown cytochemically to contain phospholipids (Nath, Gupta and Bains, 1958 and Nath, Gupta and Lal, 1958). Biochemical studies on rat liver mitochondria by Swanson and Artom (1950) have demonstrated that they contain large quantities of lipids. 80% of the lipids are phospholipids and of the phospholipids, lecithin and phosphatidylethanolamine were the most abundant.

Ooplasmic carbohydrates: Shiomi and Kitazume (1956) have reported that 6% of the ooplasm of mature, unfertilized *Drosophila* eggs is glycogen. 94% of the glycogen is soluble "lyoglycogen" and the remainder is poorly soluble "desmoglycogen". As embryogenesis proceeds, the lyoglycogen content declines; whereas the desmoglycogen content remains constant. The egg of *Bombyx mori* contains 2% glycogen (Tichomiroff, 1885). PA/S-positive materials are abundant in the ooplasm of *Drosophila*. However, these polysaccharides do not behave like glycogens with respect to the LT/S test. The most abundant carbohydrate found in the background cytoplasm behaves like a hexosamine-containing polysaccharide. Pigorini (cited by Needham, 1931) found a glucosamine-protein conjugate that made up 51% of the total protein of the silkworm oocyte. Mature ooplasm also contains a glycoprotein.

Ooplasmic lipids: In *Drosophila melanogaster* Levenbook, Travaglini and Schultz (1958) have shown that RNA makes up 2% of the ooplasm of laid, unfertilized eggs. King and Wilson (1954) demonstrated that *Drosophila* eggs contain the highest phosphorous concentration of any developmental stage (0.5%). RNA phosphorous can account for only 40% of the total phosphorous. Phospholipids probably make up a considerable amount of the phosphorous unaccounted

for, since the present study has shown that the ooplasm is very rich in these compounds. In silkworm ooplasm neutral fats and phospholipids make up about 85% and 10% of the total ether extractable lipids, respectively (Tichomiroff, 1885), and 64% of the energy required for embryogenesis is provided by fat combustion (Farkas, 1903).

The fact that insect eggs are rich in fats (the ooplasm of the silkworm contains 9% fat according to Tichomiroff) suggests that the tiny

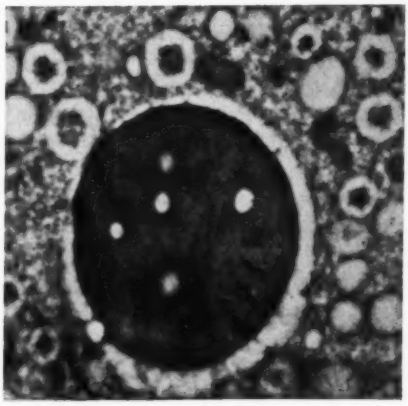

FIGURE 22

An electron micrograph of the ooplasm of a stage 10 oocyte showing an alpha sphere, several dense, ellipsoidal mitochondria, and vacuoles, some of which contain clusters of granules.

vacuoles seen in the ooplasm of *Drosophila* represent extracted fat droplets. Nath and his collaborators have shown in *Culex* and *Periplaneta* that lipids are confined to relatively small spheres which undergo radical quantitative changes in their composition as they mature. One often sees in electron micrographs of *Drosophila* oocytes tiny membrane-covered spheres containing particulate material (figure 22), and these structures may represent partially extracted lipid droplets which have undergone reactions with osmium similar to those described by Wigglesworth. Wigglesworth (1957) has pointed

out that osmium may be retained in a thin insoluble layer of lipid over the surface of a lipid droplet. The molecules of lipid at the surface of such a droplet are oriented with their hydrophilic groups outside and their paraffin chains aligned. These chains have a more or less constant composition, and the ethylenic linkages of corresponding components will lie adjacent to one another. Osmium may then bind these chains together, causing the lipid to polymerize over the surface (see Stoeckenius, 1959). Wigglesworth performed model experiments in which he fixed films of oil droplets in agar with osmium tetroxide. The oil droplets consisted of liquid paraffin containing 1% of various test lipids. When phosphatidyl ethanolamine was used the droplets formed a robust surface membrane from which innumerable trabeculae passed inwards. Interspersed among this network were numerous black granules. The appearance of such droplets is quite similar to those observed in electron micrographs of oocytes.

RNA synthesis: Autoradiographic studies (King and Burnett, 1959; Zalokar, 1960; and King and Falk, 1960) suggest that RNA synthesis occurs primarily in the nurse cell nuclei of immature egg chambers and that subsequently nuclear RNA enters the cytoplasm of the nurse cell and the ooplasm.

The contribution of RNA by trophocytes to the oocyte is known for two other species of insects with polytrophic ovaries, the silkworm (Columbo, 1956) and the bee (Morgenthaler, 1952 and Bier, 1954) and for two species with telotrophic ovaries, the bedbug (Dasgupta and Ray, 1954) and the large milkweed bug (Bonhag, 1955). Evidence from radio-tracer experiments for the nuclear origin of RNA in the salivary gland cells of *Drosophila repleta* larvae has been described by Taylor, McMaster and Caluya (1955) and in hyphae of *Neurospora* by Zalokar (1959).

Just prior to stage 14 the nuclear membrane disappears and all that remains of the *Drosophila* oocyte nucleus is a Feulgen-positive body, the karyosphere, which is located in the anterior, dorsal portion of the egg. The nuclear membrane of the oocyte nucleus also disappears in *Tenebrio* (Schlottman and Bonhag, 1956). The karyosphere in *Drosophila* has a volume of about 2.7 cubic micra, which is sufficient to contain tetrads of the four chromosomes, if each member of the tetrad has the dimensions of a corresponding chromosome

as viewed in an oogonial metaphase (King, Rubinson, and Smith, 1956). Since the chromosomal material of the mature ovarian oocyte is in such a compact state, it is unlikely that its DNA participates in the metabolic activities of the stage 14 oocyte.

Stages 12 and 14 oocytes represent closed systems (that is, the ooplasm in each case is sealed within the vitelline membrane) of equal volumes ($9x10^6$ cubic micra) and presumably of more or less identical weights. However, in sections the stage 14 oocyte is much denser when viewed with the electron microscope or with the light microscope under phase contrast or dark field illumination, and stage 14 ooplasm is richer in materials (particularly RNA) which stain by the techniques already described. It is obvious that the procedures used to provide sections (dehydration through an ethanol series to butyl methacrylate) remove more material from stage 12 than from stage 14 oocytes. The main change occurring in the oocyte once it reaches its maximum volume is the conversion of small soluble molecules into large, insoluble polymers; a conversion which appears to be independent of the intervention of the oocyte karyosphere. Some RNA synthesis has been demonstrated recently in laid, unfertilized *Drosophila* eggs (J. Schultz, personal communication).

The RNA which initially accumulates in the ooplasm arises from the nurse cell nuclei, but the subsequent build-up of ooplasmic RNA is independent of the nurse cells and the oocyte DNA. An economical working hypothesis to explain these facts would be that an RNA-forming system originally located in the nurse cell nucleus is transferred to the ooplasm during vitellogenesis. Perhaps the endoplasmic reticulum plays a vital role in this process (see pp. 274 and 300). Plaut and Rustad (1959) have presented data which suggest strongly that the cytoplasm of ameba is capable of RNA synthesis in the absence of the nucleus (see Brachet, pp. 321-351 for earlier work on this problem).

The egg coverings: Both vitelline membrane and chorion contain proteins, phospholipids, and polysaccharides. The ellipsoidal, sudanophilic epithelial bodies produced by the columnar follicle cells presumably play some role in the fabrication of the lipoidal components of the vitelline membrane or endochorion. Bonhag (1955) has described phospholipoidal particles in the follicular epithelium of *Oncopeltus* which bear some resemblance to the above epithelial bodies. Palm

(1948) reported that the follicular epithelium of *Bombus* contains two types of follicle cells, one with cytoplasm darker than that of the other. The dark cells produce particulate matter which appears to enter the oocyte; whereas the lighter cells subsequently form the chorion. Perhaps the dark follicle cells of *Drosophila* also play a role distinct from the more numerous, less dense cells.

The most thorough study on chorion formation and structure is that by Beament (1946) for *Rhodnius prolixus*. He showed that in this hemipteran the chorion consists of a complex series of proteinaceous layers which can be distinguished from each other on the basis of their staining behavior, solubility in acids, bases, oxidants, and organic solvents, and their permeability to molecules of various sizes. Among the materials present in the chorionic layers are lipoproteins, protein-oil complexes and complexes of proteins with polyphenols. Chitin is absent from the chorion and vitelline membrane. The proteinaceous vitelline membrane of *Rhodnius* contains no oil or polyphenols.

Beament (1947) has also worked out the morphogenesis of the micropylar complex for *Rhodnius,* but no comparable work has been done for *Drosophila*. The "border cells" of *Drosophila* play a vital role in the formation of the micropylar complex (see page 305). These cells are a group of follicle cells which migrate from the anterior pole of the egg posteriorly between the nurse cells until they reach the surface of the oocyte where they remain. The migration which occurs during stages 9 and 10 takes about an hour (King, 1957). Early in stage 12 (before the endochorion appears) the vitelline membrane is secreted into a depression formed by the border cells. The nipple-shaped protuberance so formed marks the beginning of the micropylar cone. According to Pantel similar cell clusters form the micropylar complex in the eggs of various parasitic dipterans.

W. M. McIndoe (unpublished work) has found that the chorion of *Drosophila* contains about twice as much protein as the thinner vitelline membrane, and that proteinaceous material from the vitelline membrane and chorion is not broken down during warm alkaline hydrolysis (0.25 N NaOH, 18 hours, 37° C). Certain structural proteins such as silk fibroin, keratin, and elastin are known to be stable in warm alkaline solutions. The stability of keratin seems to depend largely upon S-S bridges which cross-link adjacent polypeptide chains

(Frey-Wyssling, 1948). Insect egg shells are rich in sulfur. The shell of the silkworm egg, for example, contains 4% sulfur (Tichomiroff, 1885). The phenylmercuric chloride-ammoniacal silver nitrate procedure demonstrates abundant protein sulfhydryl groups in the *Drosophila* vitelline membrane and endochorion.* It may be that much of the sulfur in insect egg coverings is present in cysteine groups which confer upon the proteins of which they are constituents properties similar to such structural proteins as keratin.

The hardening of proteins also may be accomplished by "tanning" them by the introduction of aromatic cross linkages. Pryor (1940 a, b) has demonstrated that insects can produce dihydrophenols, oxidize them to quinones, and combine these with water soluble proteins to produce tanned proteins which are very resistant to most chemical reagents and enzymes. Such proteins are present in cuticle and in roach ootheca.

A 20 minute immersion in 3% sodium hypochlorite solution dissolves the chorion but not the vitelline membrane. The cystine moieties of keratin can be oxidized by various agents (including hypochlorite ions) to cysteic acid, and the products of the reaction are soluble (Kendrew, 1954).

King (1959) has observed "normal appearing" mature oocytes in whole mounts of Feulgen-stained ovaries of *Drosophila* from females homozygous for certain female-sterile mutations (*ocelliless, narrow abdomen, brief,* and *shaven*^{de}). Abnormalities in the production of beta spheres would have escaped detection, and therefore these mutants should be subjected to cytochemical studies of the type described in this report. The same argument applies to cases where flies fed upon deficient diets or upon antimetabolites lay normal-sized eggs which fail to hatch.

SUMMARY

Cytochemical studies were made of the distribution of polysaccharides, lipids, proteins and nucleic acids in developing oocytes of *Droso-*

* Recent analysis of *Drosophila* egg shells by B. R. Wilson (Dissertation Abstract (1960) *20*: no. 11 pg. 4267) cast some doubt upon this observation. The egg shells are 80% protein, but only traces of sulfur-containing amino acids were found in these proteins. They are presumably acidic in view of the abundance of aspartic and glutamic acids found in their hydrolyzates. Alanine, tyrosine, glycine, and serine were also plentiful. The shells contained 0.6% glucosamine which suggests the presence of aminopolysaccharides, and they were rich in calcium, aluminum, copper, magnesium, and silicon.

phila melanogaster. Sections two micra thick from ovaries fixed in osmium tetroxide and embedded in methacrylate were viewed with the light microscope. Adjacent sections 60 millimicra thick (or less) were observed under the electron microscope.

The plasmosomes of the nurse cell nuclei contain ribonucleoproteins, neutral mucopolysaccharides and a phospholipid-protein complex. Electron micrographs demonstrate plasmosomal emissions during early stages of vitellogenesis.

During vitellogenesis mitochondria, scattered elements of endoplasmic reticulum and dense bodies are observed in the nurse cell cytoplasm. These stream into the oocyte where the dense bodies break down and contribute their lipoidal contents to the ooplasm. The envelope of the nurse cell nucleus may play a role in the synthesis of the dense bodies and the endoplasmic reticulum.

The endoplasmic reticulum and the mitochondria of the columnar follicle cells which envelop the oocyte are concerned (among other things) in the production of lipoidal droplets which may be used in the fabrication of the lipoidal constituents of the vitelline membrane and endochorion.

Two types of yolk spheres are found in the mature egg. The alpha spheres which arise first and contain a phospholipid-protein complex, and the beta spheres which contain phospholipids and acid mucopolysaccharides. Beta spheres arise in physical association with alpha spheres. Together these spheres make up about ¼th the total volume of the egg. During early stages of their development the alpha spheres contain a polysaccharide which may be later contributed to the ooplasm.

The ooplasm contains tiny fat droplets, mitochondria and an endoplasmic reticulum which poliferates as the oocyte matures. The background ooplasm contains abundant amounts of ribonucleoprotein, glycoprotein, lipid-protein complexes and hexosamine-containing polysaccharides.

The vitelline membrane and chorion contain proteins, polysaccharides and phospholipids. Electron micrographs have shown that the vitelline membrane is laid down in the intercellular space between the cell walls of the oocyte and adjacent follicle cells; whereas the chorion is laid down upon the basement membrane of the follicle cells.

The main change occurring in the oocyte once it reaches its maxi-

mum volume is the conversion of small, soluble molecules into large, insoluble polymers (such as proteins, RNA and polysaccharides). This conversion may be independent of the intervention of the genetic material of the oocyte which is confined in the karyosphere. However, many polymers may be formed by systems previously transferred from nurse cell nuclei to the oocyte.

Acknowledgements

The author is grateful to Drs. K. R. Porter, H. W. Deane, J. H. Sang, D. F. Poulson, M. F. Wolfsberg, and K. Deutsch for their careful criticisms of the manuscript. Helpful suggestions were contributed by Drs. D. H. Moore, D. Luck, J. Rothschild, D. Smith, J. A. Bergeron, L. D. Peachey, R. D. Machado, and M. J. Moses. Sections of vestopal embedded material were cut and stained by Mrs. Sarah V. Inglis. The electron micrographs shown in Figures 16 and 17 were taken by R. G. Burnett.

References

Bahr, G. F. 1954. Osmium tetroxide and ruthenium tetroxide and their reactions with biologically important substances. *Exp. Cell Res.*, **7**, 457-479.

Baker, J. R. 1946. The histochemical recognition of lipine. *Quart. J. Micr. Sci.*, **87**, 441-70.

————. 1958. Principles of Biological Microtechnique. J. Wiley.

Bangle, R. & Alford, W. C. 1954. The chemical basis of the periodic acid Schiff reaction of collagen fibers with reference to periodate consumption by collagen and by insulin. *J. Hist. Cytochem.*, **2**, 62-76.

Beament, J. W. L. 1946. The formation and structure of the chorion of the egg in an hemipteran, *Rhodnius prolixus*. *Quart. J. Micr. Sci.*, **87**, 393-439.

————. 1947. The formation and structure of the micropylar complex in the egg-shell of *Rhodnius prolixus* Stål (Heteroptera reduviidae). *J. Exp. Biol.*, **23**, 213-223.

————. 1949. The penetration of the insect egg-shells. II. The properties and permeability of subchorial membranes during development of *Rhodnius prolixus* Stål. *Bull. Ent. Res.*, **39**, 467-488.

————. 1949. The penetration of the insect egg-shells. I. Penetration of the chorion of *Rhodnius prolixus* Stål. *Bull. Ent. Res.*, **39**, 359-383.

Bier, K. 1954. Über Phasen gesteigerter Protien - und Kohlehydratein - lagerung und die Fettverteilung im Hymenopterenovar. *Verh. Dtsch. Zool. Ges.*, **18**, 422-429.

Bonhag, P. F. 1955. Histochemical studies of the ovarian nurse tissues and oocytes of the milkweed bug, *Oncopeltus fasciatus* (Dallas). I. Cytology, nucleic acids, and carbohydrates. *J. Morph.*, **96**, 381-439.

————. 1955. Histochemical studies of the ovarian nurse tissues and oocytes of the milkweed bug, *Oncopeltus fasciatus* (Dallas). II. Sudanophilia, phospholipids, and cholesterol. *J. Morph.*, **97**, 283-312.

———. 1956. The origin and distribution of periodic acid-Schiff-positive substance in the oocyte of the earwig, *Anisolabis maritima* (Géné). *J. Morph.*, **99**, 433-464.

———. 1958. Ovarian structure and vitellogenesis in insects. *Annu. Rev. Ent.*, **3**, 137-160.

———. 1959. Histological and histochemical studies on the ovary of the American cockroach *Periplaneta americana* (L.) *Univ. Calif. Publ. Ent.*, **16**, 81-124.

BRACHET, J. 1957. Biochemical Cytology. Academic Press, N. Y.

BUCHNER, P. 1918. Vergleichende Eistudien. I. Die akzessorischen Kerne des Hymenopterenеies. *Ark. f. mikr. Anat.*, **91**, 1-202.

CAIN, A. J. 1947. The use of Nile blue in the examination of lipoids. *Quart. J. Micro. Sci.*, **88**, 383-392.

CASSELMAN, W. G. B. 1959. Histochemical Technique. J. Wiley.

CHAUDHRY, H. S. 1951. Nucleolar activity in the oocytes of some marine teleostean fishes. *J. Roy. Mic. Soc.*, **71**, 87-93.

COLOMBO, G. 1955. I'oogenesi negli Ortotteri. II. Richerchi sull' accrescimento degli oociti di *Anacridium aegyptium L. Arch. Zool. Italiano*, **40**, 235-263.

———. 1956. Richerche citologiche sull'oogenesi del Baco da seta *(Bombyx mori* L.) e considerazioni sull'oogenesi degli Insetti. *Boll. Zool.*, **23**, 279-89.

DASGUPTA, B. & RAY, H. N. 1954. A cytochemical study of the nurse cells of the bed bug. *Proc. Zool. Soc. Beng.*, **7**, 108-112.

DEANE, H. W. 1958. Intracellular lipides: their detection and significance. In *Frontiers in Cytology*. Edited by S. L. Palay. Yale U. Press, pp. 227-263.

DEUEL, H. J. 1951. The Lipids, their Chemistry and Biochemistry. vol. I: Chemistry. Interscience Publ.

FARKAS, K. 1903. Beiträge zur Energetik der Ontogenese. *Pflüg Arch. Ges. Physiol.*, **98**, 490-546.

FAWCETT, D. W., ITO, S. & SLAUTTERBACK, D. B. 1959. The occurence of intercellular bridges in groups of cells exhibiting synchronous differentiation. *J. Biophys. Biochem. Cytol.*, **5**, 453-460.

FEULGEN, R. & ROSSENBECK, H. 1924. Mikroskopisch - chemischer Nachweis einer Nucleinsäure von Typus der Thymonuclein-säure und auf die darauf beruhende elektive Färbung von Zellkernen in mikroskopischen Präparaten. *Zeit. Physiol. Chem.*, **135**, 203-48.

FLAX, M. H. & HIMES, M. H. 1952. Microspectrophotometric analysis of a metachromatic staining of nucleic acids. *Physiol. Zool.*, **25**, 297-311.

FREY-WYSSLING, A. 1948. Submicroscopic Morphology of Protoplasm and its Derivatives. Elsevier Publishing Co.

GLEGG, R. E., CLERMONT, Y. & LEBLOND, C. P. 1952. The use of lead tetra acetate, benzidine, o-dianisidine and a "film test" in investigating the periodic acid-Schiff technique. *Stain Tech.*, **27**, 277-305.

GOMORI, G. 1952. Microscopic Histochemistry. U. Chicago Press.

GUPTA, B. L. 1958. Demonstration of some "masked" lipids in the oocytes of *Chrotogonus trachypterus* with Sudan black B and phenol "unmasking" techniques. *Nature, Lond.*, **181**, 555.

HALE, A. J. 1957. The histochemistry of polysaccharides. *Intl. Rev. Cyt.*, **6**, 193-263.

HINTON, H. E. 1959. Plastron respiration in the eggs of *Drosophila* and other flies. *Nature, Lond.*, **184**, 280-1.

HSU, W. S. 1952. The history of the cytoplasmic elements during vitellogenesis in *Drosophila melanogaster. Quart. J. Micr. Sci.*, **93**, 191-206.

———. 1953. The origin of proteid yolk in *Drosophila melanogaster. Quart. J. Micr. Sci.*, **94**. 23-8.

JACOB, J. & SIRLIN, J. L. 1959. Cell function in the ovary of *Drosophila* I. DNA classes in nurse cell nuclei as determined by autoradiography. *Chromosoma*, **10**, 210-228.

KENDREW, J. C. 1954. Structural Proteins. I. in *The Proteins*. vol. II B:845-950. Ed. by H. Neurath and K. Bailey, Acad. Press, N. Y.

KING, R. C. & WILSON, L. P. 1954. Studies with radiophosphorus in *Drosophila*. IV. Experiments on flies homogenously labeled with P^{32}. *J. Exp. Zool.*, **126**, 401-418.

———, RUBINSON, A. C. & SMITH, R. F. 1956. Oogenesis in adult *Drosophila melanogaster*. *Growth*, **20**, 121-157.

———. 1957. Oogenesis in adult *Drosophila melanogaster*. II. Stage distribution as a function of age. *Growth*, **21**, 95-102.

———, BURNETT, R. G. & STALEY, N. A. 1957. Oogenesis in adult *Drosophila melanogaster*. IV. Hereditary ovarian tumors. *Growth*, **21**, 239-261.

——— & BURNETT, R. G. 1957. Oogenesis in adult *Drosophila melanogaster*. V. Mutations which affect nurse cell nuclei. *Growth*, **21**, 263-280.

———. 1957. The cytology of the irradiated ovary of *Drosophila melanogaster*. *Exp. Cell Res.*, **13**, 545-552.

——— & SANG, J. H. 1958. Modification of ovogenesis in *D. melanogaster*. *Drosophila Inform. Serv.*, **32**, 131-133.

——— & DEVINE, R. L. 1958. Oogenesis in adult *Drosophila melanogaster*. VII. The submicroscopic morphology of the ovary. *Growth*, **22**, 299-326.

——— & SANG, J. H. 1959. Oogenesis in adult *Drosophila melanogaster*. VIII. The role of folic acid in oogenesis. *Growth*, **23**, 37-53.

———. 1959. The genetic control of oogenesis in *Drosophila melanogaster*. Proceedings of the XV International Congress of Zoology, London, July 1958, p. 722-723.

——— & BURNETT, R. G. 1959. An autoradiographic study of uptake of tritiated glycine, thymidine and uridine by fruit fly ovaries. *Science*, **129**, 1674-1675.

——— & FALK, G. 1960. *In vitro* incorporation of uridine-H^3 into developing fruit fly oocytes. *J. Biophys. Biochem. Cytol.*, (in press).

——— & VANOUCEK, E. G. 1960. Oogenesis in adult *Drosophila melanogaster*. X. Studies on the behavior of the follicle cells. *Growth*, (in press).

LEVENBOOK, L., TRAVAGLINI, E. C. & SCHULTZ, J. 1958. Nucleic acids and their components as affected by the Y chromosome of *Drosophila melanogaster*. I. Composition and amount of ribonucleic acids in unfertilized egg. *Exp. Cell Res.*, **151**, 43-61.

LEWIS, I. F. & WALTON, L. 1958. Gall-information on *Hamamelis virginiana* resulting from material injected by the aphid *Hormaphis hamamelidis*. *Trans. Amer. Micr. Soc.*, **77**, 146-200.

LILLIE, R. D. 1956. The mechanism of Nile blue staining of lipofuscins. *J. Hist. Cytochem.* **4**, 377-81.

LOVERN, J. A. 1957. The Chemistry of Lipids of Biological Significance. J. Wiley.

LUFT, J. H. 1956. Permanganate—a new fixative for electron microscopy. *J. Biophys. Biochem. Cytol.*, **2**, 799-802.

MACHEBOEUF, M. 1937. Etat des Lipides dans la Matière Vivante. Actualités Scientifiques et Industrielles, No. 448. Herman et Cie., Paris.

MAZIA, D., BREWER, P. A. & ALFERT, M. 1953. The cytochemical staining and measurement of protein with mercuric bromphenol blue. *Biol. Bull.*, **104**, 57-67.

MONNÉ, L. & SLAUTTERBACK, D. B. 1950. Differential staining of various polysaccharides in sea urchin eggs. *Exp. Cell Res.*, **1**, 477-491.

MOORE, D. & GRIMELY, P. M. 1957. Problems in methacrylate embedding for electron microscopy. *J. Biophys. Biochem. Cytol.*, **3**, 255-260.

MORGENTHALER, H. U. 1952. Über den Nukleinsäuregehalt im Ovar der Bienenkönigin. *Arch. Julius Klaus-Stiftung,* **27**, 206-11.

NATH, V., GUPTA, B. L. & LAL, B. 1958. Histochemical and morphological studies of the lipids in oogenesis. I. *Periplaneta americana. Quart. J. Micr. Sci.,* **99**, 315-332.

NATH, V., GUPTA, B. L. & BAINS, G. S. 1958. Histochemical and morphological studies of the lipids in oogenesis. V. The egg-follicle of *Culex fatigans. Research Bull. Panjab Univ.,* No. 148, p. 135-148.

NEEDHAM, J. 1931. Chemical Embryology, vol. 1, Cambridge U. Press.

NONIDEZ, J. F. 1920. The internal phenomena of reproduction in *Drosophila. Biol. Bull., Woods Hole,* **39**, 207-230.

ONCLEY, J. L. 1959. Chemical characterization of proteins, carbohydrates, and lipids. *Rev. Mod. Physics,* **31**, 30-49.

OVEREND, W. G. & STACEY, M. 1949. Mechanism of the Feulgen nucleal reaction. *Nature, Lond.,* **163**, 538-540.

PANTEL, J. 1913. Recherches sur les Diptères a larves entomobies. II. Les enveloppes le l'oeuf avec leurs dépendances, les dégâts indirects du parasitisme. *Le Cellule,* **29**, 1-284.

PEARSE, A. G. E. 1954. Histochemistry. Little and Brown, Co.

PLAUT, W. & RŪSTAD, R. C. 1959. The incorporation of (^{14}C) uracil and (^{14}C) orotic acid into RNA in the cytoplasm of *Amoeba proteus. Biochim. Biophys. Acta,* **33**, 59-64.

PORTER, K. R. 1954. Observations on the fine structure of animal epidermis. Proc. Internat. Conf. on Electron Microscopy. London, July 1954, 539-546.

PRYOR, M. G. M. 1940a. On the hardening of the ootheca of *Blatta orientalis. Proc. Roy. Soc.,* **128B**, 378-393.

———. 1940b. On the hardening of the cuticle of insects. *Proc. Roy. Soc.,* **128B**, 393-407.

RICHARDS, A. G. 1952. Studies on arthropod cuticle. 7. Patent and masked carbohydrate in the epicuticle of insects. *Science,* **115**, 206-8.

SANG, J. H. & KING, R. C. 1959. Nutritional requirements for normal oogenesis in *Drosophila melanogaster. Drosophila Inform. Serv.,* **33**, 156-8.

SATIR, P. G. & PEACHEY, L. D. 1958. A simple method for reducing compression artifacts. *J. Biophys. Biochem. Cytol.,* **4**, 345-7.

SCHLOTTMAN, L. & BONHAG, P. F. 1956. Histology of the ovary of the adult mealworm. *Univ. Calif. Publ. Ent.,* **11**, 351-394.

SHIOMI, T. & KITAZUME, Y. 1956. Changes in glycogen content during early embryonic development in *Drosophila melanogaster.* (Abs.) *Drosophila Inform. Serv.,* **30**, 151-152.

SPICER, S. S. 1960. A correlative study of the histochemical properties of rodent acid mucopolysaccharides. *J. Hist. Cytochem.* **8**, 18-34.

SRIVASTAVA, D. S. 1953. Nucleolus and nucleolar extrusions in the oocytes of *Lumbricus terrestris* L. *La Cellule,* **55**, 131-137.

STACEY, M. 1946. The chemistry of mucopolysaccharides and mucoproteins. *Advanc. Carbohyd. Chem.,* **2**, 161-201.

STICH, H. 1951. Das Vorkommen von Kohlenhydraten im Ruhekern und Während der Mitose. *Chromosoma,* **4**, 429-438.

STOECKENIUS, W. 1959. An electron microscope study of myelin figures. *J. Biophys. Biochem. Cytol.,* **5**, 491-500.

SWANSON, M. A. & ARTOM, C. 1950. The lipid composition of the larger granules (mitochondria) from rat liver. *J. Biol. Chem.,* **187**, 281-7.

SWIFT, H. 1955. Cytochemical techniques for nucleic acids. In *the Nucleic Acids* II. edited by Chargaff and Davidson. Academic Press, p. 91.

TAYLOR, J. H., MCMASTER, R. D. & CALUYA, M. F. 1955. Autoradiographic study of incorporation of P^{32} into RNA at the intracellular level. *Exp. Cell. Res.*, **9**, 460-473.

TICHOMIROFF, A. 1885. Chemische Studien über die Entwicklung der Insecteneier. *Zeit. Physiol. Chem.*, **9**, 518-532.

WANG, T. Y., MAYER, D. R. & THOMAS, L. E. 1953. A lipoprotein of rat liver nuclei. *Exp. Cell Res.*, **4**, 102-106.

WARD, R. T. 1959. Observations on the origin of yolk. *Anat. Rec.*, **134**, 651.

WATSON, H. L. 1958. Staining of tissue sections for electron microscopy with heavy metals. II. Application of solutions containing lead and barium. *J. Biophys. Biochem. Cytol.*, **4**, 727-731.

WIGGLESWORTH, V. B. & BEAMENT, J. W. L. 1950. The respiratory mechanisms of some insect eggs. *Quart. J. Micr. Sci.*, **91**, 429-452.

———. 1957. The use of osmium in the fixation and staining of tissues. *Proc. Roy. Soc. B.*, **147**, 185-199.

YOSUFZAI, H. K. 1953. Cytological studies on the oogenesis of *Fasciola hepatica* L. *La Cellule*, **55**, 167-177.

WREN, J. J. & MITCHELL, H. K. 1959. Extraction methods and an investigation of *Drosophila* lipids. *J. Biol. Chem.*, **234**, 2823-2828.

ZOLOKAR, M. 1959. Nuclear origin of ribonucleic acid. *Nature, Lond.*, **183**, 1330.

———. 1960. Sites of RNA and protein synthesis in *Drosophila*. *Exp. Cell Res.*, **19**, 184-6.

ZUGIBE, F. T., BROWN, K. D. & LAST, J. H. 1959. A new technique for the simultaneous demonstration of lipid and acid polysaccharides on the same tissue section. *J. Hist. Cytochem.*, **7**, 101-106.

Growth, 1960, **24**, 325-331.

GROWTH IN YOUNG RATS USED AS AN INDEX OF EXOCRINE PANCREATIC FUNCTION

L. E. EDWARDS AND A. C. BREHME

Department of Physiology, Medical College of Virginia, Richmond

(Received for publication June 20, 1960).

INTRODUCTION

In a previous paper by two of us (Edwards and Garber, 1954) a method was described in which a rat could be rid of exocrine pancreatic secretion. Some investigators have studied the effects of the removal of pancreatic secretion from the digestive tract (Chaikoff and Entenman, 1948). Most of these studies have been concerned with choline metabolism and its relation to fatty livers. Trypsin has been shown to play a role in the prevention of fatty livers (Montgomery *et al.*, 1950). Associated with the fatty changes one often sees changes in growth (Clowes and MacPherson, 1951). In an animal deprived of exocrine pancreatic secretion, one might expect the change in growth to appear first because of the fact that the animal has a limited supply of enzymes to digest and perhaps rebuild protein, and a protein deficiency should show up very quickly.

A more thorough study of the growth changes produced by the elimination of some or all of the acinar tissue seemed worth while.

MATERIALS AND METHODS

The animals were prepared as described in a previous paper (Edwards and Garber, 1954). That is, the experimental animal was prepared by operation so that all of the pancreatic ducts were effectively ligated. This involved splicing the upper end of the common bile duct into the duodenum. The lower section of this duct was ligated at both ends. The duodenal end of this section was ligated twice in order to prevent any recannulation back into the duodenum.

In the control group, animals were prepared in which the common bile duct was spliced into the intestine in a similar manner, but all the pancreatic ducts were patent and the juice had free access to the

gut. These animals were operated on to impose the same surgical trauma and shock to the control group.

Growth curves were kept on all rats and the food was weighed daily except on Saturdays, Sundays and holidays. All the animals were kept in an air-conditioned room but not in a constant temperature room.

Total fats were determined according to Barker *et al.* (1950). The livers were minced and extracted 16 hours on a Soxhlet apparatus with a mixture of one part ether to three parts alcohol. After drying, the fats were dissolved in petroleum ether and dried. Each flask was weighed and the weight subtracted from the original tared flask weight to give the fat weight.

Autopsy slides were made on the kidney, liver, pancreas, adrenal gland and aorta for many of the animals.

The experimental animals were maintained after the operation on a diet containing 1% pancreatin (3X) in Purina Chow. The control animals were fed a basal diet composed only of Purina Chow. Some of the experimental animals were fed the pancreatin diet for a period of three weeks and then placed on the basal diet for a period of two months.

Results

The data have been separated into three arbitrary groups from the gross autopsy findings. The first group included all the animals with an estimated 10% or less of the active acinar pancreatic tissue. The second group included those animals having between 11 and 40% of the total acinar tissue remaining. In the operated controls about 90 to 100% of the acinar tissue is still active.

In order to interpret the growth curves, the log of the weight was plotted against the reciprocal of the time. This gives nearly a straight line between these two functions. The slope (K) is calculated from this line according to Zucker *et al.* (1941). This slope gives us an indication as to the overall growth of the animal. Since it is impossible to define K in terms of growth rate, we have taken the liberty in this paper of referring to K as the growth index. K does give us a way of comparing an early growth period with a later period for the same animal. In a normal growth curve, the rate of gain in weight diminishes with time. The above curve compensates for the diminishing

rate of gain in weight with age. [K′ refers to the slope of the line after the animal was placed on a no pancreatin diet.]

Assuming that changes in K values give us a fairly reliable measure of growth changes, it can be seen that they are altered in several of the experimental procedures presented here. First a sham operation, where little or no pancreatic tissue is removed, does not alter the growth index (K value) from that found in the unoperated controls, if sufficient time is allowed for recovery from the operation. If between 60% and 90% of the pancreatic acinar tissue is destroyed, the K values are altered significantly on the basal diet (Table I). This

TABLE I
ALTERATIONS IN THE GROWTH INDEX IN PANCREATIC-DEFICIENT RATS

N		K	K′
12	Normal controls	6.10 ± .90**	
33	Operated controls	5.78 ± 1.42	
20	Group I	4.74* ± 1.44	—1.74 ± 1.31
20	Group II	5.09* ± 1.74	4.03 ± 1.49
		Mean difference	P
Normal vs. operated controls		.32	< .4
Operated controls vs. Group I (K)		1.04	< .02
Operated controls vs. Group II (K)		.69	< 2.
Group I (K) vs. Group II (K)		.35	< 5.
Group I (K) vs. Group I (K′)		6.48	< .01
Group II (K) vs. Group II (K′)		1.06	< .05

LEGEND FOR TABLE I

**	Standard deviations
N	Number of animals
K & K′	So-called growth index (see text)
*	1% 3X pancreatin diet

represents a drop of about 30% in the growth index. If pancreatin is added to the diet at the 1% level for the 3X pancreatin, the K values are restored to the operated control level. If more than 90% of the acinar tissue is destroyed, a marked change in the K value takes place. Not only is no growth obtained but weight loss takes place which gives a negative K value. If pancreatin is added to the basal diet to the level of 1% of the 3X pancreatin, the growth index is restored to nearly the operated control level.

Since the amount of food eaten by the animal can alter growth, the daily food intake was measured. As to the amount of food eaten, it is noticed that the pancreatic deficient rat eats 29% more food than the

normal operated control (Table II). The greater the pancreatic deficiency (beyond a certain point) the greater the amount of food eaten by the animal. When pancreatin is added to the diet, no further increase or decrease in food intake takes place in the deficient animal.

TABLE II
CHANGES IN FOOD INTAKE IN THE PANCREATIC-DEFICIENT RAT

N		1st 2-wk. interval	2nd 2-wk. interval
12	Normal controls	14.69 ± 1.94**	16.45 ± 1.96
11	Operated controls	15.13 ± 1.35	15.88 ± 1.82
20	Group I	19.56* ± 2.83	20.67 ± 3.55
29	Group II	16.78* ± 2.50	17.99 ± 3.04

	Mean diff.	P
Normal controls (1st int.) vs. operated controls (1st int.)	.44	< .6
Operated cont. (1st int.) vs. operated cont. (2nd int.)	.75	< .3
Operated cont. (1st int.) vs. Group I (1st int.)	4.43	< .01
Operated cont. (1st int.) vs. Group II (1st int.)	1.65	< .01
Group I (1st int.) vs. Group II (1st int.)	2.78	< .01
Group I (1st int.) vs. Group I (2nd int.)	1.11	< .3
Group II (1st int.) vs. Group II (2nd int.)	1.21	< .1

LEGEND FOR TABLE II

**	Standard deviation
N	Number of animals
*	1% 3X pancreatin diet

It is known that alterations in digestion and absorption do occur in duct-ligated animals (Coffey *et al.*, 1940; Douglas *et al.*, 1953; Cohen and Annegers, 1953). Some further metabolic studies are being carried out in this laboratory.

Malnutrition and low protein diets have been shown to produce fatty livers (Gillman and Gilbert, 1954). In these experimental animals, only Group I showed any alterations in the percentage of liver fat (Table III). This was actually a decrease in percent liver fat.

One might expect that the liver would reflect inadequate pancreatic function by change in its weight. Although body weight was altered by several of the imposed procedures, no alteration was seen in the liver as measured by percentage of body weight.

DISCUSSION

The action of the pancreas in maintaining proper growth has never been thoroughly understood. Even though the exocrine secretion has been studied, its exact role has not been established. Marked altera-

tion in growth that has been demonstrated in this study when the acinar tissue is almost completely destroyed must be explained. Other investigators are aware of the fact that growth bears some relationship to the total amount of the pancreas at the lower levels of functional pancreatic tissue (Clowes and MacPherson, 1951; Coffey *et al.*, 1940; Dragstedt, 1943). One might expect the alteration seen in growth to be related to digestion and absorption of the various foodstuffs. If this is true, just where does this failure to break down or absorb a given food occur? More studies are needed to explain the mechanisms described above.

TABLE III

N		% Liver Fat	Liver % Body Wt.
20	Operated controls	4.57 ± .97**	3.39 ± .59
10	Group I	3.68* ± .41	3.42* ± .36
16	Group II	4.47* ± .98	3.50* ± .49
	Mean diff.	P	Mean diff. P
Controls vs. Group I	.89	< .01	.03 < .9
Controls vs. Group II	.10	< .8	.11 < .6
Group I vs. Group II	.79	< .01	.08 < .7

LEGEND FOR TABLE III

** Standard deviation
N Number of animals
* 1% 3X pancreatin diet

Another question is how does pancreatin alleviate most of the pancreatic deficiency seen in these experimental animals? One would expect pancreatin to be destroyed by the acid and pepsin found in the stomach. The fact that growth is resumed on a diet containing only 1% 3X pancreatin casts some doubt as to whether the pancreatic enzymes are solely involved in promoting growth.

The animal itself seems to be able to sense some loss in the absorbed food products for it is capable of increasing its food intake above that normally found in the control animal. With pancreatin added to the diet, near normal growth occurs. Without pancreatin the most deficient animals do not gain weight. The amount of extra food eaten is more in the most deficient animals than in the less deficient animals. Hence the animal is able to correct in part for minor losses in absorption and digestion by simply eating more food.

Whatever the changes seen in body weight, the liver weight seems to keep pace with these changes. Since no alterations were seen in the

liver structure or in the percentage of body weight, it seems unlikely that liver function is altered.

Malnutrition and low protein diets often affect the fat content of the liver rather than its growth and structure (Gillman and Gilbert, 1954). Since no increase was seen in liver fat, it is unlikely that the lipotropic factor was involved in the abnormal metabolism seen in these animals. Clowes and MacPherson (1951), on similarly operated animals, could not demonstrate any changes of the fat content of the liver when their rats were fed Purina Fox Chow. They were able to demonstrate an increase in liver fat on a choline deficient diet. No recovery period after the operation was allowed and no report was given on the growth of these animals.

It was realized that the estimated pancreas determined at the time of autopsy was a measure of the total amount of pancreas at that time. It appears that recannulation of pancreatic ducts, followed by regeneration of pancreatic tissue, must have taken place in some of these experiments. These changes are indicated by sudden alterations seen in the growth curves. So in some of these animals the pancreatic tissue found at autopsy is the maximum amount found rather than the preferred average amount of tissue acting over the experimental period.

Summary

Oral feeding of pancreatin corrected most of the deficiency produced by the loss of pancreatic juice in the intestine.

The most deficient animals, with little or no acinar tissue, showed a marked decrease in the growth index (K value) in going from a 1% pancreatin diet to a no pancreatin diet.

The pancreatic acinar deficient animals eat more food than the controls whether or not pancreatin is added to the diet.

No alterations were seen in the liver as measured by the percentage of body weight.

The rats having the greatest pancreatic deficiency (Group I) contained a lower percentage of liver fat than the controls.

Acknowlegments

3X pancreatin was supplied through the courtesy of Dr. David Klein of the Wilson Laboratories.

This investigation was supported in part by a research grant A-1390

from the National Institutes of Health, National Institute of Arthritis and Metabolic Diseases.

References

1. Barker, W. F., Rogers, K. E., & Moore, F. D. 1950. Effect of pancreatectomy on phospholipid synthesis in the dog. *Arch. of Surgery*, **61**, 1151-1162.
2. Chaikoff, I. L., & Entenman, C. 1948. Antifatty-liver factor of the pancreas-present status. *Advances Enzymol.*, **8**, 171-202.
3. Clowes, G. H. A., Jr., & Macpherson, L. B. 1951. Production of fatty livers by ligation of the pancreatic ducts in rats. *Am. J. Physiol.*, **165**, 628-638.
4. Coffey, R. J., Mann, F. C. & Bollman, J. L. 1940. The influence of the pancreas on the utilization of foodstuffs. *Am. J. Digestive Diseases*, **7**, 144-149.
5. Cohen, B. J., & Annegers, J. H. 1953. Fecal loss of various dietary nutrients in dogs lacking pancreatic juice. *Gastroenterology*, **25**, 67-71.
6. Douglas, G. J., Jr., Reinauer, A. J., Brooks, W. C. & Pratt, J. H. 1953. The effect on digestion and absorption of excluding the pancreatic juice from the intestine. *Gastroenterology*, **23**, 452-459.
7. Dragstedt, L. R. 1943. Some physiologic problems in surgery of the pancreas. *Annals of Surgery*, **118**, 576-593.
8. Edwards, L. E., & Garber, J. 1954. A simple method for splicing the common bile duct into the duodenum of the rat. *Gastroenterology*, **26**, 312-315.
9. Gillman, J., & Gilbert, C. 1954. Aspects of nutritional liver disease—human and experimental. *Ann. N. Y. Acad. Sci.*, **57**, 737-749.
10. Montgomery, M. L., Entenman, C., Chaikoff, I. L., & Feinberg, H. 1950. Antifatty liver activity of crystalline trypsin in insulin-treated depancreatized dogs. *J. Biol. Chem.*, **185**, 307-310.
11. Zucker, T. F., Hall, L., Young, M., & Zucker, L. 1941. The growth curve of the albino rat in relation to diet. *J. Nutrition*, **22**, 123-138.